

STREAM CO₂ DEGASSING: REVIEW OF METHODS AND LABORATORY VALIDATION
OF FLOATING CHAMBERS

By

2015

Michael J. Rawitch

Submitted to the graduate degree program in Geology and the Graduate Faculty of the University
of Kansas in partial fulfillment of the requirements for the degree of Master of Science.

Chairperson Dr. G.L. Macpherson

Dr. Andrea Brookfield

Dr. Craig Marshall

Date Defended: January 27th, 2016

The Thesis Committee for Michael J. Rawitch certifies that this is the approved version of the following thesis:

STREAM CO₂ DEGASSING: REVIEW OF METHODS AND LABORATORY VALIDATION
OF FLOATING CHAMBERS

Chairperson Dr. G.L. Macpherson

Date approved: January 27th, 2016

Abstract

Measuring the amount of CO₂ exiting headwater streams through degassing could play an important role in environmental chemistry. The objective of this project was to develop a method to measure CO₂ flux from headwater streams such as those at the Konza Prairie Long-Term Ecological Research Site and Biological Station (Konza), and to determine the effects of stream morphology and turbulence that can affect CO₂ degassing. The project comprised an in-depth critical review of literature on the topic of measuring degassing in small streams, as well as a series of experiments that developed and tested methods of quantifying the flux of CO₂ from a simulated stream. The experiments evaluated the effectiveness of multiple floating chamber designs to measure CO₂ degassing in flowing water at a range of water velocities and dissolved CO₂ concentrations. Both the literature review and experiments suggested that the floating chamber is viable method for use in headwater streams.

Acknowledgements

I have had a truly blessed experience at the University of Kansas during the course of my graduate education. My graduate advisor, Dr. Gwen Macpherson, has had an open door to any questions or concerns I have had since day one at the University. Dr. Macpherson has proven to be a tremendous mentor and teacher over the past several years. It has also been a pleasure working with Dr. Andrea Brookfield and Dr. Craig Marshall as part of my graduate committee. They are two exceptional professors who have provided many useful insights while guiding my research and coursework at the University. My fellow students have provided me with greatly valued assistance during my time at the university including Brock Norwood, Trevor Osorno, Mackenzie Creamens, Brooks Bailey, and Jaime Long. Numerous individuals in the engineering department have helped to support my research by providing facilities and useful training in the operation of those facilities. Specifically, Donny Spradling and Evan Deal have provided significant help. I have benefited from many generous donors who have made my education at the University of Kansas an unparalleled experience. A special thanks to the KU Endowment Association, the KU Geology Department, the Geological Society of America, and the Konza NSF LTER program for their funding. A network of family, friends, and colleagues have supported my intellectual pursuits through emotional support, subject matter discussions, and occasional financial assistance as I worked through the hydrogeology program. Most importantly, I would like to thank my fiancé, Dr. Merritt Sizemore, who challenged me to continue my education as she continued hers and remained supportive at all times of my academic endeavors. She brings out the best in me.

Table of Contents

Abstract.....	iii
Acknowledgements.....	iv
CHAPTER 1. METHODS FOR MEASURING ATMOSPHERIC EXCHANGE RATES FROM LOW-ORDERED STREAMS: A CRITICAL REVIEW.....	1
1. Objective.....	2
1.1. Overview of modern carbon cycle.....	2
1.2. Overview of carbon cycle in inland waters.....	3
2. Soil to stream: sources of CO ₂ and groundwater-stream carbon cycling.....	4
2.1. Soil CO ₂ production.....	4
2.2. Geochemical controls on in-stream CO ₂ concentrations.....	6
2.3. Physical hydrogeology.....	7
2.4. Hydrodynamics and geomorphology.....	9
3. Gas transfer physics overview.....	9
4. Methods for measuring gas transfer.....	11
4.1. Chambers.....	12
4.2. Tracers.....	18
4.3. Wind speed.....	21
4.4. Hydrogeomorphology.....	21
4.5. Others.....	22

5. Selecting a methodology.....	24
6. Future research.....	25
Tables.....	27
Figures	28
References.....	33
1. Introduction.....	46
2. Methods	47
2.1. Flume experiment	47
2.1.1. Water-chemistry.....	49
2.1.2. Floating chamber measurements.....	50
2.2. Stirring plate simulation.....	52
3. Results.....	53
3.1. Flume experiments.....	53
3.1.1. Fundamental parameters	53
3.1.2. CO ₂ degassing.....	55
3.2. Stirring plate simulation.....	56
4. Discussion.....	57
5. Conclusions and implications	60
Tables.....	61
Figures	74
References.....	81
APPENDICES	90

Appendix A. Gas permeability trials	91
Goal.....	91
Methods.....	91
Results.....	92
Interpretations and conclusions.....	94
Appendix B. Water-chemistry Flux.....	100
Introduction.....	100
Methods.....	100
Verifying water chemistry fluxes rates	101
Results.....	102
Assumptions tested	102
Discussion and conclusions	103
Appendix C. Gas analyzer setup and procedure	113
Field check-list:.....	113
Start-up procedure:.....	114
Span (monthly):	118
Zero (monthly):.....	118
Operation:	118
Shut-down:	119
Floating-chamber calculations:.....	120

Appendix D. Flume setup and procedure	125
Water resources laboratory	125
Step by step procedure	125
Appendix E. Geochemical speciation modeling.....	128
Appendix F. Example calculations	129
Dissociation reaction constants.....	129
Partial pressure of CO ₂	129
Water-chemistry flux	129
Floating-chamber calculations:.....	130
Appendix G. Flushing the chamber between trials.....	132
Appendix H. Supply numbers and orders.....	136
Appendix I. Results of CO ₂ concentration titration.....	137
Appendix J. Stirring plate experiment with tap water	138
Appendix J. Controlling room atmospheric CO ₂	141
References cited in all appendices	142

**CHAPTER 1. METHODS FOR MEASURING ATMOSPHERIC EXCHANGE RATES
FROM LOW-ORDERED STREAMS: A CRITICAL REVIEW**

1. Objective

The biogeochemistry of small streams has emerged as an important aspect of the carbon cycle. Researchers are quickly working to quantify and understand the processes involved in moving CO₂ between the atmosphere and terrestrial environments. To adequately quantify these fluxes, it is necessary to fully develop a functional conceptual model for a given study site and to choose the proper methodology based on site-specific characteristics. The aim of this review is to provide an overview of processes involved in producing CO₂ found in small streams and to critically discuss the methods currently available for measuring fluxes from small streams to the atmosphere.

1.1. Overview of modern carbon cycle

The amount of carbon in the earth's atmosphere, in the form of both CO₂ and CH₄, has oscillated throughout the Phanerozoic with the highest atmospheric CO₂ occurring during the Cambrian Period and concentrations more or less decreasing until recently (Berner 2004). It should be noted that since the beginning of the industrial revolution in the mid-nineteenth century, atmospheric CO₂ has jumped from 280 ppm to over 400 ppm (Tans 2016). The measured increase in atmospheric CO₂ over the past 200 years accounts for only about half of the CO₂ emitted from human activities over this time, and the rest is assumed to be sequestered in the oceans or on land. Understanding the complex behavior of carbon in the environment is difficult but also essential. The processes by which carbon is transformed and moved through the environment is referred to as the "Carbon Cycle" (Figure 1). This cycle moves carbon through the atmosphere, biosphere, geosphere, and hydrosphere with varying rates. Effectively quantifying these fluxes is crucial to more completely understand carbon cycling and the associated processes involving carbon in the environment.

1.2. Overview of carbon cycle in inland waters

Terrestrial carbon reservoirs include the terrestrial portions of the geosphere (soils, minerals, sediments), biosphere (animals and plants), and hydrosphere (lakes, reservoirs, wetlands, rivers, and streams). Inland waters can be viewed as the sum of all lakes, reservoirs, wetlands, rivers, and streams. In recent years, work has begun to focus on inland waters and the complex processes of carbon accumulation in them due to sedimentation and mineralization, transport through rivers to the oceans, and gas exchange to the atmosphere (Figure 2). Each type of inland water (lakes, reservoirs, wetlands, rivers and, streams) is affected differently by the processes of carbon accumulation, transport, and gas exchange.

The recent effort to accurately measure emissions from small low-ordered streams is of particular interest to carbon-cycle researchers. Low-ordered headwater streams play a particularly important role in gas efflux to the atmosphere because of their close connection to groundwater and their abundance (Nadeau and Rains, 2007). These low-ordered streams typically have elevated CO₂ concentrations compared to atmospheric (Hotchkiss et al., 2015) and tend to be shallow, turbulent, and have higher velocities than other inland waters (Generaux and Hemond, 1992). Halbedel and Koschorreck (2013) estimate emissions from central European streams and suggest streams emit an order of magnitude more CO₂ than reservoirs. Butman and Raymond (2011) conservatively estimate the amount of CO₂ released to the atmosphere from streams in the continental United States (between 25°N and 50°N) each year to be equivalent to 6.3% (0.5 Pg) of anthropogenic CO₂ emissions.

Many low-ordered streams are intermittent and difficult to characterize. Nadeau and Rains (2007) estimate that these low-ordered intermittent rivers account for more than half the length of rivers and streams in the United States. Yet, intermittent rivers remain underestimated

by remote sensing techniques and are often left out of large studies (Benstead and Leigh 2012; Datry et al., 2014). Global and regional carbon budgets that omit carbon gas efflux from streams may dramatically overestimate the amount of carbon stored through mineralization and in sediments (Johnson et al., 2008, and Richey et al., 2009).

The abundance of small streams and their physical and chemical characteristics make them a potentially important source of carbon to the atmosphere. Crawford et al. (2014) show that streams in a lake abundant environment are consistent sources of CO₂ and CH₄ to the atmosphere due to their supersaturation with respect to the atmosphere. This state of headwater streams being supersaturated with CH₄ and CO₂, with respect to the atmosphere, is widely documented (Teodoru et al., 2009, Billett et al., 2013, Halbedel and Koschorreck 2013, and Wallin et al., 2014), but the magnitude and variability of the processes leading to this state is less well understood.

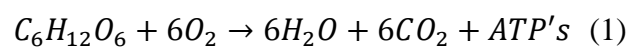
2. Soil to stream: sources of CO₂ and groundwater-stream carbon cycling

In small streams, much of the discharge in low-flow conditions is derived from groundwater, and therefore strongly reflects the geochemical properties of the groundwater. Groundwater chemistry is primarily influenced by the CO₂ produced in soil and the chemical properties of the geologic medium. The length of storage of CO₂ in groundwater and in streams is controlled by several additional factors including hydrogeology and the geomorphologic features of the stream channel. Understanding each of these influencing factors (Figure 3) is crucial to properly budgeting carbon in groundwater and in streams, and to selecting the right method for measuring gas efflux in streams (see 4 Methods for Measuring Gas Transfer).

2.1. Soil CO₂ production

Soils are the main terrestrial environment where CO₂ is produced (Figure 3). Most of the CO₂ produced in soil escapes to the atmosphere through gas efflux at the soil surface (Schlesinger 1984), but a significant fraction of the CO₂ can dissolve into the soil water and recharge aquifers (Kessler and Harvey 2001, Schlesinger and Lichter 2001, Finlay 2003, Johnson et al., 2008, and Tyspin and Macpherson 2012). Over time, this process can lead to concentrations of groundwater CO₂ that exceed atmospheric concentrations by an order of magnitude or more (Macpherson 2009). Concentrations of CO₂ can be spatially and temporally variable depending upon changes in plant and microbial biology, climate, and the hydrogeologic setting. Each of these variables will impact the mechanisms and rates at which CO₂ is created and transported through the vadose zone into aquifers.

Soil CO₂ is created by both plant root respiration (equation (1)), microbial degradation of organic matter, and respiration by soil fauna (Chapelle 2000). Together, root respiration, microbial degradation, and soil faunal respiration are referred to collectively as soil respiration. Plants respire a globally significant amount of CO₂ into soil in accordance with equation (1) (Paul 2014). Generally, plants respire continuously and photosynthesize only during the day. Microbial respiration of CO₂, during the breakdown of subsurface organic matter, is the second main source of CO₂ in soil respiration (Chapelle 2001). Plants extrude significant amounts of carbon compounds to the root zone during photosynthesis (Hütsch et al., 2002). Microbes break down these compounds into CO₂, water, and energy, thus contributing to soil CO₂ content. In addition to plants and microbes, fungi and other soil fauna (ex. nematodes) also contribute to soil respiration by breaking down carbon compounds and respiring CO₂.



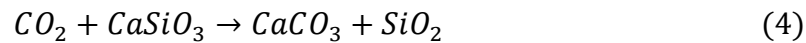
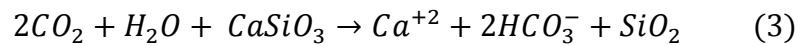
Soil CO₂ production is spatially and temporally variable and depends upon many factors including soil temperature and soil moisture. Soil temperature can speed up or slow down microbial processes and is a significant contributor globally in the production of soil CO₂. Colder temperatures usually yield lower rates of biological activity. Soil moisture also varies widely and often determines the amount of saturated and unsaturated pore space needed for respiration to occur in soils (Ouyang and Zheng, 2000). Generally speaking, soil respiration rates are positively correlated to water availability (Liu et al., 2002 and Wan et al., 2007) until water becomes a limiting factor by filling all unsaturated pore space.

2.2. Geochemical controls on in-stream CO₂ concentrations

The geochemistry of aquifers connected to streams is another key component controlling CO₂ concentrations in streams. Bedrock can serve as either a source or a sink for CO₂ created in the root zone depending upon the chemical composition of the rocks interacting with the groundwater. Soil water percolating to the water table can result in cation exchange and the dissolution of bedrock, which causes a decline in dissolved CO₂ and produces bicarbonate ion. When the groundwater is discharged into streams, it has a lower concentration of CO₂ than was originally present in the soil water as a result of bedrock weathering.

The geochemical composition of the stream channel can also serve as a control on concentrations of in-stream CO₂. Small headwater streams underlain by carbonate rocks should have strongly related concentrations of CO₂, Ca²⁺, and HCO₃⁻ since H₂CO₃ weathering of carbonate rocks is the dominant reaction producing HCO₃⁻. Less available Ca²⁺ means that less CaCO₃ will mineralize (equation (2)). Similarly, silicate weathering is also an important process in the carbon cycle, whereby CO₂ reacts with silicate minerals to produce alkalinity and divalent cations (equation (3)), or CO₂ can be removed from the atmosphere and stored in sedimentary

rocks as shown in equation (4) (Berner 1999, Goudie et al., 2012). Lithology can override other factors like climate and vegetation in creating dissolved loads for rivers, and this influence is also strong in small streams. Likewise, the outgassing of CO₂ can cause stream water to become oversaturated with respect to carbonate minerals causing mineral precipitation (Herman and Lorah 1987).



2.3. Physical hydrogeology

Production and consumption of CO₂ in soil and aquifers are relevant to stream gas efflux due to the physical transport of dissolved chemical constituents through hydrogeologic pathways to streams. The nature of the hydrogeology is an important physical constraint on the movement of CO₂ between the vadose zone, aquifers, and streams. The flow path of water through the vadose zone to the water table in shallow aquifers allows for transport of dissolved CO₂ into groundwater, and the connectivity of the groundwater to streams determines the rates of storage of carbon in shallow aquifers.

Groundwater discharge is the main driver of gas concentrations in streams (Hope et al., 2001, Doctor et al., 2008, Johnson et al., 2008, Sand-Hensen and Staehr 2012, Crawford et al., 2013, Crawford et al., 2014, and Hotckiss et al., 2015). Shallow groundwater concentrations of CO₂ are typically 10 to 100 times the atmospheric concentration (Macpherson et al., 2009), and a significant concentration gradient exists where aquifers discharge into surface water bodies and interact with the atmosphere. Streams that are heavily influenced by groundwater quickly equilibrate with the atmosphere (Johnson et al., 2008). Deep groundwater discharge does not

typically provide CO₂ to low-ordered streams, and shallow groundwater is the main contributor of groundwater derived CO₂ in low-ordered streams (Hotchkiss et al., 2015). This gradient is evident in low-ordered headwater streams where a proportionally larger amount of stream discharge comprises groundwater than in higher-ordered streams. Hotchkiss et al. (2015) estimated that more than 70% of CO₂ evaded from streams was produced terrestrially with the majority of that being from soil respiration in areas hydrologically connected to streams.

Stream-aquifer interaction can be quite complex and may take on many different forms along a single reach (Figure 4). Aquifers can interact with low-ordered streams as a source of water (gaining stream) or as a drain (losing stream). It is also possible that a low-ordered stream does not interact directly with an aquifer at a given point. This conceptual model is further complicated by the fact that changes in stream-stage can modify the stream-aquifer interaction if the hydraulic conductivity of the streambed is spatially variable. For example, it is possible that at a low stream stage a stream cannot interact with the underlying aquifer because the bottom of the streambed consists of a low hydraulic conductivity material. If the stream stage increases, water may then be able to move through more conductive material at a point closer to the top of the streambed.

A stream reach can have multiple types of interactions with an aquifer as described above. Conceptual models of stream-aquifer interactions along a reach are sometimes simplified as an open channel transporting water or as a gaining or losing stream for the entire reach of interest. For many applications, this type of conceptual model is applicable, but in small streams it may be important to take into account small-scale heterogeneities in the physical hydrogeology of a stream reach. Large rivers are proportionally influenced less by groundwater interaction while small streams are heavily influenced by groundwater and this must be taken into account

when examining any geochemical problem. In reality, any small stream represents a complicated environment when trying to interpret groundwater and stream-water interactions in detail (Bear and Cheng 2010).

2.4. Hydrodynamics and geomorphology

Other stream properties that influence the flux of CO₂ from streams include the geomorphic and geometric features of the stream that control degassing rates (Genereux and Hemond 1992 and Raymond et al., 2012). Stream order also correlates with dissolved CO₂ content in the water (Hotchkiss et al., 2015) and the proportion of streamflow derived from groundwater. Headwater streams provide a unique environment where the geomorphology of the stream and the stream order are often conducive to high rates of CO₂ release to the atmosphere. Understanding how a stream is gaining or losing and how this affects degassing rates is most important in understanding the proper method to apply in directly measuring degassing (see 4 Methods for Measuring Gas Transfer).

3. Gas transfer physics overview

Macintyre et al. (1995) provides an excellent in-depth overview of the complex physics involved in gas transfer across the air-water interface. Generally, there are three main pathways through which gas transfer occurs in streams. The first pathway is as bubble ebullition from sediments. This has proven increasingly important for measuring methane (Crawford et al., 2015), but studies have yet to prove it as a significant source of CO₂ in streams. The second pathway is through aquatic life (Hauer and Lamberti 2011, and Hotchkiss et al., 2015). Aquatic respiration can play an important role in headwater and low-ordered streams, so it should be thoroughly considered in any study but is less likely to play an important role in lower-ordered

streams and rivers. In many situations, biological inputs are insignificant when compared to terrestrial inputs in small streams. The third pathway by which gas moves from streams to the atmosphere is by diffusion through the water column. Diffusion is driven by turbulence and is often termed diffusive flux (MacIntyre et al., 1995). Diffusive flux is the dominant means by which gas moves from the dissolved state in small streams to the gas phase in the atmosphere, and it is difficult to quantify with a high degree of accuracy.

Numerous methods exist for obtaining estimates of diffusive flux of gases in aquatic environments (Table 1). Each of these methods works to measure the flux (F) or the gas transfer coefficient (k , also known as the gas transfer velocity), as shown in equation (5), assuming a known atmospheric concentration of the gas in the air above the body of water of interest (C_a) and a known concentration of the gas of interest in the water (C_w). The flux of a gas is proportional to the concentration gradient ($C_w - C_a$) times the gas transfer coefficient (k). Depending on which variable is measured (k or F) you can solve for the remaining variable of interest. Equation (5) is the governing equation for flux of a given gas from a water body to the atmosphere.

$$F = k(C_w - C_a) \quad (5)$$

The gas transfer coefficient is of particular interest because of its dynamic properties. The value of k can be thought of as the height of a column of water at a given temperature that equilibrates with the atmosphere per unit of time. The gas transfer coefficient (k) must be thought of as different from the reaeration coefficient (k_2 ; unit of time^{-1}) used in many stream studies, as it is corrected for depth, and the reaeration coefficient is not.

The gas transfer coefficient is temperature- (Demars and Manson 2013) and density-dependent (Wannikhof 1992) and is usually converted to a k_{600} value (Cole and Caraco 1998).

The k_{600} is calculated to compare values with other gas transfer rates at 20°C. The conversion of k to k_{600} is explained with equation (6) below. The number 600 corresponds with the Schmidt number of CO₂ at 20 °C in freshwater. The Schmidt number (equation (7)) relates diffusivity of gas to viscosity of water as expressed below (ν is the kinematic viscosity of water, and D is the diffusion coefficient for a gas). Kinematic viscosity is the dynamic viscosity divided by the density of the fluid. Dynamic viscosity and density can be found in reference tables like the CRC Handbook of Chemistry and Physics. Diffusion coefficients are determined experimentally or by empirical equations (MacIntyre et al., 1995). A k_{600} value can be calculated when the k and temperature are known for any particular gas by using the ratio of the Schmidt numbers.

$$\frac{k_{600}}{k} = \left(\frac{600}{Sc_{CO_2}} \right)^{-n} \quad (6)$$

$$Sc = \frac{\nu}{D} \quad (7)$$

There are numerous direct and indirect techniques for determining the flux and gas transfer coefficient of headwater streams, and all of these techniques have been used in different environments to varying degrees of success. The following sections will demonstrate the strengths and weaknesses of each technique as well as which methods are optimal to implement in low-ordered headwater streams.

4. Methods for measuring gas transfer

Headwater streams occupy a significant portion of surface area in the conterminous United States, varying between 0.2 to 1.5% of watershed area, with 20% of the total stream surface area considered headwater streams (Butman and Raymond, 2011). Streams and rivers are demonstrated net sources of CO₂ to the atmosphere, and, although estimates have been made (Cole et al., 2007), there has been little effort to directly measure CO₂ gas efflux in these

settings. One reason for this could be the propensity of gas exchange rates between the water and the atmosphere to be error prone (Raymond and Cole, 2001). Other studies (Crawford et al., 2014, Crawford et al., 2013, Sand-Jensen and Staehr, 2012, Hope et al., 2001, Doctor et al., 2008) have also demonstrated evidence that groundwater discharge into streams is necessary to explain observed CO₂ concentrations in streams for many localities. CO₂ content is also strongly influenced by the stream size, and increasing stream size corresponds to decreasing dissolved CO₂ (Finlay 2003, Johnson et al., 2008, and Hotchkiss et al., 2015). This pattern is likely due to the enhanced interaction of smaller streams with groundwater. While studies have been conducted to measure CO₂ flux from a variety of other water bodies (Cole et al., 2010; Kremer et al., 2003, and Matthews et al., 2003) more research is needed with a direct focus on smaller, headwater streams. Recent work has demonstrated how carbon flux in streams could be an important aspect of water and atmospheric chemistry (Halbedel and Koschorreck 2013). However, there is no current method of accurately measuring CO₂ degassing in many of these streams.

4.1. Chambers

The chamber method, using a floating dome, floating helmet, or floating but static chamber, has proven a logistically simple and economic method of measuring gas efflux from lentic and ocean systems (Kremer et al., 2003 and Cole et al., 2010). However, controversy remains about the chamber's accuracy under certain conditions (Matthews et al., 2003, and Vachon et al., 2010), and limited testing has been conducted on its effectiveness in a shallow, turbulent, lotic environment (Lorke et al., 2015). Despite a lack of developed evidence supporting use of chamber-based techniques, there have been numerous attempts to utilize chamber methodologies to measure carbon gas fluxes (CO₂ and CH₄) in environments with

flowing-turbulent water (Crawford et al., 2013, Campeau et al., 2014, Campeau and Giorgio, 2014, Crawford et al., 2014, Billett et al., 2015, and Müller et al., 2015).

The floating chamber method involves placing a gas impermeable container that is sealed onto the surface of the water body of interest and supporting the chamber with some sort of buoyant floatation device on the exterior of the device. The chamber must maintain a seal with the surface of the water for the duration of the measurement (usually five minutes or more). As soon as the chamber is placed onto the surface of the water gas concentration samples must be taken periodically beginning at time zero. Two general methods apply when collecting the periodic gas samples. In the first method, the gas is pumped through a field portable gas analyzer (usually an Infrared Gas Analyzer), and recirculated to the chamber. This method provides a high temporal resolution measurement of gas concentrations for the duration of the experiment, and the gas recirculation avoids causing any significant pressure changes during the duration of the experiment. In the second method, which is less costly, gas samples are drawn from the chamber and injected into a pre-evacuated cylinder. The samples are then processed in the laboratory by gas chromatography. A similar method, suspending a chamber in the water as opposed to allowing it to float, has also been applied in small streams (Crawford et al., 2013, and Crawford et al., 2014).

The data collected during the allotted period is then plotted with time on the abscissa and concentration on the ordinate (Figure 5). Using a linear regression model to build a best-fit curve, the equation for the curve can then be used to determine the rate of accumulation (Figure 5), or the flux, of a particular gas into the chamber from the water body of interest. This accumulation rate can be converted to a flux, using equation (8). The flux measured by the chamber (F_{chamber}) is in $\mu\text{mol m}^{-2} \text{s}^{-1}$ is equal to the slope of the fitted curve ($\frac{dc}{dt}$) in $\mu\text{mol mol}^{-1} \text{s}^{-1}$

for the floating chamber measured concentrations over time. Pressure (p) is the pressure in Pa inside the chamber, the chamber volume (V) is the chamber volume in m^3 , R is the universal gas constant, T_{KA} is the temperature of the air Kelvin, and A is the floating chamber surface area in m^2 (Müeller et al., 2015).

$$F_{chamber} = \frac{dc}{dt} \left(\frac{pV}{RT_{KA}A} \right) \quad (8)$$

Most researchers apply a linear regression technique; however there is also some debate as to the most appropriate regression technique. Silva et al. (2015) provides a thorough analysis of regression techniques applied to chambers, and shows that linear regression can underestimate fluxes by between 10 and 50%. Silva et al. (2015) further suggests the use of a non-linear regression method (a quadratic regression model) instead of the linear regression should be used situationally depending on which regression R^2 value was greater (linear or quadratic). Contrary to this study, Matthews et al. (2003) suggests that linear regression overestimates the flux if the temperature of the chamber gas changes over time and is not compensated for in other calculations. Linear regression likely works in many circumstances at early times in data collection (Anthony et al., 1995) and is used in many studies (Matthews et al., 2003, Alin et al., 2011, Campeau et al., 2014); however, at late times in data collection it may be best to use a non-linear method. This suggests that diffusive gas flux into chambers is not linear but may be approximated as such at early times. The non-linearity results from the fact that the chamber-measured diffusive flux is dependent on the concentration difference between the water and the air inside of the chamber. Because this concentration difference will become smaller over time, it does not follow a linear trend (Cole et al., 2010).

There has been some research into the specific design characteristics to address critiques of the floating chamber's accuracy, and many different designs have been employed to fit the

particular needs of projects. Different chamber designs have been shown to provide differing results (Lambert et al., 2005), so special attention should be paid to chamber design. Sealing the chamber onto the surface of the water creates a microenvironment inside the chamber, so many of the designs try to replicate the conditions of the actual environment which is being measured. Increasing temperature due to solar radiation or decreasing wind shear on the water surface by covering it with a chamber can decrease the measured flux from a water surface. Studies have combatted these issues by covering the outside of the chamber with reflective material to minimize solar heating (Vachon et al., 2010, Lambert et al., 2005), painting the chamber white to reduce heating (Sand-Jensen et al. 2012), and placing a small fan inside of the chamber to replicate the wind shear on the water of the exterior environment (Sebacher et al., 1983). In sheltered riparian headwater stream environments, solar radiation and wind shear do not often play as large a role as in studies of less sheltered lentic systems. In turbulent environments, it is also important to regulate the bobbing motion of the floating chamber as this can cause pressure and volume fluctuations during the course of a measurement. In high turbulence environments, it is also possible for the chamber to break the seal with the water surface if it is not properly supported against this occurrence.

The two main schools of thought about the detrimental characteristics of chamber deployment in streams are 1) the chamber overpredicts the flux from streams because it induces artificial turbulence as flowing water collides with the sides of the chamber, or 2) the chamber is difficult to deploy in areas where gas transfer is highest (Krenz et al., 2013). Gas transfer is typically highest in the areas of the stream that are the most shallow and turbulent. This deployment issue causes an underestimation of fluxes from streams. Cole et al. (2010) provide a brief warning against using the floating chamber design in an environment with flowing-water:

“...these chambers are not designed for use in flowing waters”. Despite this warning, numerous studies continue to implement chamber based designs in streams (Alin et al., 2011, Crawford et al. 2013, Crawford et al. 2014, Campeau et al., 2014, Sand-Jensen et al., 2012), and rivers (Beaulieu et al., 2012, and Teoduru et al., 2015).

Users of the chamber in oceanographic environments were the first to question and test the floating chamber for artificially high flux measurements due to chamber-induced turbulence. Many of the recommendations from these studies could prove useful for researchers designing their own versions of the chamber for use in streams. Vachon et al. (2010) provide quantitative evidence that chambers in a lake environment actually induce turbulence as the chamber moves on the surface of the water, and chambers can overestimate gas fluxes by several hundred percent in this type of environment. This study also finds that using the floating chamber is most problematic in calm environments and less of an issue when the water is already moving. The chamber is more biased towards high measurements in calm environments because the chambers' movement on the surface of the water causes a disturbance that is more turbulent relative to the natural state of the water. Other studies qualitatively agree that floating chambers placed on the surface of the water (not reaching into the water column) create more disturbance to the air-water interface than those that are submerged several centimeters into the water (Lambert et al., 2005). Vachon et al. (2010) also suggests that the bottom of the chamber be sealed at least six centimeters below the surface of the water, an unreasonable solution for shallow headwater streams. Matthews et al. (2003) suggest that not having the chamber deployed with its edges below the surface of the water, and instead even with the top of the water, may cause chambers to overestimate fluxes by three to five times in a lotic environment. Campeau et al. (2014) visually observes that chambers likely add bias to flux estimates in streams by

disturbing the water surface and level of turbulence, but to date no study has quantified this disturbance.

Despite the possible concerns of the floating chamber method, some research has provided solutions to improve floating chamber accuracy. MacIntyre et al. (1995) reports that “minimizing the height of the box” used to construct the chamber can allow greater concentration changes to be observed over time, which will improve the accuracy of the measurement. Guerin et al. (2006) measures emissions from rivers downstream of a tropical reservoir using a floating chamber deployed from a small boat. During the course of this study, the small boat and chamber were left drifting to avoid pushing the chamber against the water turbulence. Lorke et al. (2015) tests this method and finds that anchoring the chamber in place allows for comparatively higher flux measurement. Although this technique does hold some promise, it is still not a viable option for many smaller streams that are not navigable.

Krenz et al. (2013) examined CO₂ emissions from a boreal watershed in Sweden and used the floating chamber technique on both lakes and streams. They found the floating chamber to be generally unsuitable due to limitations in chamber placement in the stream reaches. Other authors argue that floating chambers underestimate emission rates because they actually reduce surface water turbulence inside of the chamber and remove the effect of wind (MacIntyre et al., 1995 and Billet and Moore 2008). Recently, Crawford et al. (2014) note the likely effect of chamber bias but state that this uncertainty is difficult to quantify and must be more thoroughly studied. This literature summary suggests that a floating chamber should be used with caution if applied in streams, but it should not be ruled out for this type of study.

Despite the possible limitations described above, researchers continue to use the floating chamber method because of its many advantages. MacIntyre et al. (1995) states that the chamber

method actually removes uncertainty in measured fluxes that is often present with many indirect measurements (such as wind derived values for k), but the method is limited during high winds in highly turbulent waters, or circumstances where excessive heating from solar insolation occurs. When MacIntyre et al. (1995) published this review they did not account for limitations of chamber deployments in flowing water, but their limitations still hold true for chambers used in streams. The largest advantage of the floating chamber is that it is logistically simple to deploy and it collects a direct measurement of gas flux at a point. The value of point measurements is especially advantageous in headwater streams because of sporadic groundwater interactions that other methods are not able to characterize fully. The chamber provides an easy to use technique at low cost (Mazot and Bernard, 2015). Although the results have not yet been quantified in streams, previous studies (Cole et al., 2010) show that careful application of the chamber technique yields results comparable to trusted methods in lakes.

4.2. Tracers

Gas transfer rates in streams and rivers can be measured indirectly using a gas-tracer method. The tracer method involves the addition of a volatile tracer gas at an upstream point and monitoring the change in concentration of the gas along the stream reach of interest. The gas exchange rate is then calculated as an average rate for the entire reach of interest based on the dissipation of the tracer gas. Propane and sulfur hexafluoride (SF_6) are two common gases that are used as volatile tracers. The tracer methodology has been used in lotic systems varying from large rivers (MacIntyre et al., 1995) to first order streams (Wannikhof et al., 1990) and is widely accepted as a gas transfer methodology in lakes (Cole et al., 2010). The degassing rate of the volatile tracer is proportional to the degassing rate of a given gas of interest by the ratio of the Schmidt numbers.

The k for a gas of interest can be calculated when you know the k for any particular gas and the temperature by using the ratio of the Schmidt numbers (equation (9)). The value for n (a fitting parameter) can vary between 1.00 and -0.66 (MacIntyre et al., 1995).

$$\frac{k_{tracer}}{k_{gas2}} = \left(\frac{Sc_{tracer}}{Sc_{gas2}} \right)^n \quad (9)$$

One of the greatest pitfalls of the application of the tracer method in small streams is that it fails to take into account groundwater inflow and groundwater concentrations of various gases of interest (Webster and Meyer 1997) or streamflow loss in losing streams, and a conservative tracer must be used in conjunction with the volatile tracer. For the application of the tracer method, Hauer and Lamberti (2011) suggest avoiding stretches of streams with a proportionally large influx from groundwater or water from lateral tributaries. A conservative tracer is often used in tandem with the volatile tracer gas when it is impossible to avoid sources of inflow. Examples of conservative tracers include tritium (Wannikohf et al., 1990), rhodamine dye (Runkel 2015), sodium bromide (Edwardson et al., 2003), and sodium chloride (Mallard et al., 2015). The amount of dilution of the conservative tracer provides an estimate of groundwater flux into the stream. Stream reaches for conservative tracer studies can be several kilometers long, so the distribution of the conservative tracer is carefully monitored over time. The first and last appearances of the dye are noted, while regular timed measurements record the peak dye concentration in the stream. The stream reach can also be segmented, provided enough personnel are present to conduct the experiment.

Despite the use of conservative tracers, groundwater inflow is a notoriously difficult parameter to measure accurately (McCallum et al., 2012). The conservative tracer concentration can diminish at a point in time due to dispersion of the tracer in the stream, lateral inflow from surface water and groundwater, any other losses due to gas exchange, hyporheic exchange, or

sorption. The non-ideal nature of degassing in streams limits the effectiveness of the tracer method in streams and makes properly parameterizing the processes causing tracer dilution to be a challenge (Knapp et al., 2015).

Using the tracer method in a reach with groundwater inflow can yield overestimations of gas transfer in streams. Research has found that it is vital to account fully for the groundwater volume and concentration of important gases in groundwater entering the reach (McCutchan et al., 2002, and Hall and Tank 2005). It has been demonstrated that groundwater flux into a stream can significantly impact the concentration of gases in a stream (Choi et al., 1998), and can be a significant source of dissolved organic matter (Tank et al., 2010) that stream carbon budgets often ignore. Groundwater flux and concentrations along a stream study reach may also be heterogeneous (Bear and Cheng 2010), and an infrastructure of wells in hydrologic contact with the stream must be in place to provide for more accurate measurements of gases in groundwater and their discharge into streams.

In summary, the use of tracers for measuring gas exchange in streams is considered an adequate means of measuring degassing in some streams but depends largely upon the hydrogeologic setting for its accuracy and usability. Complex hydrogeologic settings involving changing interactions between the stream and groundwater, hyporheic exchange, or variable dissolved gas concentrations in groundwater can all prove problematic with tracer methods. Quantifying the precise rates at which the conservative gas is injected into the stream is also difficult (Benson et al., 2014). Additionally, the tracer method often releases gases to the environment (SF_6) that are powerful greenhouse gases, and should not be used extensively (Gålfalk et al., 2013 and Benson et al. 2014). Other drawbacks to the tracer method include its

tendency to be time-consuming, labor intensive, and expensive; however, it is considered effective in areas with minimal groundwater inflow.

4.3. Wind speed

Indirect measurements of gas transfer can be inferred by collecting wind speed measurements and applying empirical models to estimate k for a system. The wind speed in these models is essentially used as a proxy for the turbulent energy at the water surface (Cole et al., 2010). This type of model has been improved upon since the mid-1980s for use in lakes, estuaries, oceans, and rivers (Wanninkhof et al., 1985, Alin et al., 2011, and Striegl et al., 2012) but has potentially severe limitations for use in small and wind-sheltered environments (Cole et al., 2010). The degassing rate in headwater streams is directly related to the turbulence at the water surface. Contrary to lakes or oceans, where many wind derived k models were developed, headwater streams are sheltered riparian environments that are often incised below the surrounding topography by erosional processes. In-stream hydrogeomorphic factors more likely dominate gas transfer processes in headwater streams. It has been demonstrated that gas transfer is independent of wind speeds at velocities recorded in headwater-stream environments (Occampo-Torres et al., 1994), but other studies have shown that wind-derived values for k may be inappropriate for headwater streams (Liu et al., 2013). Given the nature of wind derived gas transfer methodologies, they are unlikely to provide accurate estimations for gas transfer in headwater streams.

4.4. Hydrogeomorphology

Equations based upon hydrogeomorphic variables are another method used to provide an indirect measured estimate of the stream k (Cox 2003). The predictive equations for k commonly include measurements of water velocity, water depth, and channel slope. Equations are also

sometimes known to contain additional variables to describe the bed-roughness, geomorphology (Froude number or friction velocity), the difference in elevation between the ends of a reach of interest, or the travel time of a packet of water through a reach (Parker and Gray 1987). Various predictive equations describing gas transfer have been proposed for almost one hundred years (Streeter and Phelps 1925, Tsivoglou and Neal 1976, and Raymond et al., 2012) but no equation has yet effectively scaled to streams of all sizes. This is especially true in small headwater streams where groundwater discharge is the dominant source of dissolved gases (Raymond et al., 2012).

Predictive equations are appealing because of the apparent potential to easily scale across large geographic areas, but accurate scaling is not possible with current models. It is possible that with geospatial data improving in resolution, and with continued in situ measurements of gas transfer, that models based on predictive equations could one day yield more accurate estimates. Further research is also needed to better understand which parameters dominate gas transfer at a particular site, and therefore, which equation is applicable in a particular type of setting. Currently, there is no “one-size fits all” equation for headwater streams, and direct measurements are needed to validate any mathematical model and reduce uncertainties.

4.5. Others

Several studies have assessed CO₂ degassing from streams by calculating the excess CO₂ present in river water that was originally sourced from groundwater (Jones and Mulholland, 1998, Neal et al., 1998, Neal et al., 2002, Worrall and Lancaster, 2005, and Worrall et al., 2007), using river and groundwater chemistry. The “excess CO₂” method essentially involves a calculated value of the equilibrium partial pressure of CO₂ for a given water concentration and compares it to the CO₂ content of the entire river system (equation (10)). All streamwater CO₂

that is not used in ecosystem productivity, and that is not transported downstream, is assumed to be lost to the atmosphere through CO₂ degassing as the streamwater equilibrates. This “excess CO₂” method assumes degassing to equilibrium saturation with respect to the atmosphere, although measurements of stream and river chemistry invariably show that they are not in equilibrium with the atmosphere, with respect to CO₂ (e.g., Szramek and Walter, 2004). In situ measurements may underestimate fluxes because they fail to account for the highest concentrations of CO₂ at the groundwater source, due to limited groundwater samples. The challenges of using water chemistry to infer CO₂ degassing, then, are that this approach requires an extensive chemical database to create accurate models for watershed scale studies, and that the model must make some assumptions about the distribution and sourcing of chemical species that are likely to be oversimplified. If enough data are available, the excess CO₂ method may be a good “first cut” at determining carbon fluxes from streams for a given watershed.

$$Excess\ CO_2 = \frac{CO_{2\text{water}}}{CO_{2\text{equilibrium with atmosphere}}} \quad (10)$$

The methods listed previously are conventional approaches to measuring gas efflux in streams. An unconventional method, using sound pressure correlation, may hold promise as a reliable and cheap means of obtaining estimates of degassing. Morse et al., (2007) recorded the sound pressure along a stream reach and uses this as a proxy for in-stream turbulence. The magnitude of the sound pressure correlated with reaeration results from a simultaneous tracer gas release yielding an equation to predict the rate of gas transfer based on the sound magnitude of the stream. Correlating sound pressure with gas transfer is appealing because of the ease of application, relatively cheap cost compared to other methods, and widespread possibility for application. Further testing is needed to validate the sound pressure method of estimating

reaeration in different types of stream environments, and the method requires an area with a low noise pollution level.

5. Selecting a methodology

A review of the literature reveals that the importance of hydrogeologic influence in small streams is often overlooked and oversimplified despite its importance in selecting an appropriate method for measuring gas efflux. The apparent lack of comprehension of the effects of hydrogeology in small streams may distort estimates provided for these systems. The unique environment of small streams necessitates careful selection of methods necessary to obtain accurate measurements of gas efflux. Due to the complex nature of stream and groundwater interactions, they are often overlooked or simplified for this type of study. Many scientists have employed a flawed conceptual model of smaller streams that does not fully account for groundwater inflow and other spatially heterogeneous characteristics of the stream.

As noted, several methods currently exist for measuring the same gas transfer properties of streams, although they are not always applied appropriately. Taking into account what is known or unknown about the stream-aquifer hydrology is crucial to selecting the proper methodology. Although the connection of a stream reach with groundwater should be considered, it is not the only factor limiting which methodology should be utilized. Other considerations discussed earlier in this paper include the accessibility of the reach of interest, the level of turbulence in the stream, and the budget of a given project.

Weighing only the hydrology of a stream reach and ignoring alternative considerations allows us to demonstrate two general scenarios where the tracer method is not applicable and where the tracer method is applicable. It is best to apply methods other than the tracer method in streams that are gaining with a large proportion of discharge derived from groundwater (more

than 20%), streams where the hydrologic connection with the aquifer is not well understood, or streams that can be both gaining and losing along different stream segments and at different points in the discharge curve. A large number of the small headwater streams fall into the category where the tracer method should not be used. Specifically, chamber-based methodologies and the sound pressure correlation method can be used where groundwater inflow to stream segments is significant and should be used in place of the tracer method in this scenario. The tracer method is applicable in gaining streams with a small proportion of flow derived from groundwater discharge (less than 20% of discharge) or a losing stream. Chamber-based methodologies and the sound pressure correlation method may also be applicable in this scenario as they are not mutually exclusive to a single stream type.

Several additional methods discussed in this paper include wind-based equations, the excess CO₂ method, and hydrogeomorphic equations. Wind-based equations are not applicable for measurement of degassing in headwater streams because this type of stream is usually wind-sheltered and hydrogeomorphic variables dominate atmospheric exchange rates. The excess CO₂ method may be a useful method for rough estimates of regional CO₂ inputs from inland waters but it requires an extensive geospatial database that is impractical for many research projects, and the fundamental assumption that rivers come into equilibrium with atmospheric CO₂ will likely overestimate degassing rates. Hydrogeomorphic equations have proven to be largely site specific, so until these equations are better defined for use in heterogeneous headwater streams, they should be used with caution and with an appropriate estimate of error.

6. Future research

Future investigation into the potential error associated with the discussed methods should be pursued to validate the use of the floating chamber, sound pressure correlation, and

hydrogeomorphic equations in small streams. Validating the accuracy of floating chamber measurements for use in small streams with flowing water should be established. Additionally, comparative studies between the various methods in headwater stream environments would prove useful. The cost effective nature of the floating chamber, and its ability to incorporate hydrogeologic differences, make it an extremely viable option. Sound pressure correlation also provides a promising and economically viable alternative for measuring atmospheric exchange rates, but to date, has only been used and verified in one study (Morse et al., 2007), and requires further development for widespread use in many different environments. Hydrogeomorphic equations have a tremendous potential upside if they are scalable but have proven to be largely site specific. As more comprehensive geospatial datasets, with higher spatial resolution data, continue to become available, more steps should be taken to pursue the application of mathematical models of gas efflux based on hydrogeomorphic variables.

It has been thoroughly demonstrated (Teodoru et al., 2009, Billett et al., 2013, Halbedel and Koschorreck 2013, and Wallin et al., 2014) that many small streams are more than just conduits transporting carbon downstream, but instead are complex systems which can emit significant amounts of carbon to the atmosphere. Accurate measurement of gas transfer in small streams is necessary to obtain reasonable estimates for use in carbon budgets. A crucial challenge for researchers is to limit the potential error inherent with each method for estimating atmospheric exchange rates and incorporate these into carbon budgets built using these methods. In order to apply the proper method in any given stream, scientists need to fully understand the hydrogeologic connection of the stream with groundwater.

TablesTABLE 1. METHODS FOR MEASURING CO₂ DEGASSING

Method Name	Source(s)
Chambers	Crawford et al., 2014
Chemical Tracers	Genereux and Hemond, 1992
Hydrogeomorphic Equations	Raymond et al., 2012, Owens et al., 1964, and Streeter and Phelps 1925
Wind-based Equations	Cole et al., 2010
Excess CO ₂	Neal et al., 1998
Sound Pressure Correlation	Morse et al., 2007

Figures

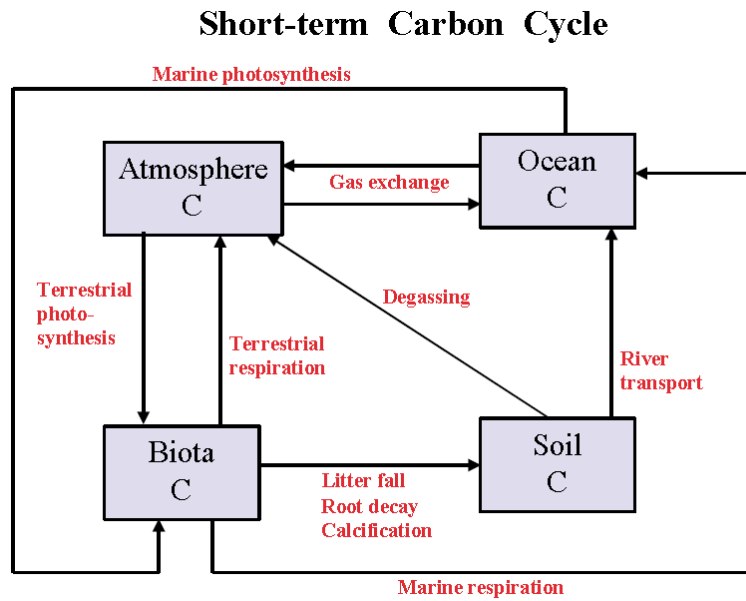


Figure 1. Box diagram showing the short-term carbon cycle adopted from Berner (1999). Boxes represent reservoirs, and arrows represent fluxes between reservoirs.

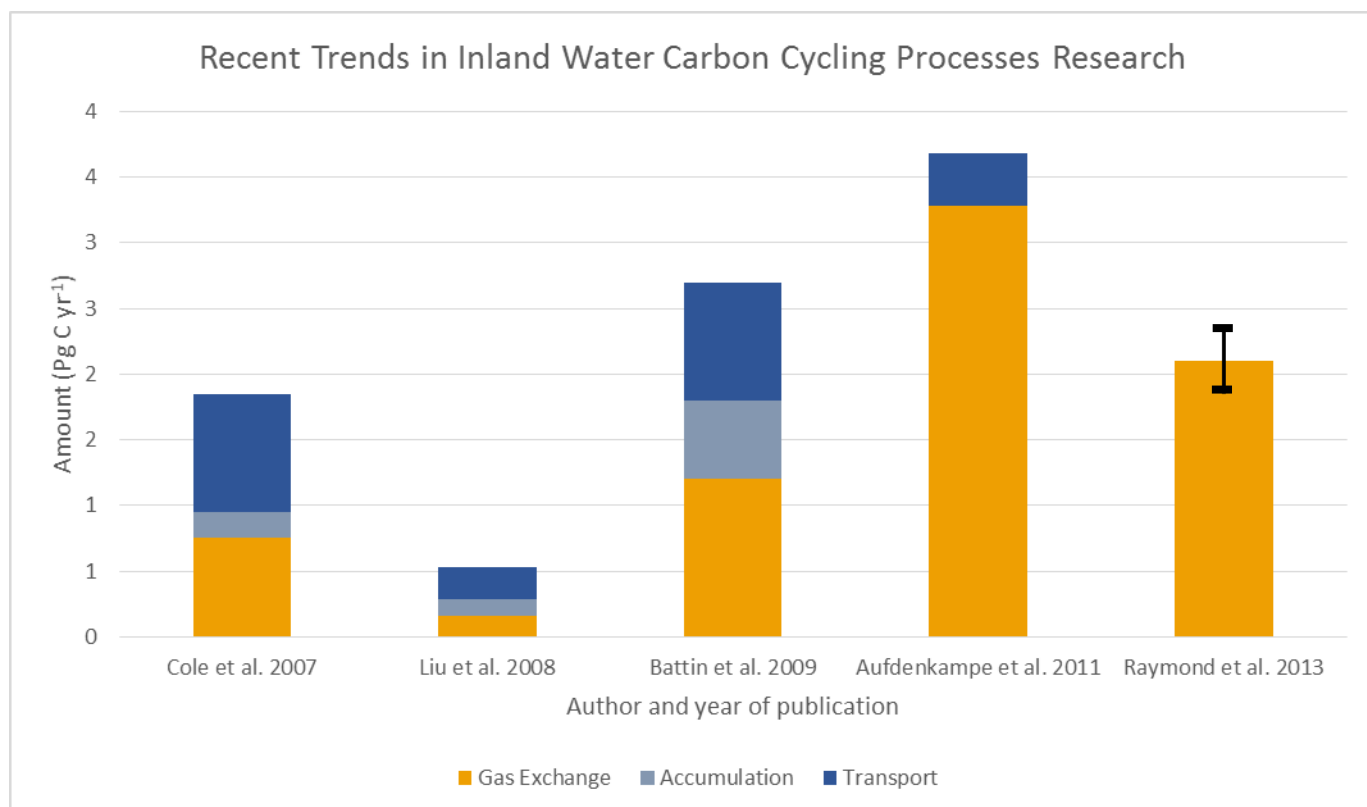


Figure 2. Recent estimates of the distribution of fluxes in carbon cycle research in inland waters are presented in the figure above. Global estimates of gas exchange between inland waters and the atmosphere are expressed as dark yellow bars, accumulation through mineralization and burial in sediments is expressed in light blue, and transport via rivers to the ocean is expressed in dark blue.

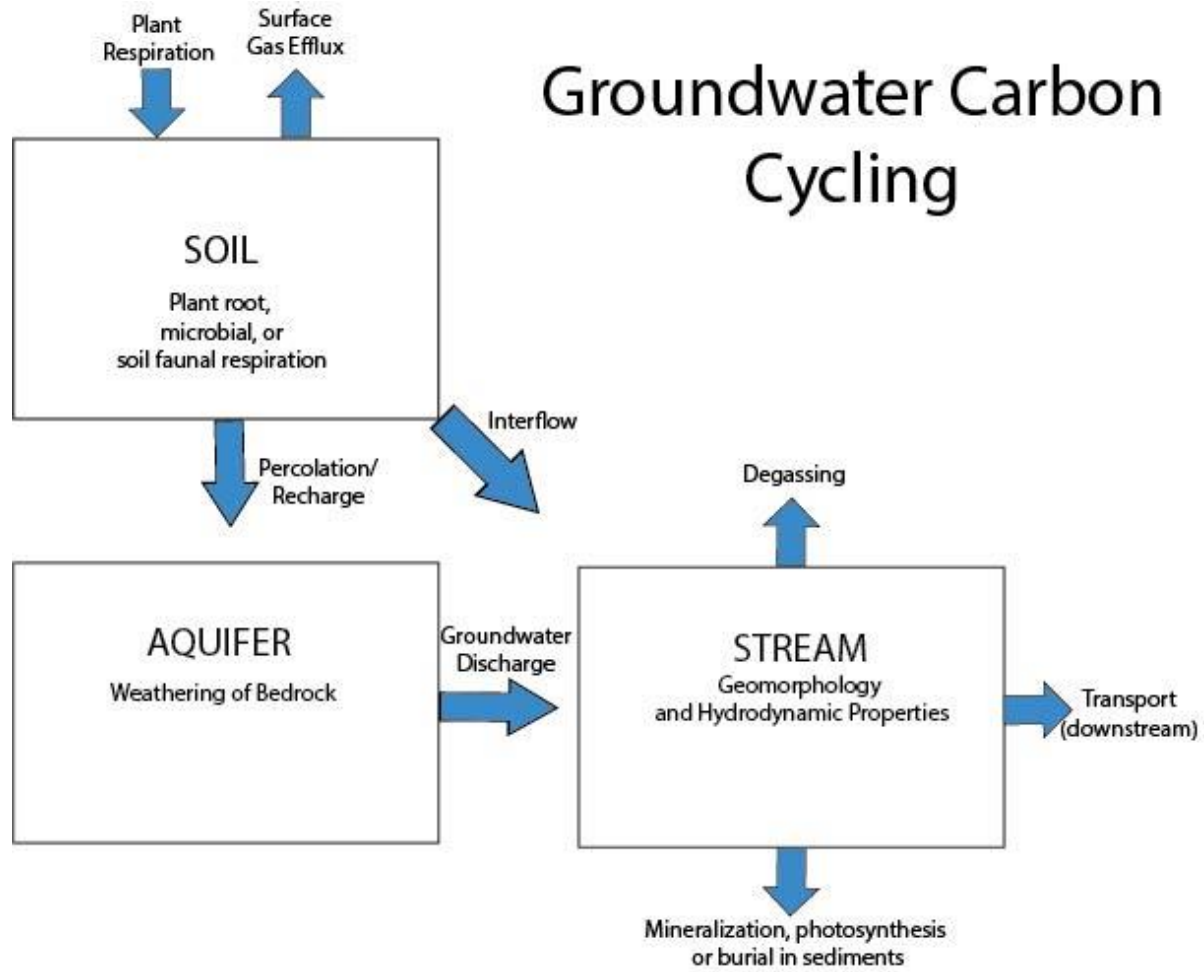


Figure 3. Conceptual model of the production and movement of CO₂ in small headwater streams. Modified from Jones and Mulholland 1998. Boxes and capitalized words describe reservoirs, arrows describe fluxes of CO₂, and wording inside of boxes describes transformative processes.

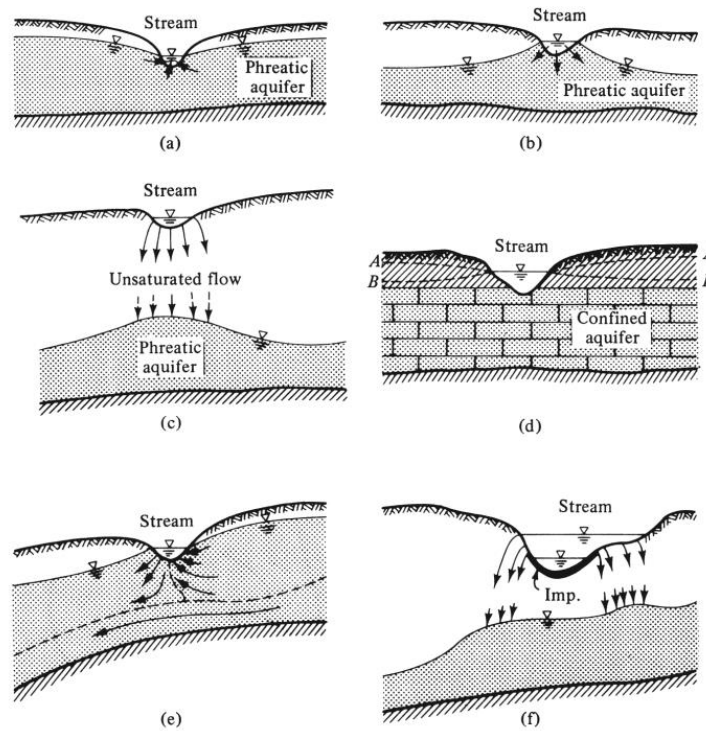


Figure 4. Diagram showing the varied interactions between surface water in streams and groundwater. Adapted from Bear and Cheng 2010. (a) Gaining stream (b) Losing stream. (c) Losing stream (deep water table). (d) Losing stream (piezometric surface B), or gaining stream (piezometric surface A) intersecting a confined aquifer. (e) A stream which is both losing and gaining. (f) A partly clogged losing stream.

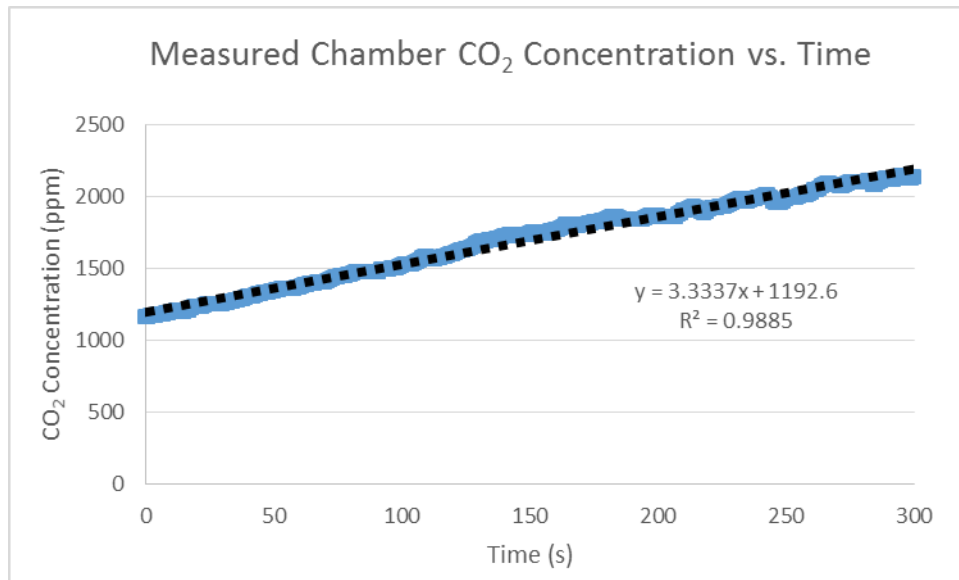


Figure 5. Example of typical concentration change inside of a floating chamber. Note that this chamber was being measured in a laboratory experiment with a high ambient CO₂ level which is why the intercept of the line is higher than typical atmospheric concentrations of CO₂.

References

- Anthony, W., Hutchinson, G., and Livingston, G., 1995, Chamber measurement of soil-atmosphere gas exchange: Linear vs. diffusion-based flux models: *Soil Science Society of America Journal*, v. 59, no. 5, p. 1308-1310.
- Alin, S. R., de Fátima FL Rasera, M., Salimon, C. I., Richey, J. E., Holtgrieve, G. W., Krusche, A. V., and Snidvongs, A., 2011, Physical controls on carbon dioxide transfer velocity and flux in low-gradient river systems and implications for regional carbon budgets: *Journal of Geophysical Research: Biogeosciences (2005–2012)*, v. 116, no. G1.
- Bear, J., and Cheng, A.-D., 2010, *Modeling groundwater flow and contaminant transport*, Springer, p. 97-100.
- Beaulieu, J. J., Shuster, W. D., and Rebbholz, J. A., 2012, Controls on gas transfer velocities in a large river: *Journal of Geophysical Research*, v. 117, no. G2007.
- Benson, A., Zane, M., Becker, T. E., Visser, A., Uriostegui, S. H., DeRubeis, E., Moran, J. E., Esser, B. K., and Clark, J. F., 2014, Quantifying reaeration rates in alpine streams using deliberate gas tracer experiments: *Water*, v. 6, no. 4, p. 1013-1027.
- Benstead, J. P., and Leigh, D. S., 2012, An expanded role for river networks: *Nature Geoscience*, v. 5, p. 678-679
- Berner, R. A., 1999, A new look at the long-term carbon cycle: *GSA Today*, v. 9, no. 11, p. 1-6.
- Berner, R. A., 2004, *The Phanerozoic carbon cycle: CO₂ and O₂*, Oxford University Press.
- Billett, M., and Harvey, F., 2013, Measurements of CO₂ and CH₄ evasion from UK peatland headwater streams: *Biogeochemistry*, v. 114, no. 1-3, p. 165-181.

- Billett, M., Garnett, M., and Dinsmore, K., 2015, Should Aquatic CO₂ Evasion be Included in Contemporary Carbon Budgets for Peatland Ecosystems? : *Ecosystems*, v. 18, no. 3 p. 471-480.
- Billett, M., and Moore, T., 2008, Supersaturation and evasion of CO₂ and CH₄ in surface waters at Mer Bleue peatland, Canada: *Hydrological Processes*, v. 22, no. 12, p. 2044-2054.
- Butman, D., and Raymond, P. A., 2011, Significant efflux of carbon dioxide from streams and rivers in the United States: *Nature Geoscience*, v. 4, no. 12, p. 839-842.
- Campeau, A., and Giorgio, P. A., 2014, Patterns in CH₄ and CO₂ concentrations across boreal rivers: Major drivers and implications for fluvial greenhouse emissions under climate change scenarios: *Global change biology*, v. 20, no. 4, p. 1075-1088.
- Campeau, A., Lapierre, J. F., Vachon, D., and Giorgio, P. A., 2014, Regional contribution of CO₂ and CH₄ fluxes from the fluvial network in a lowland boreal landscape of Québec: *Global Biogeochemical Cycles*, v. 28, no. 1, p. 57-69.
- Chapelle, F., 2001, *Ground-water microbiology and geochemistry*, John Wiley & Sons, p. 304.
- Chapelle, F. H., 2000, The significance of microbial processes in hydrogeology and geochemistry: *Hydrogeology Journal*, v. 8, no. 1, p. 41-46.
- Choi, J., Hulseapple, S., Conklin, M., and Harvey, J., 1998, Modeling CO₂ degassing and pH in a stream-aquifer system: *Journal of Hydrology*, v. 209, no. 1, p. 297-310.
- Cole, J. J., and Caraco, N. F., 1998, Atmospheric exchange of carbon dioxide in a low-wind oligotrophic lake measured by the addition of SF₆: *Limnology and Oceanography*, v. 43, no. 4, p. 647-656.
- Cole, J. J., Prairie, Y. T., Caraco, N. F., McDowell, W. H., Tranvik, L. J., Striegl, R. G., Duarte, C. M., Kortelainen, P., Downing, J. A., Middelburg, J. J., and Melack, J., 2007, Plumbing

- the Global Carbon Cycle: Integrating Inland Waters into the Terrestrial Carbon Budget: *Ecosystems*, v. 10, no. 1, p. 172-185.
- Cole, J. J., Bade, D. L., Bastviken, D., Pace, M. L., and Van de Bogert, M., 2010, Multiple approaches to estimating air-water gas exchange in small lakes: *Limnology and Oceanography: Methods*, v. 8, p. 285-293.
- Cox, B., 2003, A review of dissolved oxygen modelling techniques for lowland rivers: *Science of the Total Environment*, v. 314, p. 303-334.
- Crawford, J. T., Lottig, N. R., Stanley, E. H., Walker, J. F., Hanson, P. C., Finlay, J. C., and Striegl, R. G., 2014, CO₂ and CH₄ emissions from streams in a lake-rich landscape: Patterns, controls, and regional significance: *Global Biogeochemical Cycles*, v. 28, no. 3, p. 197-210.
- Crawford, J. T., Dornblaser, M. M., Stanley, E. H., Clow, D. W., and Striegl, R. G., 2015, Source limitation of carbon gas emissions in high-elevation mountain streams and lakes: *Journal of Geophysical Research: Biogeosciences*. v. 118, p. 1-14
- Crawford, J. T., Striegl, R. G., Wickland, K. P., Dornblaser, M. M., and Stanley, E. H., 2013, Emissions of carbon dioxide and methane from a headwater stream network of interior Alaska: *Journal of Geophysical Research: Biogeosciences*, v. 118, no. 2, p. 482-494.
- Datry, T., Larned, S. T., and Tockner, K., 2014, Intermittent Rivers: A Challenge for Freshwater Ecology: *BioScience*, v. 64, no. 3, p. 229-235.
- Demars, B., and Manson, J., 2013, Temperature dependence of stream aeration coefficients and the effect of water turbulence: A critical review: *Water research*, v. 47, no. 1, p. 1-15.
- Doctor, D. H., Kendall, C., Sebestyen, S. D., Shanley, J. B., Ohte, N., and Boyer, E. W., 2008, Carbon isotope fractionation of dissolved inorganic carbon (DIC) due to outgassing of

- carbon dioxide from a headwater stream: *Hydrological Processes*, v. 22, no. 14, p. 2410-2423.
- Edwardson, K. J., Bowden, W. B., Dahm, C., and Morrice, J., 2003, The hydraulic characteristics and geochemistry of hyporheic and parafluvial zones in Arctic tundra streams, north slope, Alaska: *Advances in Water Resources*, v. 26, no. 9, p. 907-923.
- Finlay, J. C., 2003, Controls of streamwater dissolved inorganic carbon dynamics in a forested watershed: *Biogeochemistry*, v. 62, no. 3, p. 231-252.
- Gålfalk, M., Bastviken, D., Fredriksson, S., and Arneborg, L., 2013, Determination of the piston velocity for water-air interfaces using flux chambers, acoustic Doppler velocimetry, and IR imaging of the water surface: *Journal of Geophysical Research: Biogeosciences*, v. 118, no. 2, p. 770-782.
- Genereux, D. P., and Hemond, H. F., 1992, Determination of gas exchange rate constants for a small stream on Walker Branch Watershed, Tennessee: *Water Resources Research*, v. 28, no. 9, p. 2365-2374.
- Goudie, A. S., and Viles, H. A., 2012, Weathering and the global carbon cycle: geomorphological perspectives: *Earth-Science Reviews*, v. 113, no. 1, p. 59-71.
- Guérin, F., Abril, G., Richard, S., Burban, B., Reynouard, C., Seyler, P., and Delmas, R., 2006, Methane and carbon dioxide emissions from tropical reservoirs: significance of downstream rivers: *Geophysical Research Letters*, v. 33, no. 21., p. 161-172.
- Guérin, F., Abril, G., Serça, D., Delon, C., Richard, S., Delmas, R., Tremblay, A., and Varfalvy, L., 2007, Gas transfer velocities of CO₂ and CH₄ in a tropical reservoir and its river downstream: *Journal of Marine Systems*, v. 66, no. 1-4, p. 161-172.

- Halbedel, S., and Koschorreck, M., 2013, Regulation of CO₂ emissions from temperate streams and reservoirs: *Biogeosciences*, v. 10, no. 11, p. 7539-7551.
- Hall, R. O., and Tank, J. L., 2005, Correcting whole-stream estimates of metabolism for groundwater input: *Limnology and Oceanography: Methods*, v. 3, p. 222-229.
- Hall, R. O., and Tank, J. L., 2005, Correcting whole-stream estimates of metabolism for groundwater input: *Limnology and Oceanography: Methods*, v. 3, p. 222-229.
- Hauer, F. R., and Lamberti, G. A., 2011, *Methods in stream ecology*, Academic Press, p. 203.
- Haynes, W. M., 2014, *CRC handbook of chemistry and physics*, CRC press.
- Herman, J. S., and Lorah, M. M., 1987, CO₂ outgassing and calcite precipitation in Falling Spring Creek, Virginia, USA: *Chemical Geology*, v. 62, no. 3, p. 251-262.
- Hotchkiss, E., Hall Jr, R., Sponseller, R., Butman, D., Klaminder, J., Laudon, H., Rosvall, M., and Karlsson, J., 2015, Sources of and processes controlling CO₂ emissions change with the size of streams and rivers: *Nature Geoscience*, vol. 8, no. 9, p. 696-699.
- Hope, D., Palmer, S. M., Billett, M. F., and Dawson, J. J., 2001, Carbon dioxide and methane evasion from a temperate peatland stream: *Limnology and Oceanography*, v. 46, no. 4, p. 847-857.
- Hütsch, B. W., Augustin, J., and Merbach, W., 2002, Plant rhizodeposition—an important source for carbon turnover in soils: *Journal of Plant Nutrition and Soil Science*, v. 165, no. 4, p. 397-407.
- Jones Jr, J. B., and Mulholland, P. J., 1998, Carbon dioxide variation in a hardwood forest stream: an integrative measure of whole catchment soil respiration: *Ecosystems*, v. 1, no. 2, p. 183-196.

- Jonsson, A., Algesten, G., Bergström, A.-K., Bishop, K., Sobek, S., Tranvik, L. J., and Jansson, M., 2007, Integrating aquatic carbon fluxes in a boreal catchment carbon budget: *Journal of Hydrology*, v. 334, no. 1, p. 141-150.
- Johnson, M. S., Lehmann, J., Riha, S. J., Krusche, A. V., Richey, J. E., Ometto, J. P. H., and Couto, E. G., 2008, CO₂ efflux from Amazonian headwater streams represents a significant fate for deep soil respiration: *Geophysical Research Letters*, v. 35, no. 17.
- Kessler, T. J., and Harvey, C.F., 2001, The global flux of carbon dioxide into groundwater *Geophysical research letters*, vol. 28, no. 2, p. 279-282.
- Knapp, J. L., Osenbrück, K., and Cirpka, O. A., 2015, Impact of non-idealities in gas-tracer tests on the estimation of reaeration, respiration, and photosynthesis rates in streams: *Water research*, v. 83, p. 205-216.
- Kremer, J.N., Nixon, S.W., Buckley, B., and Roques, P., 2003, Technical Note: Conditions for Using the Floating Chamber Method to Estimate Air-Water Gas Exchange: *Estuaries*, v. 26, no. 4A, p. 985-990.
- Krenz, J., 2013, Measuring CO₂ emissions from a small boreal lake and its connecting streams using automatic floating chambers [M.S. thesis]: Swedish University of Agricultural Sciences.
- Lambert, M., and Fréchet, J.-L., 2005, Analytical techniques for measuring fluxes of CO₂ and CH₄ from hydroelectric reservoirs and natural water bodies, *Greenhouse Gas Emissions—Fluxes and Processes*, Springer, p. 37-60.
- Liu, X., Wan, S., Su, B., Hui, D., and Luo, Y., 2002, Response of soil CO₂ efflux to water manipulation in a tallgrass prairie ecosystem: *Plant and Soil*, v. 240, no. 2, p. 213-223.

- Liu, H., 2014, Inorganic and Organic Carbon Variations in Surface Water, Konza Prairie LTER Site, USA and Maolan Karst Experimental Site, China [M.S. thesis]: University of Kansas Geology.
- Lorke, A., Bodmer, P., Noss, C., Alshboul, Z., Koschorreck, M., Somlai, C., Bastviken, D., Flury, S., McGinnis, D., and Maeck, A., 2015, Technical Note: Drifting vs. anchored flux chambers for measuring greenhouse gas emissions from running waters, vol. 12, no. 17.
- MacIntyre, S., Wanninkhof, R., and Chanton, J., 1995, Trace gas exchange across the air-water interface in freshwater and coastal marine environments, Biogenic trace gases: Measuring emissions from soil and water, p. 52-97
- Macpherson, G., 2009, CO₂ distribution in groundwater and the impact of groundwater extraction on the global C cycle: Chemical Geology, v. 264, no. 1, p. 328-336.
- Macpherson, G., Roberts, J., Blair, J., Townsend, M., Fowle, D., and Beisner, K., 2008, Increasing shallow groundwater CO₂ and limestone weathering, Konza Prairie, USA: Geochimica et Cosmochimica Acta, v. 72, no. 23, p. 5581-5599.
- Mallard, J., McGlynn, B., and Covino, T., 2014, Lateral inflows, stream-groundwater exchange, and network geometry influence stream water composition: Water Resources Research, v. 50, no. 6, p. 4603-4623.
- Matthews, C. J. D., St. Louis, V. L., and Hesslein, R. H., 2003, Comparison of Three Techniques Used To Measure Diffusive Gas Exchange from Sheltered Aquatic Surfaces: Environmental Science & Technology, v. 37, no. 4, p. 772-780.
- Mazot, A., and Bernard, A., 2015, CO₂ degassing from volcanic lakes, Volcanic Lakes, Springer, Berlin Heidelberg, p. 341-354.

- McCallum, J. L., Cook, P. G., Berhane, D., Rumpf, C., and McMahon, G. A., 2012, Quantifying groundwater flows to streams using differential flow gaugings and water chemistry: *Journal of Hydrology*, v. 416, p. 118-132.
- McCutchan Jr, J., Saunders III, J., Lewis Jr, W., and Hayden, M. G., 2002, Effects of groundwater flux on open-channel estimates of stream metabolism: *Limnology and Oceanography*, v. 47, no. 1, p. 321-324.
- Morse, N., Bowden, W. B., Hackman, A., Pruden, C., Steiner, E., and Berger, E., 2007, Using sound pressure to estimate reaeration in streams: *Journal of the North American Benthological Society*, v. 26, no. 1, p. 28-37.
- Müller, D., Warneke, T., Rixen, T., Müller, M., Jamahari, S., Denis, N., Mujahid, A., and Notholt, J., 2015, Lateral carbon fluxes and CO₂ outgassing from a tropical peat-draining river: *Lateral*, v. 12, p. 10389-10424.
- Nadeau, T. L., & Rains, M. C., 2007, Hydrological connectivity between headwater streams and downstream waters: How science can inform policy. *Journal of the American Water Resources Association*, v. 43(1), p. 118–133.
- Neal, C., House, W. A., and Down, K., 1998, An assessment of excess carbon dioxide partial pressures in natural waters based on pH and alkalinity measurements: *Science of the Total Environment*, v. 210, p. 173-185.
- Neal, C., Watts, C., Williams, R. J., Neal, M., Hill, L., and Wickham, H., 2002, Diurnal and longer term patterns in carbon dioxide and calcite saturation for the River Kennet, south-eastern England: *Science of the total environment*, v. 282, p. 205-231.

- Ocampo-Torres, F., Donelan, M., Merzi, N., and Jia, F., 1994, Laboratory measurements of mass transfer of carbon dioxide and water vapour for smooth and rough flow conditions: *Tellus B*, v. 46, no. 1, p. 16-32.
- Ouyang, Y., and Zheng, C., 2000, Surficial processes and CO₂ flux in soil ecosystem: *Journal of Hydrology*, v. 234, no. 1, p. 54-70.
- Owens, M., Edwards, R., and Gibbs, J., 1964, Some reaeration studies in streams: *Air and water pollution*, v. 8, p. 469.
- Parker, G. W., and Gay, F. B., 1987, A procedure for estimating reaeration coefficients for Massachusetts streams: US Geological Survey, no.86-4111.
- Paul, E. A., 2014, *Soil microbiology, ecology and biochemistry*, Academic press, p. 47.
- Raymond, P. A., and Cole, J. J., 2001, Gas exchange in rivers and estuaries: Choosing a gas transfer velocity: *Estuaries and Coasts*, v. 24, no. 2, p. 312-317.
- Raymond, P. A., Zappa, C. J., Butman, D., Bott, T. L., Potter, J., Mulholland, P., Laursen, A. E., McDowell, W. H., and Newbold, D., 2012, Scaling the gas transfer velocity and hydraulic geometry in streams and small rivers: *Limnology & Oceanography: Fluids & Environments*, v. 2, no. 0, p. 41-53.
- Richey, J. E., Krusche, A. V., Johnson, M. S., Da Cunha, H. B., and Ballester, M. V., 2009, The role of rivers in the regional carbon balance: *Amazonia and Global Change*, v. 186, p. 489-504.
- Runkel, R. L., 2015, On the use of rhodamine WT for the characterization of stream hydrodynamics and transient storage: *Water Resources Research*. v. 51

- Sand-Jensen, K., and Staehr, P. A., 2012, CO₂ dynamics along Danish lowland streams: water–air gradients, piston velocities and evasion rates: *Biogeochemistry*, v. 111, no. 1-3, p. 615-628.
- Schlesinger, W., 1984, Soil organic matter: a source of atmospheric CO₂: The role of terrestrial vegetation in the global carbon cycle, p. 111-127.
- Schlesinger W. H. and Lichter J., 2001, Limited carbon storage in soil and litter of experimental forest plots under increased atmospheric CO₂. *Nature*, v. 411, p. 466–469.
- Sebacher, D. I., Harriss, R. C., and Bartlett, K. B., 1983, Methane flux across the air-water interface: air velocity effects: *Tellus B*, v. 35B, no. 2, p 103-109.
- Silva, J. P., Lasso, A., Lubberding, H. J., Peña, M. R., and Gijzen, H. J., 2015, Biases in greenhouse gases static chambers measurements in stabilization ponds: Comparison of flux estimation using linear and non-linear models: *Atmospheric Environment*, v. 109, p. 130-138.
- Streeter, H., and Phelps, E., 1925, A Study of the Pollution and Natural Purification of the Ohio River, Illinois Factors Concerned in the Phenomenon of Oxidation and Reaeration: *Public Health Service Bulletin*, v. 146.
- Striegl, R. G., Dornblaser, M., McDonald, C., Rover, J., and Stets, E., 2012, Carbon dioxide and methane emissions from the Yukon River system: *Global Biogeochemical Cycles*, v. 26, no. 4.
- Tank, J. L., Rosi-Marshall, E. J., Griffiths, N. A., Entekin, S. A., and Stephen, M. L., 2010, A review of allochthonous organic matter dynamics and metabolism in streams: *Journal of the North American Benthological Society*, v. 29, no. 1, p. 118-146.

- Tans, P., 2016, Trends in Carbon Dioxide, National Oceanic and Atmospheric Administration Earth Systems Research Laboratory Trends in Carbon Dioxide.
- Teodoru, C. R., Del Giorgio, P. A., Prairie, Y. T., and Camire, M., 2009, Patterns in pCO₂ in boreal streams and rivers of northern Quebec, Canada: *Global Biogeochemical Cycles*, v. 23, no. 2.
- Teodoru, C., Nyoni, F., Borges, A., Darchambeau, F., Nyambe, I., and Bouillon, S., 2015, Dynamics of greenhouse gases (CO₂, CH₄, N₂O) along the Zambezi River and major tributaries, and their importance in the riverine carbon budget: *Biogeosciences*, v. 12, no. 8, p. 2431-2453.
- Tsivoglou, E., and Neal, L., 1976, Tracer measurement of reaeration: III. Predicting the reaeration capacity of inland streams: *Journal (Water Pollution Control Federation)*, v. 48, no. 12, p. 2669-2689.
- Tsy-pin, M., and Macpherson, G., 2012, The effect of precipitation events on inorganic carbon in soil and shallow groundwater, Konza Prairie LTER Site, NE Kansas, USA: *Applied Geochemistry*, v. 27, no. 12, p. 2356-2369.
- Vachon, D., Prairie, Y. T., and Cole, J. J., 2010, The relationship between near-surface turbulence and gas transfer velocity in freshwater systems and its implications for floating chamber measurements of gas exchange: *Limnology and Oceanography*, v. 55, no. 4, p. 1723.
- Wallin, M. B., Löfgren, S., Erlandsson, M., and Bishop, K., 2014, Representative regional sampling of carbon dioxide and methane concentrations in hemiboreal headwater streams reveal underestimates in less systematic approaches: *Global Biogeochemical Cycles*, v. 9, no. 7, p. 1-9

- Wan, S., Norby, R. J., Ledford, J., and Weltzin, J. F., 2007, Responses of soil respiration to elevated CO₂, air warming, and changing soil water availability in a model old-field grassland: *Global Change Biology*, v. 13, no. 11, p. 2411-2424.
- Wanninkhof, R., Mulholland, P., and Elwood, J., 1990, Gas exchange rates for a first-order stream determined with deliberate and natural tracers: *Water Resources Research*, v. 26, no. 7, p. 1621-1630.
- Wanninkhof, R., Ledwell, J. R., and Broecker, W. S., 1985, Gas exchange-wind speed relation measured with sulfur hexafluoride on a lake: *Science*, v. 227, no. 4691, p. 1224-1226.
- Wanninkhof, R., 1992, Relationship between wind speed and gas exchange over the ocean: *Journal of Geophysical Research: Oceans (1978–2012)*, v. 97, no. C5, p. 7373-7382.
- Webster, J., and Meyer, J. L., 1997, Organic matter budgets for streams: a synthesis: *Journal of the North American Benthological Society*, v. 16, no. 1, p. 141-161.
- Worrall, F., Guilbert, T., and Besien, T., 2007, The flux of carbon from rivers: the case for flux from England and Wales: *Biogeochemistry*, v. 86, no. 1, p. 63-75.
- Worrall, F., and Lancaster, A., 2005, The release of CO₂ from riverwaters—the contribution of excess CO₂ from groundwater: *Biogeochemistry*, v. 76, no. 2, p. 299-317.
- Zheng, L., Spycher, N., Varadharajan, C., Tinnacher, R. M., Pugh, J. D., Bianchi, M., Birkholzer, J., Nico, P. S., and Trautz, R. C., 2015, On the mobilization of metals by CO₂ leakage into shallow aquifers: exploring release mechanisms by modeling field and laboratory experiments: *Greenhouse Gases: Science and Technology*, v. 5, p. 1-16.

CHAPTER 2. TESTING THE APPLICATION OF THE FLOATING CHAMBER IN
SHALLOW, FLOWING WATER

1. Introduction

Recently, streams and rivers have been recognized as potentially significant sources of carbon to the atmosphere (Cole et al., 2007, Battin et al. 2009, Butman and Raymond 2011, Hotchkiss et al., 2015). The magnitude of degassing from streams and rivers has been quantified globally in only a few studies (Liu et al., 2008, Battin et al., 2009, and Aufdenkampe et al., 2011), and more direct and site-specific measurements of gas efflux are needed to improve these estimates. Numerous methods exist for obtaining estimates of the flux of gases in environments with flowing water. These techniques include wind-based estimates (Raymond and Cole, 2001), the use of gas tracers as a proxy for the gas of interest (Generaux and Hemond 1992), estimates based on hydrogeomorphic equations (Raymond et al., 2012, Owens et al., 1964, and Streeter and Phelps 1925), chamber-based techniques (Crawford et al., 2013), and more (Neal et al., 1998 and Morse et al., 2007).

Chamber-based methodologies have proven a logistically simple and economic method of measuring gas efflux from lentic and ocean systems (Kremer et al., 2003, Cole et al., 2010, Mazot and Bernard, 2015). However, controversy remains about the accuracy of chamber measurements under certain conditions (Matthews et al., 2003; Vachon et al., 2010), and limited testing has been conducted on chambers effectiveness in a shallow, turbulent, flowing-water environment (Cole et al., 2010, and Lorke et al., 2015). Despite a lack of developed evidence supporting the use of chamber-based techniques, there have been numerous attempts to utilize them to measure gas fluxes in environments with turbulent flowing water (Table 1).

The floating chamber works by encapsulating a portion of water surface with an impermeable chamber and measuring the change in concentration of a gas of interest inside of the chamber over time. Often times, the chamber is supported by flotation devices in the water

(i.e. floating chamber, floating dome, floating helmet, or static chamber method) but the chamber can also be suspended directly over the water. Different chamber designs have been shown to provide differing results (Lambert et al., 2005), so special attention should be paid to chamber design.

There are two principal limitations of chamber use in flowing water caused by chamber design and field conditions: 1) the chamber over predicts the flux from streams due to induced artificial turbulence because the chamber disturbs the water surface, and 2) the chamber is difficult to deploy in areas where there is significant turbulence. Failing to be able to use the chamber in the most turbulent areas causes an underestimation of fluxes from streams.

Users of the chamber in oceanographic and lake environments were the first to question and test the floating chamber for accuracy of flux measurements (Matthews et al., 2003 and Vachon et al., 2010). It has been visually observed (Campeau et al., 2014) that chambers likely add bias to flux estimates in streams by disturbing the water surface and level of turbulence, but to date, few studies have attempted to quantify this turbulence (Lorke et al., 2015). The main objectives of this study are to verify the results of verifying chamber-based measurements of flux in a laboratory study and to evaluate the effects of chamber design.

2. Methods

2.1. Flume experiment

Laboratory experiments were conducted in the University of Kansas Water Resources Laboratory flume system (Table 2). The system simulates a simplified, headwater stream environment with a shallow flume channel (Figure 1), water velocities (between 0.13 and 0.23 m s⁻¹) similar to those observed in low-gradient, low-ordered headwater streams, and a concentration of dissolved CO₂ similar to groundwater discharge ($\log p\text{CO}_2 \approx -1.5$, where $p\text{CO}_2$

is the partial pressure of carbon dioxide). Water in the system is recirculated to a constant head tank that feeds a 0.76 m x 19.2 m channel (Figure 1). The sides and bottom of the channel are smooth and have relatively no roughness or topography compared to a natural stream channel. This allows the flume to behave in a near ideal manner and eliminates stream hydrodynamic properties as a variable in experiments. The height of the water in the flume channel was also maintained consistently throughout all experiments by the use of a 15.25 cm weir on the downstream end of the flume channel (Figure 1).

The water reservoir for the flume system contained approximately 35,000 liters of water during the experiments. The reservoir system circulated water between a constant head tank and a holding tank (see appendix D) while CO₂ was added to the water reservoir system from compressed gas cylinders using diffusion stones. As CO₂ was being added to the water reservoir, the water was prevented from flowing through the flume channel. Restricting the flow through the channel effectively sealed the water in the flume system from the atmosphere. There was a small headspace remaining in the water reservoir system where CO₂ concentrations were in excess of 30,000 ppmv. The high headspace concentration of CO₂ forced the CO₂ to dissolve into the water reservoir system and allowed extremely limited degassing while the flume channel was closed. The water was allowed to dissolve CO₂ for a designated time period (1.5 hours) until concentrations reached levels similar to those measured in naturally occurring groundwater ($\log p\text{CO}_2 \approx -1.5$).

Water velocity and the height of water in the flume were measured for each experimental trial. The velocity of the water was measured by observing the approximate residence time in the flume channel of a colored tracer dye between a point at the upstream end of the flume channel

and a point at the downstream end of the flume channel (Figure 2). The length of the flume was then divided by the residence time to obtain an approximate velocity.

An AZ-77535 CO₂/Temperature/RH meter measured the indoor, atmospheric conditions of the room periodically throughout the duration of the experiments. The atmospheric concentrations of CO₂ in the room were maintained using two ventilation fans in the ceiling of the laboratory (see appendix K). Air temperature was maintained using the buildings heating ventilation and air conditioning system.

2.1.1. Water-chemistry

Dissolved CO₂ content was calculated for all trials using a geochemical speciation model with inputs derived from measurements of flume water samples (Table 3). All water samples were filtered using a 0.45 µm syringe filter within 48 hours of collection. Measurements were made and water samples were collected at fixed points near the floating chamber location, and at sampling points in the upstream and downstream portions of the flume (Figure 1). A pH Thermo Scientific Orion meter with an Orion 8157BNUMD Ross Ultra pH/ATC Triode was used to monitor pH and temperature for all 42 chamber sampling events. Samples for alkalinity were stored in glass bottles with Teflon-lined lids, and refrigerated for preservation. Alkalinity was determined for 35 water samples by titrating the sample with 0.01702 N HNO₃ using the inflection point method. The water chemistry of the flume system was assumed to remain constant since all experiments used the same water supply, so two samples for determining cations and anions were used to represent the water chemistry. Cations were preserved in pre-cleaned low-density polyethylene (LDPE) bottles acidifying to 2% (v/v) with HNO₃. Cation concentrations were measured using a JY Ultima2 inductively-coupled plasma, optical emission spectrometer. Water samples for anions were stored in glass bottles with a Teflon-lined lid,

refrigerated for preservation, and analyzed using a Dionex 4000i ion chromatograph. Results were modeled using PHREEQC Interactive 3.1.7-9213 (Parkhurst and Appelo, 1999).

2.1.2. Floating chamber measurements

A large version of the floating chamber (LFC) and a smaller, streamlined version of the floating chamber (SFC) were tested (Table 5). The LFC was modified from Liu (2014), and provided a larger footprint than the SFC. The SFC was designed to be more hydrodynamic than the first version, and was smaller, with the goal of improving capabilities of measuring CO₂ degassing in narrow, shallow streams. It was manufactured using 3D printed ABS plastic, coated with paraffin wax to reduce gas permeability (see appendix A), and had a modified float-support structure.

The LFC was used in 26 experimental trials, and the SFC was used in 16 experimental trials, over a range of water velocities. Both chamber designs were tethered in place at the mid-section of the flume using fishing line. The chambers were gently placed onto the water surface and then allowed to float freely until the line became taught.

Using equation (1), a chamber-based CO₂ flux ($F_{Chamber}$) was calculated for each experimental trial. Chamber measurements were obtained by sealing the chamber with the water surface for approximately five minutes to obtain a representative data set; chamber volume in L (V), the area of the water surface sealed by the chamber in m² ($A_{Chamber}$), and the dimensions of the chamber varied between the two chamber designs tested (Table 5). The change in mole fraction (μmole per mole) of CO₂ inside of each chamber ($\frac{d(pCO_2)}{dt}$) was measured at one Hz by circulating chamber air through a LI-820 CO₂ Infrared Gas Analyzer (IRGA). The air sampled was drawn from the top of both chamber designs, filtered through a Drierite® granule filter to remove moisture, analyzed, and then recirculated back to the chamber to avoid incurring

pressure changes inside of the chamber. In between sampling events, the chamber CO₂ concentration was allowed to equilibrate with the room atmosphere to avoid CO₂ accumulation inside the chamber (see appendix G). The air temperature in degrees Celsius (converted to K for equation (1)), measured using a hand-held meter as described in section 2.1, and R , the ideal gas constant (L atm mole⁻¹ K⁻¹) are also required to solve for $F_{chamber}$. Atmospheric pressure (p) was assumed to be 1 atm for all trials following a sensitivity analysis that showed a less than 0.01% fluctuation for the maximum and minimum observed values for atmospheric pressure on the days the trials were run (barometric pressure from www.wunderground.com for Lawrence, KS was between 29.85 and 29.9 inches Hg \approx 1.00 atm). To determine $\frac{d(pCO_2)}{dt}$ a linear regression was fit to the linear portion of the measured change in CO₂ mole fraction per second ($R^2 > 0.90$).

$$F_{Chamber} = \left(\frac{d(pCO_2)}{dt} \right) \left(\frac{p * V}{R * T * A_{chamber}} \right) \quad (1)$$

The $F_{Chamber}$ obtained in equation (1) can be applied to the flux equation (equation (2)) suggested by Cole and Caraco (1998). Using equation (2), the $F_{Chamber}$ is divided by the difference between the calculated dissolved CO₂ concentration (CO_{2water}) and CO₂ room atmospheric concentration (CO_{2air}) to solve for the gas transfer coefficient (k). This effectively normalizes the flux we obtained for any variations in CO₂ concentrations in the air or water during the flume experiments. The gas transfer coefficient can be thought of as representing the depth of water that equalizes with atmospheric gas concentrations per unit of time.

$$F_{Chamber} = k (CO_{2water} - CO_{2air}) \quad (2)$$

The gas transfer coefficient is temperature dependent, so it is often corrected to a given temperature of 20° C (equation (3)). The new temperature corrected value of k is expressed as k_{600} . The temperature correction is accomplished by multiplying k by the ratio of the Schmidt numbers of CO₂ at the temperature of interest (S_{CO_2}), and at 20° C (Schmidt number of CO₂ is

equal to 600 at 20° C). The ratio is raised to the power of ½, which is appropriate for use in rough surface waters (Jähne et al 1987).

$$k_{600} = k \left(\frac{600}{SC_{CO_2}} \right)^{\frac{1}{2}} \quad (3)$$

2.2. Stirring plate simulation

A second set of laboratory experiments (Table 6) were conducted to verify the results demonstrated by the flume experiments. During this set of experiments, two water samples (water from the flume system at two different CO₂ concentrations, i.e. flume water) were charged with CO₂ bubbling from a diffusion stone. Each water sample was divided into two 800 mL portions and poured into glass beakers with a depth of 15.25 cm to match the approximate depth of water within the flume channel during the flume experimental trials. The first glass beaker was placed on a magnetic stirring plate while the second sample remained adjacent to it in the same room. One sample was stirred using a magnetic stir bar at a rate of approximately 90 revolutions per minute (rpm) to simulate the water velocity observed in flume experiments; 90 rpm provided a radial velocity similar to the average linear water velocity of the flume system detailed in section 2.1. Water velocities were confirmed by visually observing the travel time around the circumference of the beaker of a dye. The beaker circumference was then divided by the travel time of the dye to obtain a water velocity. For both the stirred and non-stirred samples, pH, temperature, and millivolts were recorded periodically for duration of the experiment using an Orion Star A329 meter with an Orion 81007UWMMD Ross Ultra pH/ATC triode. Laboratory atmosphere CO₂ concentrations were recorded using a hand-held AZ-77535 CO₂/Temperature/RH meter.

The flux from the beaker (F_{beaker}) was determined by calculating the change in dissolved CO₂ (ΔCO_2) over the duration of the experiment, and dividing this by the product of the surface area of the beaker (A_{beaker} , in m²) and the duration of the experiment in seconds (t), as shown in equation (4). A value for k_{600} was then calculated using the same procedure as outlined for calculating k_{600} for the $F_{Chamber}$.

$$F_{Beaker} = \frac{\Delta CO_2}{A_{beaker} * t} \quad (4)$$

3. Results

3.1. Flume experiments

3.1.1. Fundamental parameters

The air temperature during the flume experiments ranged between 23 °C and 29 °C with a mean of 25 °C, and flume water temperatures ranged from 20 °C to 29 °C with a mean of 24.5°C. The depth of water in the flume channel was measured at a point at the upstream end of the flume and at the downstream end of the flume, and remained at approximately 17 cm for all trials. The average residence time of water in the flume was 79 seconds, and residence time ranged between 52 seconds and 105 seconds for all experiments, as determined by water velocity and length of the flume.

Water velocity was calculated using four different measurements of the water height over an H-weir located at the upstream portion of the flume were taken. The water height was then plotted against corresponding measurements of water velocity taken using the dye method. The four corresponding measurements of the dye velocity and height of water over the H-weir were used to build a calibration curve (Figure 2). The calibration curve provided a corresponding velocity to a given water height over the H-weir. For the remaining trials the water height over

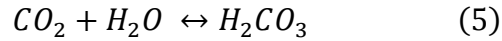
the H-weir was measured and a water velocity was calculated using the calibration curve. The corrected data points shown in Figure 2 are the four points used to build the calibration curve, and the calibration data points display the remaining data plotted using the equation derived for the calibration equation.

Water velocities in the 16 SFC trials ranged between 0.17 and 0.18 m s⁻¹, and between 0.13 and 0.23 m s⁻¹ in the 26 LFC trials. The mean water velocity of all trials was 0.18 m s⁻¹. The precision of the water velocity measurement is estimated to be ±0.05 m s⁻¹.

Geochemical speciation modeling using the water chemistry data (Table 3) confirmed that the flume water was under-saturated during all trials with respect to all minerals, so mineral precipitation was negligible during the experiments (see appendix E). In particular, under saturation with respect to calcite and other carbonate minerals was important to maintain the integrity of our experimental assumptions. The water in the flume was always supersaturated with CO₂ compared to the atmosphere of the lab (log $p\text{CO}_{2\text{-water}}$ between -1.46 and -2.37). The mean ratio of dissolved CO₂ in water to the room atmospheric concentration of CO₂ was 16 to 1. Laboratory atmospheric CO₂ concentrations were partially controlled with the ventilation system in the laboratory (see appendix K), but fluctuated between trials to between 400 and 5,000 ppmv CO₂ (mean concentration of 2,000 ppmv CO₂). The large fluctuation in CO₂ was due to leakage from the basement reservoir headspace to the laboratory room containing the flume.

The pH ranged from 6.58 to 7.50 with a mean pH of 6.81. Alkalinity remained relatively constant during all trials (mean alkalinity was 136 mg l⁻¹, one standard deviation was 4 mg l⁻¹, and range was 14 mg l⁻¹). Assuming there was negligible mineral precipitation, any change in the H⁺ concentration of the water was due to changes in the CO₂ or HCO₃⁻ concentrations (equations (5) and (6), below). Alkalinity concentrations (dominated by HCO₃⁻) remained consistent

throughout the experiment, so changes in CO₂ were the primary driver of changes in pH (equations (6) and (7), below), which permitted the use of pH as a proxy for CO₂ concentrations in the water.



$$pH = -\log(H^+) \quad (7)$$

Negligible mineral precipitation and change in the alkalinity concentration suggests that the chemistry over the length of the flume would likely only be influenced by movement of species between the water and the atmosphere. The constant oversaturation of aqueous CO₂, with respect to the laboratory atmosphere suggests that the channel was most likely to degas CO₂ rather than absorb CO₂ gas.

3.1.2. CO₂ degassing

More than 90% (39 of 42) of all chamber measurements were accepted using the criterion of an R² value of 0.90 or larger for a linear fit to the measured change in CO₂ over time (Table 4). Throughout the course of the experiments the chamber visibly disturbed the surface of the water as water flowed down-flume, and the water around and under the chamber. The disturbance was too small to quantify using any techniques available to this research project. Comparing the two chamber design types revealed that 93% (25 of 27) of LFC chamber measurements were accepted. Similarly, 94% (15 of 16) measurements taken from the SFC were accepted using the same criteria. SFC values for k_{600} ranged between 2.48×10^{-8} and 5.67×10^{-8} m s⁻¹ with an average value of 4.86×10^{-8} m s⁻¹. The LFC values for k_{600} ranged between 5.69×10^{-10} and 9.17×10^{-8} with a mean value of 2.70×10^{-8} m s⁻¹. The values of k_{600} measured during all flume experimental trials with both chamber designs ranged between 5.69×10^{-10} m s⁻¹ and

$9.17 \times 10^{-8} \text{ m s}^{-1}$ with a mean value of $2.39 \times 10^{-8} \text{ m s}^{-1}$ and one standard deviation of $3.42 \times 10^{-8} \text{ m s}^{-1}$.

The lowest water velocities (below 0.16 m s^{-1}) provided the lowest value for k by an order of magnitude. Nine of ten data points (trials 18 to 27 in Table 4) used to calculate the average k at the lowest water velocity were obtained during consecutive sampling events, and provided similarly low values. The tenth data point (trial 17 in Table 4) obtained during a different sampling event provided a value that was comparable to the medium and high water velocity values for k . The nine data points that provided the lowest values for k also had abnormally high laboratory atmospheric concentrations of CO_2 recorded during the trials (mean of 4,900 ppmv CO_2 compared to a mean of 1,200 ppmv for all other trials).

3.2. Stirring plate simulation

The stirring plate simulations were designed to simulate conditions similar to those observed in the floating chamber during the flume experiments. Stirring plate water velocities were approximately 0.1 m s^{-1} , which is comparable to velocities in the flume channel experiments (0.13 to 0.23 m s^{-1}). As in the flume experiments, pH was used as a proxy for the concentration of dissolved CO_2 .

Measurements of the pH change over the length of the flume during flume experiments were smaller than or at the accuracy of the pH probe used (± 0.01 , see appendix B). The stirring plate simulation was run over a longer time period than the residence time in the flume, allowing for more degassing to occur and thus allowing pH to change measurably.

Fluxes of CO_2 from the water in the beakers to the laboratory atmosphere were modeled using PHREEQC (see appendix E). The calculated fluxes were then used with the measured concentration gradient between the air and the water to calculate a value for k (equation (6)).

Calculated values for k were then temperature corrected to a k_{600} . The values of k_{600} measured during the stirring plate simulations ranged between $6.49 \times 10^{-9} \text{ m s}^{-1}$ and $3.40 \times 10^{-8} \text{ m s}^{-1}$ with a mean value of $2.06 \times 10^{-8} \text{ m s}^{-1}$.

4. Discussion

The flume experiments were able to adequately simulate a simplified headwater stream environment, chemically and physically. Log $p\text{CO}_2$ concentrations ranged from -1.46 to -2.37, which is a good approximation of some groundwater and soil water (Macpherson 2009). Although the laboratory atmospheric concentrations were typically higher than those observed in most headwater streams, the water was consistently saturated in CO_2 with respect to the laboratory atmosphere. Alkalinity remained constant during our lab experiments and behaved comparably to other lab experiments of a similar nature (Abongwa et al., 2015). The range of velocities falls within the same range observed in many low-gradient, low-ordered headwater streams, and the temperature remained within a range acceptable for most stream environments.

The limited residence time of the water in the flume did not allow the water to degas enough CO_2 to result in a significant pH change that could be measured within the accuracy of the pH probe (± 0.01). Similar unresolvable changes in the pH were observed in the stirring plate experiment over the same time periods as the approximate residence time of water in the flume. Over longer time periods, greater pH changes were observed in the stirring plate simulations, and the rate of CO_2 degassing became more apparent.

The k_{600} values for both chamber designs were of a similar magnitude (Figure 3), and chamber design did not have a significant effect on altering gas transfer. Since the two chamber designs resulted in comparable measurements, they are grouped together for additional interpretation. A weak linear trend of k versus water velocity was observed for all of the data.

Since k is a function of turbulence and the main control on turbulence in the flume is the water velocity, k at a given water velocity should be approximately the same. Given this logic, and the inherent uncertainty likely present in our velocity measurements, values for k_{600} were grouped into three categories based on water velocity (high, medium, and low velocity) in order to provide a clear and concise picture of how k varies across water velocities in the flume channel (Figure 4).

Since all of our chamber measurements were made with the chamber fixed in one place (anchored rather than floating), there should be a linear dependency of k on the water velocity. A similar trend was observed by Teodoru et al. (2015) when measuring degassing in the Congo River using a static floating chamber where abnormally high values for k were obtained. Teodoru et al. (2015) noticed a clear linear dependency of k on the stream or river discharge; water velocities estimated from their discharge data and river cross sections ranged from less than half of our minimum velocity to more than 1.5 times our highest velocity, with the intermediate stream velocity value having the highest rate of degassing. The weak relationship between k and water velocity in our experiments (Figure 3), and the strong correlation between k and atmospheric concentration observed in trials 18 to 27, suggests that k may be more dependent on the concentration gradient of CO_2 between the atmosphere and the water, across the range of observed water velocities, than the water velocity. The multiple experiments done the lowest velocities suggest a possible non-linear effect at low velocities. Nevertheless, considering the limited impact of the relatively small changes in water velocity on k among all flume trials and the stirring plate simulations, we are assuming the average k at all water velocities in the flume is comparable to the k 's obtained in the stirring plate simulations.

The results of the stirring plate experiment behaved as expected across several concentrations of dissolved CO₂, suggesting that they are a reliable simulation of flume behavior. The water velocities were in a range similar to the velocities observed in the flume, and the CO₂ flux out of the beaker on the stirring plate was always higher than the flux of the non-stirred beaker (Figure 7). Chemically, the flux corresponded well to the concentration gradient (Figure 7): higher aqueous CO₂ resulted in a higher CO₂ degassing flux. The k was independent of the water concentration (similar magnitude despite varying dissolved CO₂ concentrations), but dependent on the water velocity (lower k in non-stirring than corresponding stirring trial).

Comparing the k_{600} 's of the flume experiment with the k_{600} 's of the stirring plate experiment revealed that they are of the same magnitude (Figure 6). This suggests that the floating chamber does provide an accurate measurement of flux and k , and that previous estimates using this technique should be accepted, at least over the range of water velocities tested here. Observed fluxes, using the chamber, also correspond with observed fluxes using the chamber in the field (Table 1).

Previous research into the use of the floating chamber, by Matthews et al. (2003) in a lake environment, suggests that the floating chamber method may produce artificially high measurements of CO₂ caused by the disturbance of the surface boundary layer. In a different study, Vachon et al. (2010) used an acoustic doppler velocimeter to demonstrate that the floating chamber technique in a lake setting disturbs the surface boundary layer and the chamber design overestimates fluxes due to enhanced turbulence. Although multiple authors have acknowledged the effect of chambers disturbing the water surface, there have been relatively few attempts to adequately quantify this disturbance (Matthews et al., 2003, Kremer et al., 2003, Vachon et al., 2010, and Lorke et al., 2015) and only one known study attempting to quantify the effect of

chamber-induced turbulence on fluxes in systems with flowing water (Lorke et al., 2015). Lorke et al. (2015) suggested that static chambers used in flowing water consistently measure higher flux values than chambers allowed to drift. The Lorke et al. (2015) study suggested a mechanism by which anchored chambers increase the turbulence under chambers and elevate the observed flux values due to this artificially induced turbulence.

Our results are not consistent with the findings of Lorke et al. (2015). A comparison of the floating chamber method with the stirring plate simulations shows that the floating chamber provides a reasonable estimate of flux. The floating chamber may indeed be a reliable method for measuring gas fluxes in small headwater streams.

5. Conclusions and implications

This study adds supporting evidence to the idea that the floating chamber can accurately measure gas fluxes in environments with flowing water. Careful consideration should be taken when applying chamber based methodologies in environments where water flows against the sides of the chamber and where the structure of the chamber disturbs the interface between the surface water and the atmosphere. When considering methods for quantifying gas flux from streams and rivers, the floating chamber remains a relevant and viable method due to its low cost and simple field application. Accurate measurements of gas fluxes from streams and rivers are necessary to establish residence times of important elements in the environment and to adequately build atmospheric climate models. Validating the methodology of past chamber measurements in environments with small streams and rivers is an important contribution to biogeochemical cycle research.

Tables

TABLE 1. CO₂ GAS EFFLUX MEASUREMENTS USING FLOATING CHAMBERS

Author (s)	Year	Environment	Gases Measured	Fluxes Measured	Chamber Design Specifics
Striegl et al.	2012	Yukon rivers and streams	CO ₂ and CH ₄	6 to 548 mmol C m ⁻² d ⁻¹ 0.07 to 4.80 mol C m ² d ⁻¹	Allowed to float alongside a boat in rivers and anchored in place in streams
Dinmore et al.	2010	Peatland streams	CO ₂ , CH ₄ , and N ₂ O	1200 µg C m ⁻² s ⁻¹ 2 µg C m ⁻² s ⁻¹ 0.025 µg N m ⁻² s ⁻¹	Opaque injection-molded polypropylene box with dimensions of 61 cm x 30 cm x 15 cm with a volume of 0.0191 m ³
Chen et al.	2015	River with hydroelectric reservoirs	N ₂ O	10 to 30 µg m ⁻² h ⁻¹	Thermometer located at the top of the chamber to measure inside air temperature
Borges et al.	2015	Rivers	CO ₂ and CH ₄	186 to 1,149 mmol m ⁻² d ⁻¹ 0.5 to 18 mmol m ⁻² d ⁻¹	Infra-red Gas Analyzer (IRGA) for CO ₂ and in-line gas extraction for CH ₄
Alin et al.	2011	Low-gradient rivers	CO ₂	0 to 25 µmol m ⁻² s ⁻¹	Equipped with an internal fan to simulate wind
ones et al.	2015	Streams and pools in karstic cave systems	H ₂ S	0 to 80 µmol m ⁻² s ⁻¹	Chamber was connected to a handheld gas detector

Müller et al.	Luan and Wu	Deshmukh et al.	Crawford et al.	Krenz	Juuntinen et al.
2015	2015	2015	2013	2013	2013
Tropical peat-draining river	Drainage ditches	Downstream of a subtropical hydroelectric reservoir	High elevation mountain streams	Oxygenated wetland streams	Small boreal lake and its connecting streams
					Northern peatland-stream-lake continuum
CO ₂	CH ₄	CH ₄	CO ₂ and CH ₄	CO ₂	CO ₂ and CH ₄
1.8 to 28.5 gC m ⁻² d ⁻¹	0 to 16 CH ₄ mg m ⁻² d ⁻¹	1.14 to 3.3 mmol m ⁻² d ⁻¹	-40 to 146 mmol CO ₂ m ⁻² d ⁻¹ and -21.2 to 642 μmol CO ₂ m ⁻² d ⁻¹	1-20 μmol m ⁻² s ⁻¹ and 0-15 μmol m ⁻² s ⁻¹	479 g C m ² a ⁻¹ and 0.4 –17.4 g C m ² a ⁻¹
Equipped with a vent tube to maintain atmospheric pressure, and edges extended 1 cm into the water	50 cm in height, 26.3 cm in diameter, and equipped with a capillary tube to maintain atmospheric pressure	Allowed to float alongside a boat, and connected to an IRGA	Suspended clear chamber	Suspended clear chamber	Chamber walls were submerged 5 cm below the water surface. 6.6 L volume and 451 cm ² area footprint. 6.6 L, 452 cm ² area, with sidewalls penetrating 5 cm into the water column. Allowed to drift next to a boat, and sampled for 20-60 minutes.

Sand-Jensen and Staehr	Beaulieu et al.	Gómez-Gerner et al.	Neu et al.	Billet and Harvey	Billett et al.	Teodoru et al.
2012	2012	2014	2011	2013	2015	2015
Danish lowland streams	Large rivers	Intermittent Mediterranean fluvial network	Amazonian first-order headwater stream	Amazonian first-order headwater stream	Peatland streams	River and major tributaries
CO ₂	CO ₂ , CH ₄ , and N ₂ O	CO ₂ and CH ₄	CO ₂ and CH ₄	CO ₂ and CH ₄	¹⁴ C and δC ¹³ isotope	CO ₂ and CH ₄
170–1,200 mmol m ⁻² day ⁻¹	*reported gas transfer coefficients (<i>k</i>) and not fluxes	120 ± 33 mmol m ⁻² d ⁻¹ and 13.9 ± 10.1 mmol m ⁻² d ⁻¹	5,994 ± 677 g C m ⁻² y ⁻¹ and 987 ± 221 g C m ⁻² y ⁻¹		N/A	3380 mg C m ⁻² d ⁻¹ , 48.6 mg C m ⁻² d ⁻² , and
Constructed as a half-cylinder 94 cm long and 18 cm in internal diameter made of PVC painted white to prevent heating	20 L acrylic chambers with a 0.164 m ² footprint and a height of 17.8 cm, equipped with a 1 cm diameter vent hole, supported within an air-filled flotation collar, chamber walls extended 1–2 cm into the water.	Monitored the gas concentrations in the chamber every 30 seconds for a total of 10 min after passing through an in-line moisture trap at a rate of 2.9 L min ⁻¹ .	Dynamic Plexiglas floating chamber (0.125 m ² footprint with 13.5 L volume) connected to an IRGA		In-line molecular sieve for CO ₂ isotopes	Temperature continuously monitored, 17 L volume, and extended 7 cm below water surface

Huotari et al.	Belger et al.	Han et al.	Sawakuchi et al.	Ran et al.	Campeau et al.	Campeau and Del Giorgio
2013	2011	2013	2012	2015	2014	2014
Boreal river	Amazonian rivers and streams	Rivers	Large tropical rivers in the amazon basin	The Yellow River	Boreal rivers and streams	Boreal rivers and streams
CO ₂	CO ₂ and CH ₄	CO ₂ , CH ₄ , and N ₂ O	CH ₄	CO ₂	CO ₂ and CH ₄	CO ₂ and CH ₄
83±37 μmol m ⁻² d ⁻¹	2193 mg C m ⁻² d ⁻¹ , and 60 mg C m ⁻² d ⁻¹	1023 mg m ⁻² h ⁻¹ , 89 mg m ⁻² h ⁻¹ , and 151 μg m ⁻² h ⁻¹	59 to 2974 mmol m ⁻² y ⁻¹	7.9±1.2 Tg C yr ⁻¹	888 mg C m ⁻² d ⁻¹ and 97.8 mg C m ⁻² d ⁻¹	*Reported as k ₆₀₀
Not described in detail	Vented, with a fan to circulate air inside, 25 cm diameter with a volume of 10 L, sample time was 15 minutes, and gas samples were taken at 5 minute intervals with a syringe	Static chamber with gas samples analyzed using chromatography	7.5 L volume chamber with a 30 cm diameter and covered with reflective aluminum tape to reduce heating	Volume of 0.042 m ³ and a footprint of 0.2 m ² , walls 3–5 cm into the water column for 40-70 minutes.	Measurements of chamber concentration taken every minute for 10 minutes	Covered with aluminum foil to reduce solar heating and equipped with an internal thermometer to monitor temperature

Denfeld et al.	Fatima et al.	Khadka et al.	Sha et al.	Bedharik et al.	Bastien and Demarty	Xia et al.
2013	2013	2014	2011	2015	2013	2013
Arctic river basin including streams and rivers	Amazonian Rivers	River system	Riverine wetlands	Third-order stream	Rivers	Sewage-enriched river
CO ₂	CO ₂	CO ₂	CH ₄	CH ₄	CO ₂ and CH ₄	N ₂ O
0 to 26 g C m ⁻² d ⁻¹	0.8 to 15.3 μmol m ⁻² s ⁻¹	400 to 1200 g C m ⁻² y ⁻¹	0 to 160 mg CH ₄ m ⁻² h ⁻¹	0.07 to 0.73 mmol m ⁻² d ⁻¹	0 to 5,000 mg CO ₂ m ⁻² d ⁻¹ , and 0 to 15 mg CH ₄ m ⁻² d ⁻¹	62 μg N m ⁻² h ⁻¹
Circular plastic chamber with a fixed headspace, and allowed to float freely alongside a boat. Recirculated air sample through an IRGA.	0.125 m ² footprint, 10.6 L volume, made of Plexiglas with a 1 mm diameter hole to provide for pressure equalization, recirculated air sample through an IRGA, and	28 L volume plastic storage bin with an 0.11 m ² footprint, and allowed to penetrate 6 cm into the water column, recirculated air sample through an IRGA, left on	Rectangular 0.21 m ² footprint and 56 L plastic storage containers equipped with foam for buoyancy, and wrapped with duct tape for waterproofing.	3.1 L volume and 0.024 m ² footprint equipped with styrene floats, sampled every 30 minutes with a syringe for three hours.	17.6 L volume and 0.16 m ² footprint, sampled for seven minutes continuously with air recirculating to an analyzer	Constructed of round polypropylene “cake” containers 0.0064 m ³ and 0.07 m ² footprint, were floated with Styrofoam annuli, and penetrated 1-2 cm into the water column. Covered with silver paper to prevent heating

TABLE 2. FLUME CO₂ DEGASSING EXPERIMENTS

Experiment	Design	Hypotheses
Stream velocity influence	Multiple trials with varying water velocities will test the FC (floating chamber) in a flume with a known concentration of dissolved CO ₂ in the water.	As the water velocity is increased the degassing rate will increase due to artificial turbulence from the FC.
Water dynamic chamber design	Two separate FC design will be tested to see the effect of how water dynamic design plays a role in measurements. The designs test for artificial turbulence induced by the FC.	The SFC will have a lower degassing rate because it has lower FC artificially induced turbulence.

TABLE 3. WATER CHEMISTRY OF FLUME WATER

Ions	Concentration (mg L⁻¹)
Ca	42
Mg	4.8
Na	21
K	3.1
Si	4.1
Cl	1.3
SO ₄	44
NO ₃	1.0
F	0.99
Sr	0.2
Zn	0.4

TABLE 4. FLOATING CHAMBER RESULTS

Trial #	Chamber Slope (ppmv s ⁻¹)	R ² – linear regression	Air Temperature (°C)	Chamber Design	Water Velocity (m s ⁻¹)	Air Concentration	Log(pCO ₂) Water	Flux (μmol s ⁻¹ m ⁻²)	<i>k</i> (m s ⁻¹)	<i>k</i> ₆₀₀ (m s ⁻¹)
1	1.65	0.989	25	LFC	N/A	862	N/A	11.0	3.44 x 10 ⁻⁸	3.22 x 10 ⁻⁸
2	2.12	0.998	26	LFC	0.19	788	N/A	14.1	5.63 x 10 ⁻⁸	5.14 x 10 ⁻⁸
3	2.07	0.997	23.2	LFC	0.22	264	-1.67	13.9	2.24 x 10 ⁻⁸	2.08 x 10 ⁻⁸
4	1.95	0.994	23.2	LFC	0.23	320	-1.66	13.1	2.07 x 10 ⁻⁸	1.90 x 10 ⁻⁸
5	3.89	0.987	23.2	LFC	0.23	1985	-1.67	26.2	4.59 x 10 ⁻⁸	4.21 x 10 ⁻⁸
6	4.46	0.997	23.2	LFC	0.23	2116	-1.70	30.0	5.72 x 10 ⁻⁸	5.24 x 10 ⁻⁸
7	3.43	0.976	23.2	LFC	0.23	1856	-1.80	23.1	5.62 x 10 ⁻⁸	5.12 x 10 ⁻⁸
8	5.46	0.999	23.2	LFC	0.22	1914	-1.66	36.7	6.26 x 10 ⁻⁸	5.70 x 10 ⁻⁸
9	5.26	0.995	23.2	LFC	0.22	2047	-1.67	35.4	6.23 x 10 ⁻⁸	5.66 x 10 ⁻⁸

20	0.06	0.08	0.06	4.05	2.32	2.28	1.65	0.60	1.02	1.47	5.46
	0.947	0.974	0.961	0.998	0.970	0.924	0.919	0.601	0.461	0.996	0.980
25	25	25	25	23.2	23.2	23.2	23.2	23.8	23.8	23.2	23.2
LFC	LFC	LFC	LFC	LFC	LFC	LFC	LFC	LFC	LFC	LFC	LFC
0.13	4959	5019	1398	1425	1773	2692	2904	2737	1610	1773	
	-1.52	-1.51	-1.60	-1.60	-1.57	-1.58	-1.58	-1.58	-2.24	-1.85	
0.4	0.6	0.4	27.2	15.6	15.3	11.1	4.0	6.9	9.9	36.7	
5.46×10^{-10}	7.43×10^{-10}	5.55×10^{-10}	3.91×10^{-8}	2.24×10^{-8}	2.07×10^{-8}	1.60×10^{-8}	5.82×10^{-9}	9.90×10^{-9}	8.10×10^{-8}	1.01×10^{-7}	
5.69×10^{-10}	7.77×10^{-10}	5.79×10^{-10}	3.71×10^{-8}	2.14×10^{-8}	1.98×10^{-8}	1.53×10^{-8}	5.60×10^{-9}	9.52×10^{-9}	7.35×10^{-8}	9.17×10^{-8}	

31		30	29	28	27	26	25	24	23	22	21
5.75	4.07	3.57	3.50	3.11	0.13	-0.10	0.10	0.09	0.07	0.06	
0.996	0.983	0.985	0.983	0.991	0.982	0.976	0.957	0.926	0.957	0.962	
25.6	25.3	25.3	25	25	25	25	25	25	25	25	25
SFC	SFC	SFC	SFC	SFC	LFC	LFC	LFC	LFC	LFC	LFC	LFC
0.17	0.17	0.17	0.17	0.17	0.13	0.13	0.13	0.13	0.13	0.13	0.13
852	1051	894	1011	793	4787	4824	4845	4874	4910	4938	
-1.79	-1.89	-1.94	-1.96	-2.01	-1.50	-1.49	-1.50	-1.50	-1.51	-1.52	
25.6	18.2	15.9	15.6	13.9	0.9	-0.7	0.6	0.6	0.5	0.4	
5.68×10^{-8}	5.22×10^{-8}	5.11×10^{-8}	5.34×10^{-8}	5.26×10^{-8}	1.14×10^{-9}	8.27×10^{-10}	8.11×10^{-10}	7.43×10^{-10}	6.32×10^{-10}	5.85×10^{-10}	
5.31×10^{-8}	4.88×10^{-8}	4.78×10^{-8}	4.99×10^{-8}	4.92×10^{-8}	1.18×10^{-9}	8.59×10^{-10}	8.42×10^{-10}	7.70×10^{-10}	6.58×10^{-10}	6.09×10^{-10}	

42	41	40	39	38	37	36	35	34	33	32
1.00	0.67	1.49	1.63	1.75	1.61	6.66	10.4	11.8	9.18	7.57
0.974	0.908	0.940	0.985	0.964	0.814	0.994	0.997	0.994	0.976	0.992
28.8	28.6	28.2	28.5	28.3	28.1	23.2	25.6	25.7	25.8	25.6
SFC	SFC	SFC	SFC	SFC	SFC	SFC	SFC	SFC	SFC	SFC
0.18	0.18	0.18	0.18	0.18	0.18	0.17	0.17	0.17	0.17	0.17
798	1067	817	791	843	864	1417	753	755	1850	1043
-2.35	-2.38	-2.29	-2.30	-2.29	-2.24	-1.74	-1.57	-1.48	-1.53	-1.68
4.4	3.0	6.6	7.2	7.7	7.1	29.9	46.3	52.6	40.9	33.7
4.07×10^{-8}	3.26×10^{-8}	5.20×10^{-8}	5.80×10^{-8}	6.14×10^{-8}	4.95×10^{-8}	6.06×10^{-8}	6.02×10^{-8}	5.53×10^{-8}	5.03×10^{-8}	5.78×10^{-8}
3.55×10^{-8}	2.84×10^{-8}	4.54×10^{-8}	5.08×10^{-8}	5.38×10^{-8}	4.34×10^{-8}	5.67×10^{-8}	5.63×10^{-8}	5.17×10^{-8}	4.70×10^{-8}	5.40×10^{-8}

TABLE 5. FLOATING CHAMBER DESIGN CHARACTERISTICS

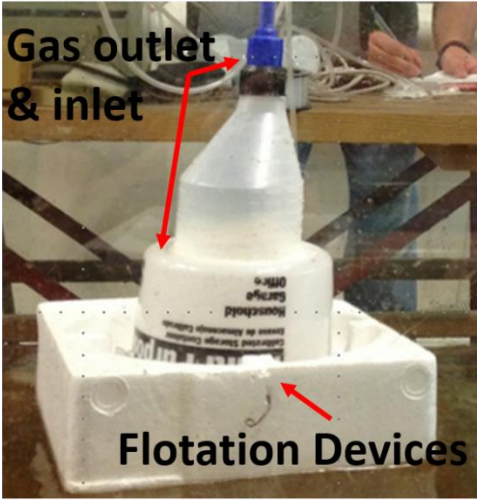
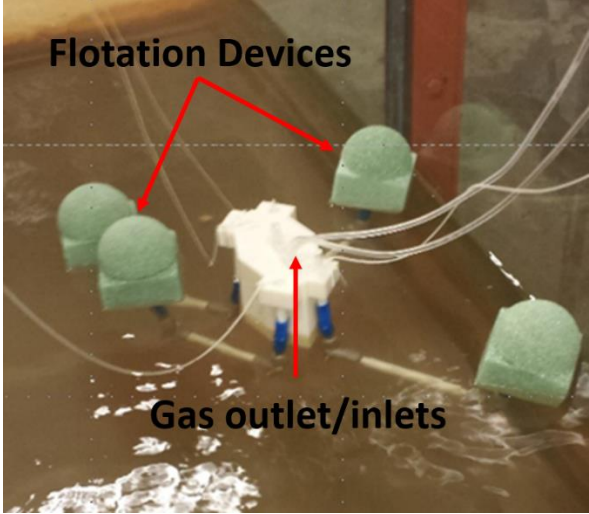
Large Floating Chamber (LFC)	Stream-lined Floating Chamber (SFC)
	
<p>Area: 0.035 m²</p> <p>Volume: 5.73 L</p> <p>Material: Inverted polypropylene bucket sealed to an inverted funnel.</p> <p>Other characteristics: Styrofoam floats immediately adjacent to where the device contacted the water surface.</p>	<p>Area: 0.0094 m²</p> <p>Volume: 1.03 L</p> <p>Material: 3D printed ABS P-240 plastic coated in paraffin wax to reduce gas permeability.</p> <p>Other characteristics: Styrofoam floats were extended away from the device where it contacted the water surface.</p>

TABLE 6. CO₂ DEGASSING BEAKER STIRRING PLATE SIMULATIONS

Water Sample	Stirring Rate (rpm)	Duration (min.)
High CO ₂ Flume Water	0	110
High CO ₂ Flume Water	90	110
High CO ₂ Flume Water	90	166
Normal CO ₂ Flume Water	90	166

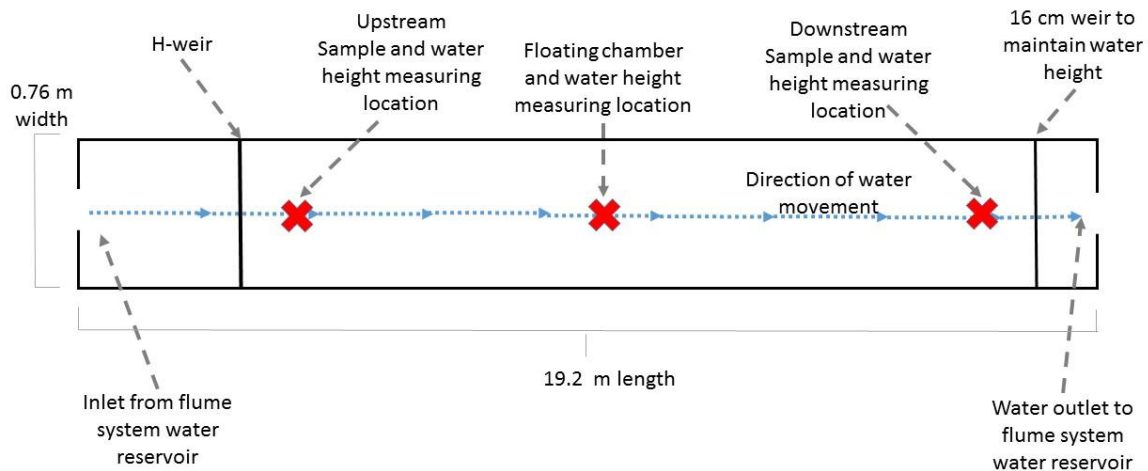
Figures

Figure 1. Schematic detailing the flume channel from a map view. Relevant details for experiments are noted.

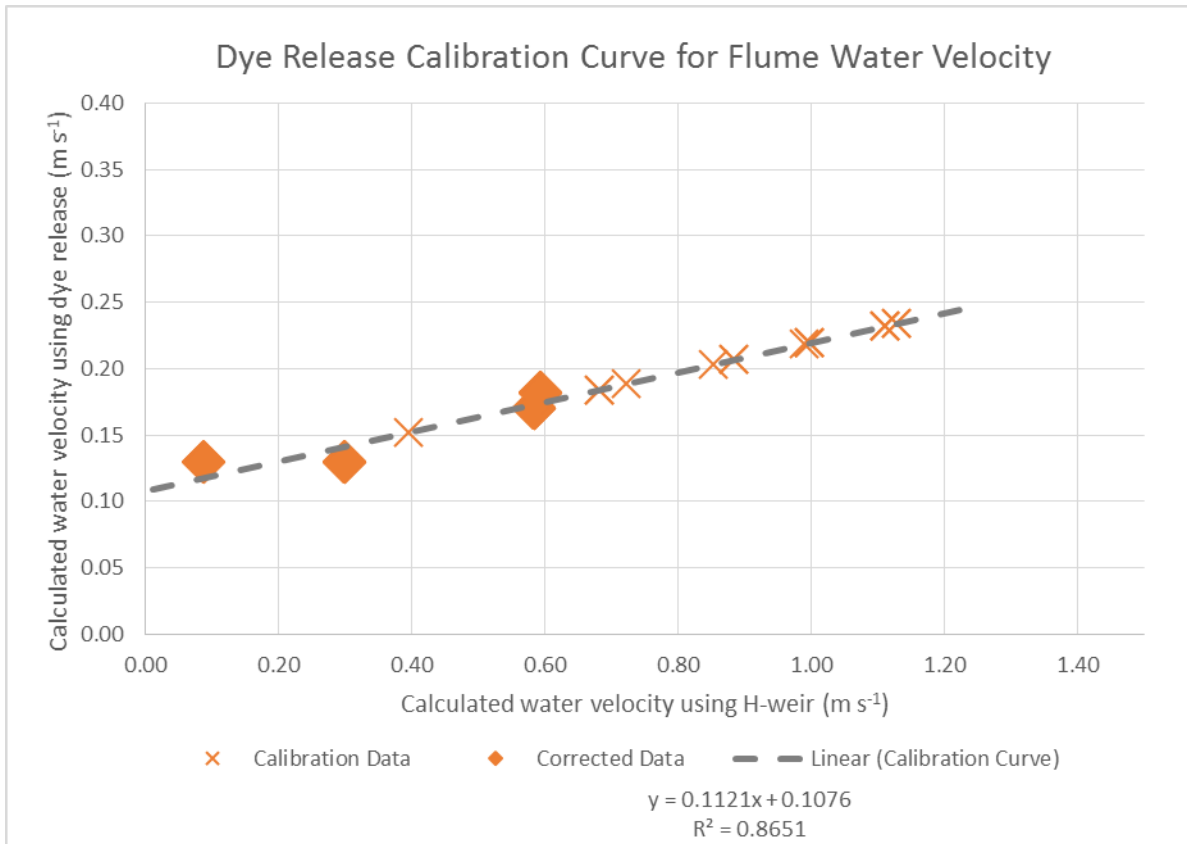


Figure 2. Calibration curve for calculating flume water velocity in m s^{-1} .

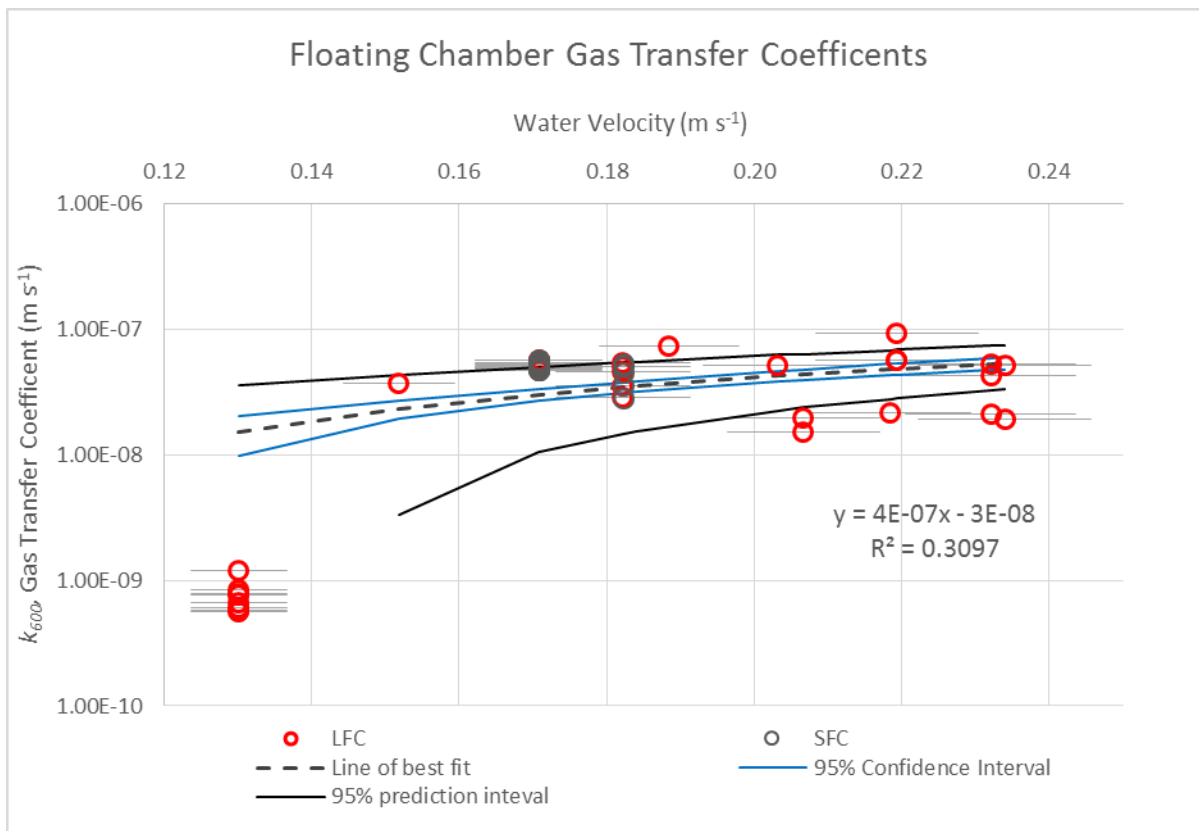


Figure 3. All accepted measurements of floating chamber gas transfer corrected for temperature.

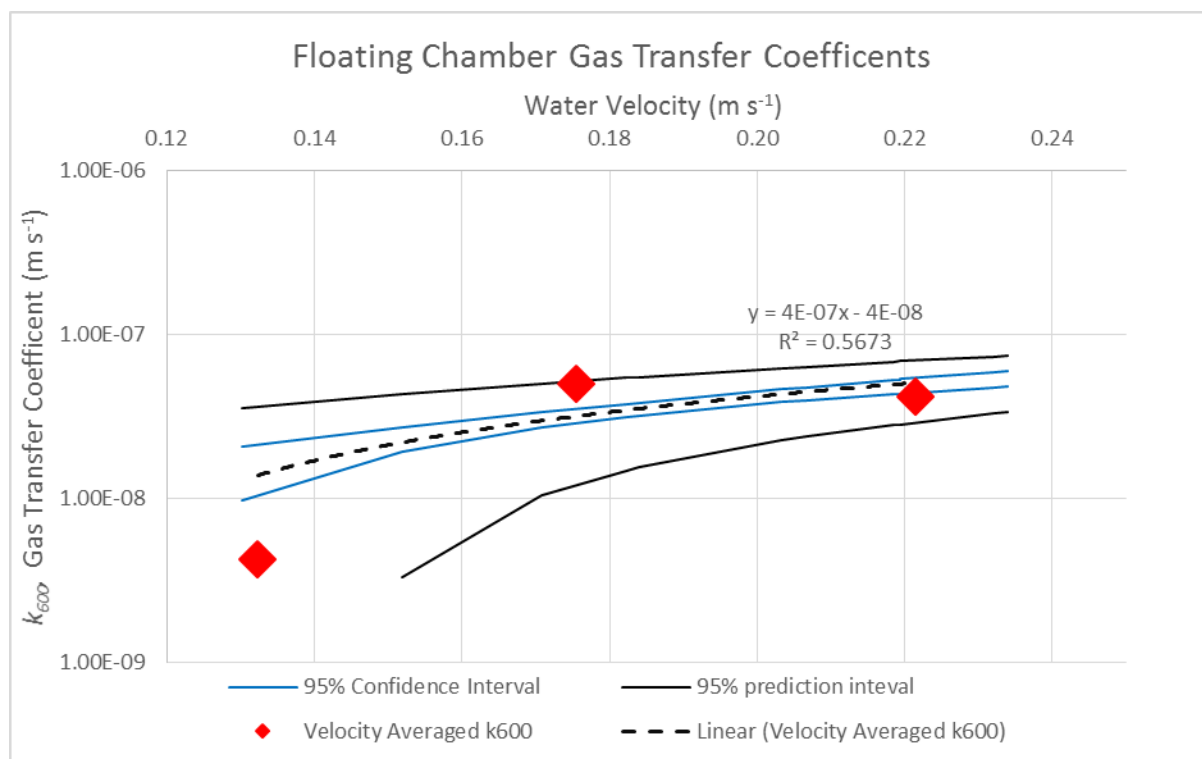


Figure 4. Gas transfer coefficients corrected for temperature (k_{600}) and averaged by water velocity. The highest water velocity incorporates all points greater than or equal to 0.20 m s^{-1} , the medium water velocity averages all points between 0.16 m s^{-1} and 0.19 m s^{-1} , and the lowest water velocity averages all points below or equal to 0.15 m s^{-1} .

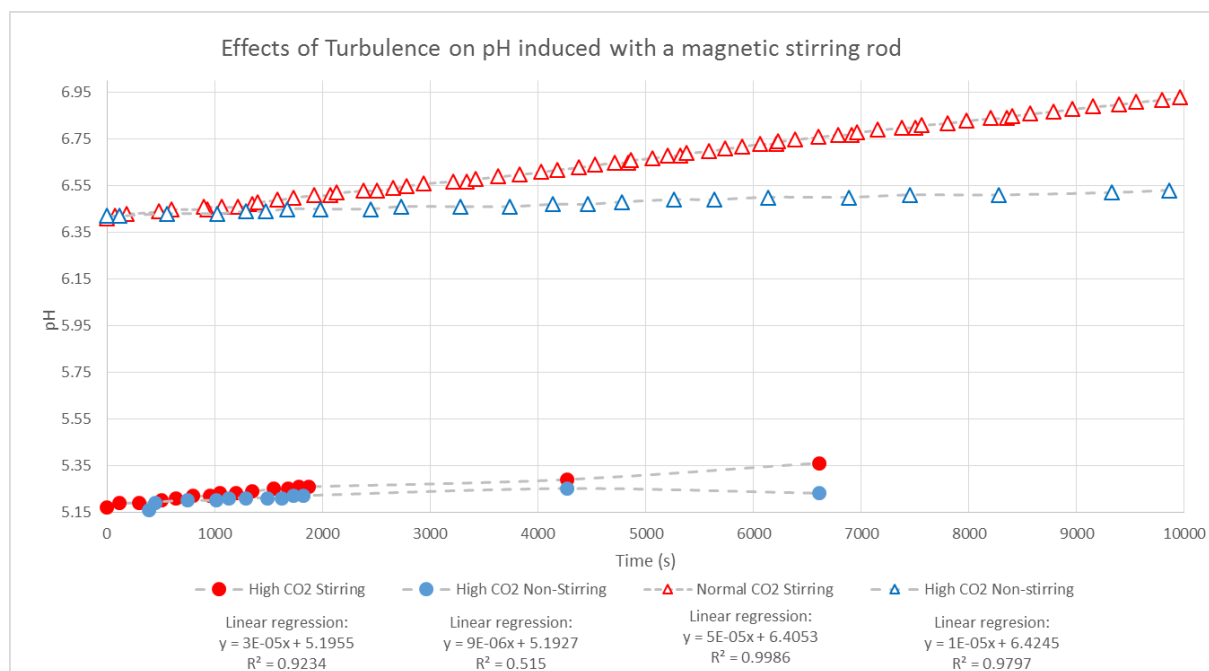


Figure 5. Results of the stirring plate simulations at two different CO₂ concentrations. Error bars of 0.01 representing the accuracy of the pH meter are smaller than the symbols.

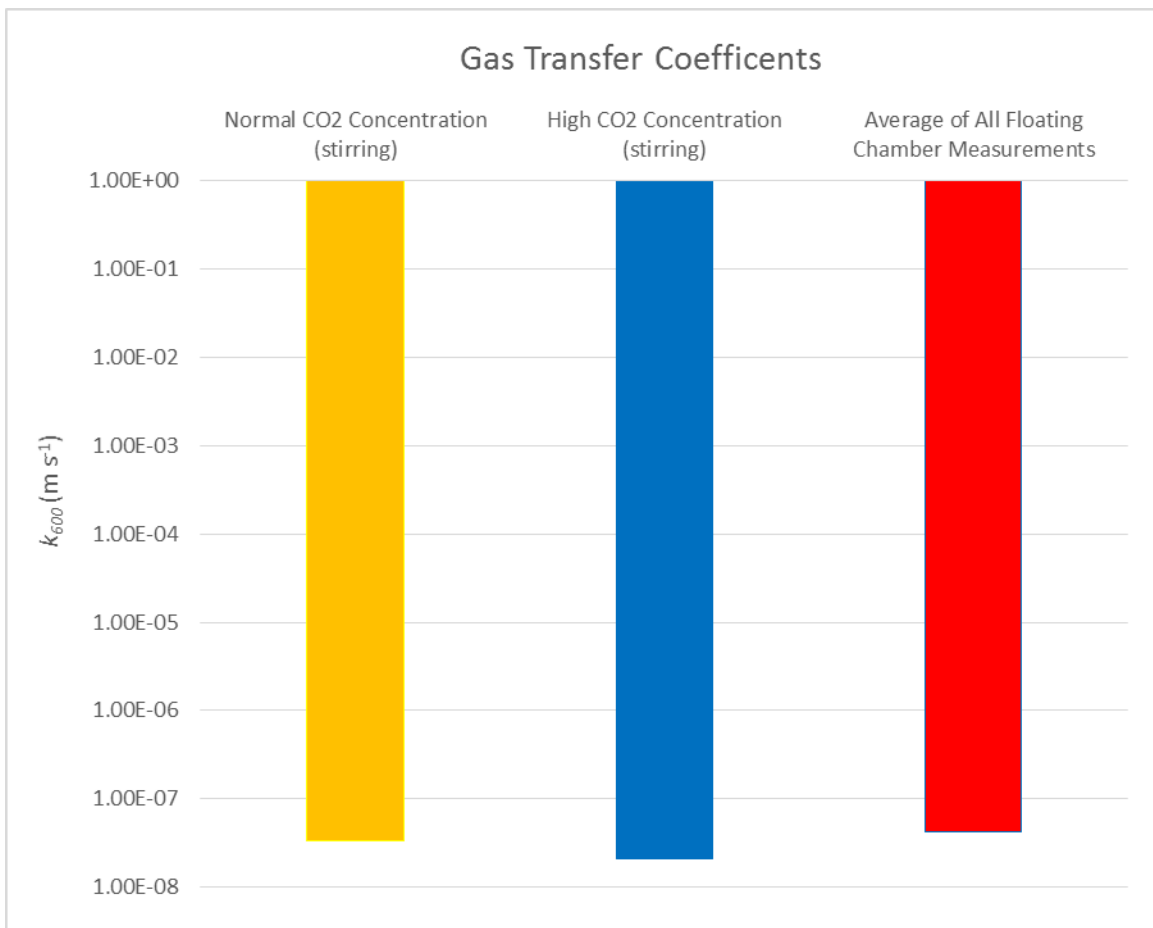


Figure 6. Gas transfer coefficients averaged for all flume experiments, and shown for both stirring plate simulations of the flume system.

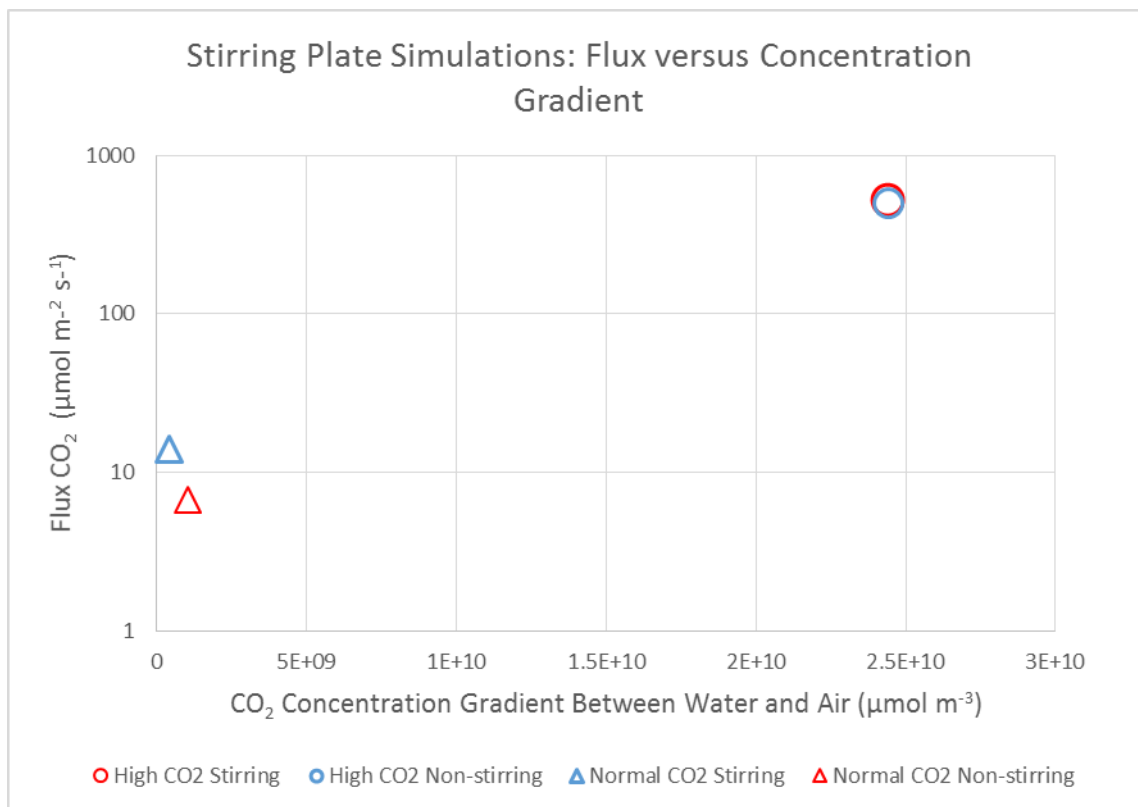


Figure 7. Response of flux to the CO₂ gradient between the atmosphere and the water for stirring plate simulations.

References

- Abongwa, P. T., and Atekwana, E. A., 2013, Assessing the temporal evolution of dissolved inorganic carbon in waters exposed to atmospheric CO₂(g): A laboratory approach: *Journal of Hydrology*, v. 505, p. 250-265.
- Alin, S., Maria de Fátima, F.L., Krusche, A. V., Richey, J. E., Ballester, M. V., and Victória, R. L., 2013, Spatial and temporal variability of pCO₂ and CO₂ efflux in seven Amazonian Rivers: *Biogeochemistry*, v. 116, no. 1-3, p. 241-259
- Alin, S. R., Maria de Fátima, F.L. M., Salimon, C. I., Richey, J. E., Holtgrieve, G. W., Krusche, A. V., and Snidvongs, A., 2011, Physical controls on carbon dioxide transfer velocity and flux in low-gradient river systems and implications for regional carbon budgets: *Journal of Geophysical Research: Biogeosciences (2005–2012)*, v. 116, no. G1.
- Aufdenkampe, A. K., Mayorga, E., Raymond, P. A., Melack, J. M., Doney, S. C., Alin, S. R., Aalto, R. E., and Yoo, K., 2011, Riverine coupling of biogeochemical cycles between land, oceans, and atmosphere: *Frontiers in Ecology and the Environment*, v. 9, no. 1, p. 53-60.
- Bastien, J., and Demarty, M., 2013, Spatio-temporal variation of gross CO₂ and CH₄ diffusive emissions from Australian reservoirs and natural aquatic ecosystems, and estimation of net reservoir emissions: *Lakes & Reservoirs: Research & Management*, v. 18, no. 2, p. 115-127.
- Battin, T. J., Luysaert, S., Kaplan, L. A., Aufdenkampe, A. K., Richter, A., and Tranvik, L. J., 2009, The boundless carbon cycle: *Nature Geoscience*, v. 2, no. 9, p. 598-600.
- Beaulieu, J. J., Shuster, W. D., and Rebolz, J. A., 2012, Controls on gas transfer velocities in a large river: *Journal of Geophysical Research*, v. 117, no. G2.

- Bednařík, A., Čáp, L., Maier, V., and Rulík, M., 2015, Contribution of Methane Benthic and Atmospheric Fluxes of an Experimental Area (Sitka Stream): *Clean –Soil, Air, Water*, v. 43, p. 1-7.
- Belger, L., Forsberg, B. R., and Melack, J. M., 2011, Carbon dioxide and methane emissions from interfluvial wetlands in the upper Negro River basin, Brazil: *Biogeochemistry*, v. 105, no. 1-3, p. 171-183.
- Billett, M., Garnett, M., and Dinsmore, K., 2015, Should Aquatic CO₂ Evasion be Included in Contemporary Carbon Budgets for Peatland Ecosystems? : *Ecosystems*, v. 18, no. 3 p. 471-480.
- Billett, M., and Harvey, F., 2013, Measurements of CO₂ and CH₄ evasion from UK peatland headwater streams: *Biogeochemistry*, v. 114, no. 1-3, p. 165-181.
- Borges, A. V., Darchambeau, F., Teodoru, C. R., Marwick, T. R., Tamooh, F., Geeraert, N., Omengo, F. O., Guérin, F., Lambert, T., and Morana, C., 2015, Globally significant greenhouse-gas emissions from African inland waters: *Nature Geoscience*, vol. 8, no. 8, p. 637.
- Butman, D., and Raymond, P. A., 2011, Significant efflux of carbon dioxide from streams and rivers in the United States: *Nature Geoscience*, v. 4, no. 12, p. 839-842.
- Campeau, A., Lapierre, J. F., Vachon, D., and Giorgio, P. A., 2014, Regional contribution of CO₂ and CH₄ fluxes from the fluvial network in a lowland boreal landscape of Québec: *Global Biogeochemical Cycles*, v. 28, no. 1, p. 57-69.
- Campeau, A., and Giorgio, P. A., 2014, Patterns in CH₄ and CO₂ concentrations across boreal rivers: Major drivers and implications for fluvial greenhouse emissions under climate change scenarios: *Global change biology*, v. 20, no. 4, p. 1075-1088.

- Chen, J., Cao, W., Cao, D., Huang, Z., and Liang, Y., 2015, Nitrogen Loading and Nitrous Oxide Emissions from a River with Multiple Hydroelectric Reservoirs: *Bulletin of Environmental Contamination and Toxicology*, vol. 94, no. 5, p. 633-639.
- Cole, J. J., and Caraco, N. F., 1998, Atmospheric exchange of carbon dioxide in a low-wind oligotrophic lake measured by the addition of SF₆: *Limnology and Oceanography*, v. 43, no. 4, p. 647-656.
- Cole, J. J., Prairie, Y. T., Caraco, N. F., McDowell, W. H., Tranvik, L. J., Striegl, R. G., Duarte, C. M., Kortelainen, P., Downing, J. A., Middelburg, J. J., and Melack, J., 2007, Plumbing the Global Carbon Cycle: Integrating Inland Waters into the Terrestrial Carbon Budget: *Ecosystems*, v. 10, no. 1, p. 172-185.
- Cole, J. J., Bade, D. L., Bastviken, D., Pace, M. L., and Van de Bogert, M., 2010, Multiple approaches to estimating air-water gas exchange in small lakes: *Limnology and Oceanography: Methods*, v. 8, p. 285-293.
- Crawford, J. T., Striegl, R. G., Wickland, K. P., Dornblaser, M. M., and Stanley, E. H., 2013, Emissions of carbon dioxide and methane from a headwater stream network of interior Alaska: *Journal of Geophysical Research: Biogeosciences*, v. 118, no. 2, p. 482-494.
- Crawford, J. T., Dornblaser, M. M., Stanley, E. H., Clow, D. W., and Striegl, R. G., 2015, Source limitation of carbon gas emissions in high-elevation mountain streams and lakes: *Journal of Geophysical Research: Biogeosciences*, v. 118, p. 1-14
- Denfeld, B. A., Frey, K. E., Sobczak, W. V., Mann, P. J., and Holmes, R. M., 2013, Summer CO₂ evasion from streams and rivers in the Kolyma River basin, north-east Siberia: *Polar Research*, v. 32, 19704.

- Deshmukh, C., Guérin, F., Pighini, S., Vongkhamsao, A., Guédant, P., Rode, W., Godon, A., Chanudet, V., Descloux, S., and Serça, D., 2015, Low methane (CH₄) emissions downstream of a monomictic subtropical hydroelectric reservoir (Nam Theun 2, Lao PDR). *Biogeosciences Discuss*, v. 12, p. 1113-11347.
- Dinsmore, K. J., Billett, M. F., Skiba, U. M., Rees, R. M., Drewer, J., and Helfter, C., 2010, Role of the aquatic pathway in the carbon and greenhouse gas budgets of a peatland catchment: *Global Change Biology*, v. 16, no. 10, p. 2750-2762.
- Genereux, D. P., and Hemond, H. F., 1992, Determination of gas exchange rate constants for a small stream on Walker Branch Watershed, Tennessee: *Water Resources Research*, v. 28, no. 9, p. 2365-2374.
- Gómez-Gener, L., Obrador, B., von Schiller, D., Marcé, R., Casas-Ruiz, J. P., Proia, L., Acuña, V., Catalán, N., Muñoz, I., and Koschorreck, M., Hot spots for carbon emissions from Mediterranean fluvial networks during summer drought: *Biogeochemistry*, v. 33 (2), p. 349-360.
- Han, Y., Zheng, Y.-f., Wu, R.-j., Yin, J.-f., Xu, J.-x., and Xu, P., 2013, Greenhouse gases emission characteristics of Nanjing typical waters in Spring: *China Environmental Science*, v. 8, p. 004.
- Hotchkiss, E., Hall Jr, R., Sponseller, R., Butman, D., Klaminder, J., Laudon, H., Rosvall, M., and Karlsson, J., 2015, Sources of and processes controlling CO₂ emissions change with the size of streams and rivers: *Nature Geoscience*, vol. 8, no. 9, p. 696-699.
- Huotari, J., Haapanala, S., Pumpanen, J., Vesala, T., and Ojala, A., 2013, Efficient gas exchange between a boreal river and the atmosphere: *Geophysical Research Letters*, v. 40, no. 21, p. 5683-5686.

- Jähne, B., Münnich, K. O., Börsinger, R., Dutzi, A., Huber, W., and Libner, P., 1987, On the parameters influencing air-water gas exchange: *Journal of Geophysical Research: Oceans* (1978–2012), v. 92, no. C2, p. 1937-1949.
- Jones, D. S., Polerecky, L., Galdenzi, S., Dempsey, B. A., and Macalady, J. L., 2015, Fate of sulfide in the Frasassi cave system and implications for sulfuric acid speleogenesis: *Chemical Geology*, v. 410, p. 21-27.
- Juutinen, S., Väiliranta, M., Kuutti, V., Laine, A., Virtanen, T., Seppä, H., Weckström, J., and Tuittila, E. S., 2013, Short-term and long-term carbon dynamics in a northern peatland-stream-lake continuum: A catchment approach: *Journal of Geophysical Research: Biogeosciences*, v. 118, no. 1, p. 171-183.
- Khadka, M. B., Martin, J. B., and Jin, J., 2014, Transport of dissolved carbon and CO₂ degassing from a river system in a mixed silicate and carbonate catchment: *Journal of Hydrology*, v. 513, p. 391-402.
- Kremer, J.N., Nixon, S.W., Buckley, B., and Roques, P., 2003, Technical Note: Conditions for Using the Floating Chamber Method to Estimate Air-Water Gas Exchange: *Estuaries*, v. 26, no. 4A, p. 985-990.
- Krenz, J., 2013, Measuring CO₂ emissions from a small boreal lake and its connecting streams using automatic floating chambers [M.S. thesis]: Swedish University of Agricultural Sciences.
- Lambert, M., and Fréchet, J.-L., 2005, Analytical techniques for measuring fluxes of CO₂ and CH₄ from hydroelectric reservoirs and natural water bodies, *Greenhouse Gas Emissions—Fluxes and Processes*, Springer, p. 37-60.

- Liu, H., 2014, Inorganic and Organic Carbon Variations in Surface Water, Konza Prairie LTER Site, USA and Maolan Karst Experimental Site, China [M.S. thesis]: University of Kansas Geology.
- Liu, Z., Dreybrodt, W., and Wang, H., 2008, A possible important CO₂ sink by the global water cycle: Chinese Science Bulletin, v. 53, no. 3, p. 402-407.
- Lorke, A., Bodmer, P., Noss, C., Alshboul, Z., Koschorreck, M., Somlai, C., Bastviken, D., Flury, S., McGinnis, D., and Maeck, A., 2015, Technical Note: Drifting vs. anchored flux chambers for measuring greenhouse gas emissions from running waters. Biogeosciences Discuss., v. 12, p. 1461-14645.
- Luan, J., and Wu, J., 2015, Long-term agricultural drainage stimulates CH₄ emissions from ditches through increased substrate availability in a boreal peatland: Agriculture, Ecosystems & Environment, v. 214, p. 68-77.
- Macpherson, G., 2009, CO₂ distribution in groundwater and the impact of groundwater extraction on the global C cycle: Chemical Geology, v. 264, no. 1, p. 328-336.
- Matthews, C. J. D., St. Louis, V. L., and Hesslein, R. H., 2003, Comparison of Three Techniques Used To Measure Diffusive Gas Exchange from Sheltered Aquatic Surfaces: Environmental Science & Technology, v. 37, no. 4, p. 772-780.
- Mazot, A., and Bernard, A., 2015, CO₂ degassing from volcanic lakes, Volcanic Lakes, Springer, Berlin Heidelberg, p. 341-354.
- Morse, N., Bowden, W. B., Hackman, A., Pruden, C., Steiner, E., and Berger, E., 2007, Using sound pressure to estimate reaeration in streams: Journal of the North American Benthological Society, v. 26, no. 1, p. 28-37.

- Müller, D., Warneke, T., Rixen, T., Müller, M., Jamahari, S., Denis, N., Mujahid, A., and Notholt, J., 2015, Lateral carbon fluxes and CO₂ outgassing from a tropical peat-draining river: *Lateral*, v. 12, p. 10389-10424.
- Neal, C., House, W. A., and Down, K., 1998, An assessment of excess carbon dioxide partial pressures in natural waters based on pH and alkalinity measurements: *Science of the Total Environment*, v. 210, p. 173-185.
- Neu, V., Neill, C., and Krusche, A. V., 2011, Gaseous and fluvial carbon export from an Amazon forest watershed: *Biogeochemistry*, v. 105, no. 1-3, p. 133-147.
- Owens, M., Edwards, R., and Gibbs, J., 1964, Some reaeration studies in streams: *Air and water pollution*, v. 8, p. 469.
- Parkhurst, D. L., and Appelo, C., 1999, User's guide to PHREEQC (Version 2): A computer program for speciation, batch-reaction, one-dimensional transport, and inverse geochemical calculations.
- Ran, L., Lu, X. X., Yang, H., Li, L., Yu, R., Sun, H., and Han, J., 2015, CO₂ outgassing from the Yellow River network and its implications for riverine carbon cycle: *Journal of Geophysical Research: Biogeosciences*, vol. 120, p. 1334-1347.
- Raymond, P. A., and Cole, J. J., 2001, Gas exchange in rivers and estuaries: Choosing a gas transfer velocity: *Estuaries and Coasts*, v. 24, no. 2, p. 312-317.
- Raymond, P. A., Zappa, C. J., Butman, D., Bott, T. L., Potter, J., Mulholland, P., Laursen, A. E., McDowell, W. H., and Newbold, D., 2012, Scaling the gas transfer velocity and hydraulic geometry in streams and small rivers: *Limnology & Oceanography: Fluids & Environments*, v. 2, no. 0, p. 41-53.

- Richey, J. E., Krusche, A. V., Johnson, M. S., Da Cunha, H. B., and Ballester, M. V., 2009, The role of rivers in the regional carbon balance: Amazonia and Global Change, v. 186, p. 489-504.
- Sand-Jensen, K., and Staehr, P. A., 2012, CO₂ dynamics along Danish lowland streams: water–air gradients, piston velocities and evasion rates: *Biogeochemistry*, v. 111, no. 1-3, p. 615-628.
- Sawakuchi, H., Rasera, M., Krusche, A., and Ballester, M., Methane Emission from Tropical Rivers, in *Proceedings EGU General Assembly Conference Abstracts 2012*, v. 14, p. 11440.
- Sha, C., Mitsch, W. J., Mander, Ü., Lu, J., Batson, J., Zhang, L., and He, W., 2011, Methane emissions from freshwater riverine wetlands: *Ecological Engineering*, v. 37, no. 1, p. 16-24.
- Streeter, H., and Phelps, E., 1925, A Study of the Pollution and Natural Purification of the Ohio River, Illinois Factors Concerned in the Phenomenon of Oxidation and Reaeration: *Public Health Service Bulletin*, v. 146.
- Striegl, R. G., Dornblaser, M., McDonald, C., Rover, J., and Stets, E., 2012, Carbon dioxide and methane emissions from the Yukon River system: *Global Biogeochemical Cycles*, v. 26, no. 4.
- Teodoru, C., Nyoni, F., Borges, A., Darchambeau, F., Nyambe, I., and Bouillon, S., 2015, Dynamics of greenhouse gases (CO₂, CH₄, N₂O) along the Zambezi River and major tributaries, and their importance in the riverine carbon budget: *Biogeosciences*, v. 12, no. 8, p. 2431-2453.

- Vachon, D., Prairie, Y. T., and Cole, J. J., 2010, The relationship between near-surface turbulence and gas transfer velocity in freshwater systems and its implications for floating chamber measurements of gas exchange: *Limnology and Oceanography*, v. 55, no. 4, p. 1723.
- Xia, Y., Li, Y., Li, X., Guo, M., She, D., and Yan, X., 2013, Diurnal pattern in nitrous oxide emissions from a sewage-enriched river: *Chemosphere*, v. 92, no. 4, p. 421-428.

APPENDICES

Appendix A. Gas permeability trials

Goal

The material used to create the stream-lined floating chamber (SFC) was highly permeable to gas. Twenty-six experiments detailed in the following appendix were designed and implemented to test the gas permeability of several materials used to coat the 3D plastic structure, and also to test if any CO₂ was emitted from the 3D plastics. The goals of the experiments were to find a material to coat the 3D printed chamber to make it gas impermeable, and to ensure that the 3D plastic did not emit CO₂.

Methods

A custom floating chamber design (SFC) was created in Google SketchUp 2015, and three-dimensionally printed with a Uprint 3D Printer system using high density ABS P-240 plastic. Before this design was completed multiple experimental trials were conducted using high density, low density, and solid plastic coated with gas impermeable substances (flex seal, a silicone epoxy, and paraffin wax), and tested for gas permeability. The 3D printer prints the material in a dense honeycomb structure supported by soluble support plastic. The ABS plastic is malleable at high temperatures and needs the support plastic to maintain stability, but the support plastic is no longer needed at room temperatures.

The printer was used to create a tube design with two ports that served as a gas inlet and outlet for a tight seal with gas impermeable tubing (Figure 1). A known concentration of 2026 CO₂ ppmv gas was then circulated through the tube in a sealed loop with the analyzer. Since the tubing in the stem was gas impermeable any observed change in the concentration of the CO₂ is assumed to be due to leaks at gas connections or leaks in the 3D plastic printed testing apparatus. The change in concentration over time inside of the chamber was monitored using a LI-820 CO₂ Infrared Gas Analyzer.

A second set of experiments monitored the air flowing through the tube. The tube was left open to the atmosphere for four trials, and then air was allowed to circulate directly to the analyzer (bypassing the tube) for four trials. The data was then assessed for any significant differences. If the air passing through the tube contained a higher concentration of CO₂ then it would indicate that the 3D plastic emitted CO₂.

Results

The three main processes that appear to be effecting gas concentration changes are tube leaking, diffusion into the plastic on the inside of the tube, and leaks in the system itself (IRGA tubing, etc.). The diffusion and systems leaks are not relevant to our experiment because we cannot correct for the system leak, and we will not have diffusion in the chamber because the inside will be coated. To remove diffusive flux into the plastic and system leaking I created a function to model the effect of these two processes on system concentrations:

Diffusion: Created a polynomial equation to simulate diffusion based on data from the diffusion of CO₂ back into the tube from the plastic in trial 3 (Figure 6).

$$Diffusion\ Out = -30.893 * \ln(t) + 1990$$

Advective leaking: Took data from previous system test to estimate a linear leak rate.

$$Advective\ Leaking = -0.0294 + 1980$$

Summing these two processes gives the blue modeled line in Figure 2. At late times this can be approximated with a linear function for simplicity as demonstrated on the graph. The other two lines on the graph in Figure 2 are simulations with a paraffin wax cover and high density plastic. These are also approximated at late times with a linear function. The slope of these two lines includes diffusion, system leaking, and tube leaking.

Assuming the rates provided from the data, there will be an approximate error from tube leakage, diffusion, and system leakage of 11 ppm at high concentrations (above 1,350 ppm). Removing the modeled error from system leakage and diffusion (sum of 4 ppm) we are left with a total approximate error caused by tube leakage of 7 ppm at high concentrations.

At lower concentrations this rate will be somewhat lower due to the polynomic nature of the gas diffusion through the plastic. In other words as the gradient between the high CO₂ air in the tube and the atmosphere grows less the approximate error should be less. Concentrations in the floating chamber are likely always going to be less than 700 ppm, so we can approximate a 5 ppm error over five minutes caused when using plastic that is coated twice with paraffin wax.

	Leak Rate (ppmv s ⁻¹)	Seconds in 5 minutes	Apx. Error (ppmv) = time in seconds * Leak Rate in ppm
Observed Leak Rate	0.037	300	11.1
Modeled Leak Rate	0.0124	300	3.72
		*Observed leak rate minus modeled leak rate =	7.4
			^Predicted leak rate at high ppmv

Table comparing modeled versus observed leaking rates for 3D printed ABS plastic.

It was also observed (Figure 3) that there was not a significant emission from the printed plastic, so in that regard the plastic proved a suitable material for use in a CO₂ measuring device. All other combinations of plastic printing techniques (low density/high density), and sealant materials tested (flex seal and silicone) proved to be gas permeable (Figures 4, 5, 7, and 8). It was also observed that the 3D plastic requires more than 48 hours post printing to properly dry

and allow the caustic solution used to dissolve 3D printed support plastic to fully evaporate (Figures 8 and 9).

Interpretations and conclusions

The proper application of two or more coats of paraffin wax (more than 48 hours after removing the 3D printed plastic from the caustic soda bath) to the interior and exterior of the 3D printed chamber makes the chamber sufficiently gas impermeable to be used to measure concentration changes inside of the chamber over time. Further, the plastic material does not emit CO₂.

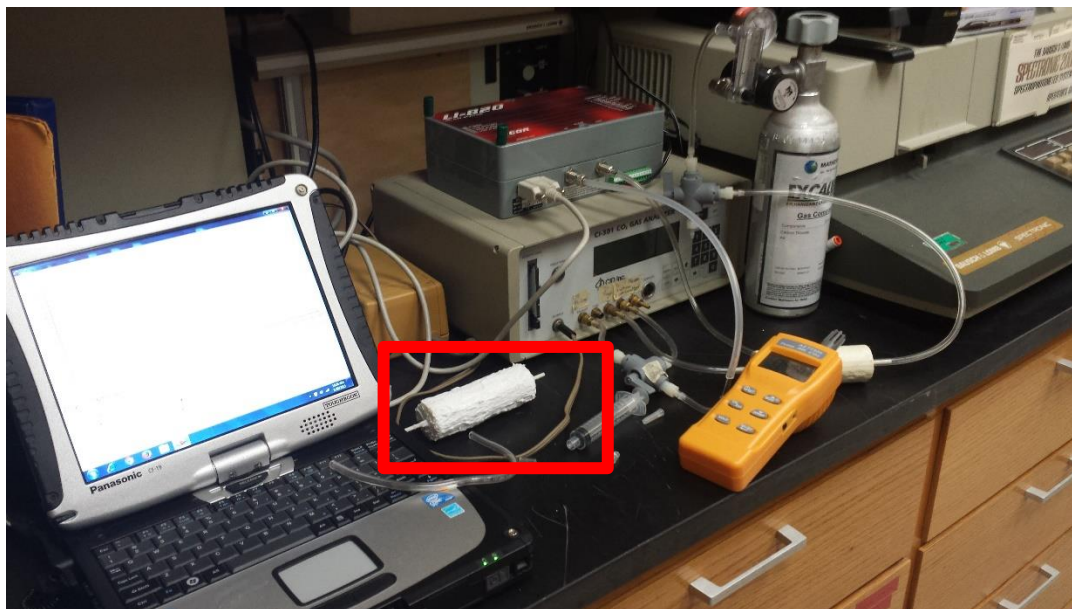


Figure 1. Experimental setup for the experiments to test the gas permeability of the ABS plastic used in the SFC. The experimental tube described in the methods section is highlighted by a red rectangle in the image.

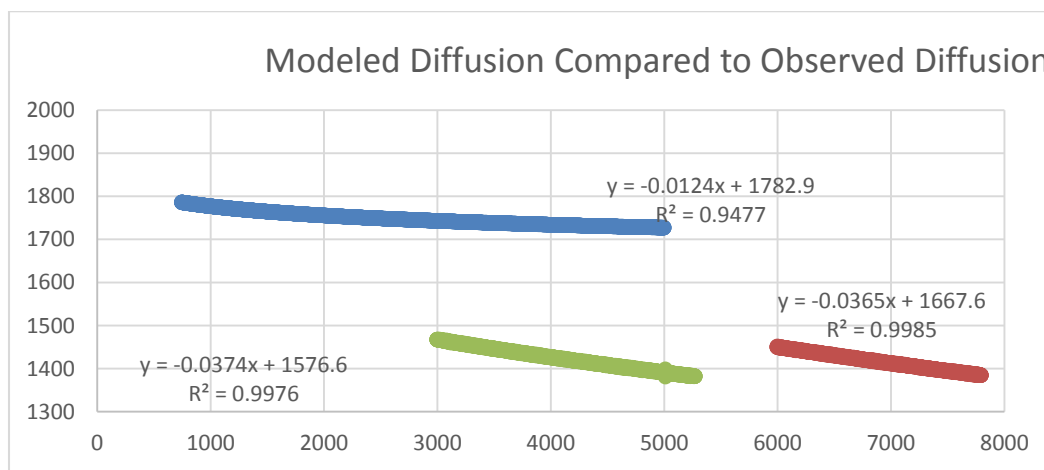


Figure 2. Modeled leakage (blue) versus observed leakage from paraffin wax coated trials (green and maroon).

Trial	1-Room	2-Tube	3-Room	4-Tube	5-Room	6-Tube	7-Room	8-Tube
Average CO ₂ ppm	587	582	563	572	559	641	669	658
Standard Deviation CO ₂ ppm	13	5	3	4	11	5	3	2

Figure 3. There were no patterns in the differences between room air, and room air filtered through the tube in 8 trials.

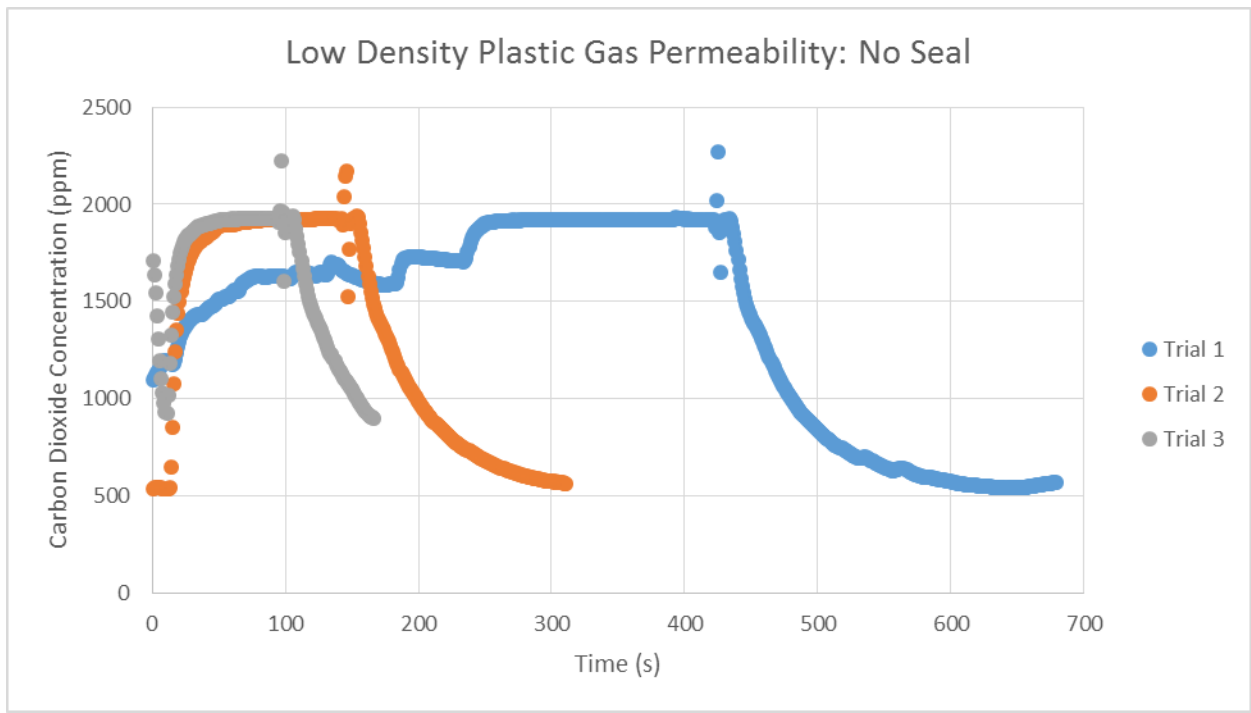


Figure 4. The low density plastic is highly permeable to gases.

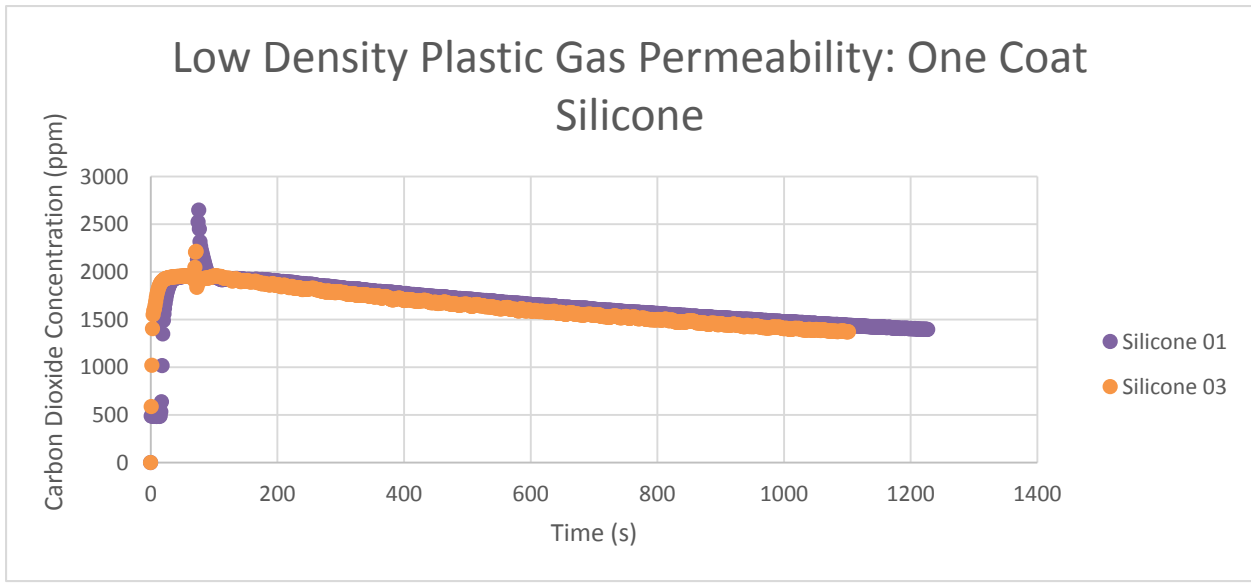


Figure 5. One coat of silicone epoxy dramatically decreases the gas permeability of low density plastic, but the rate of leaking is still too great for the purposes of a gas container.

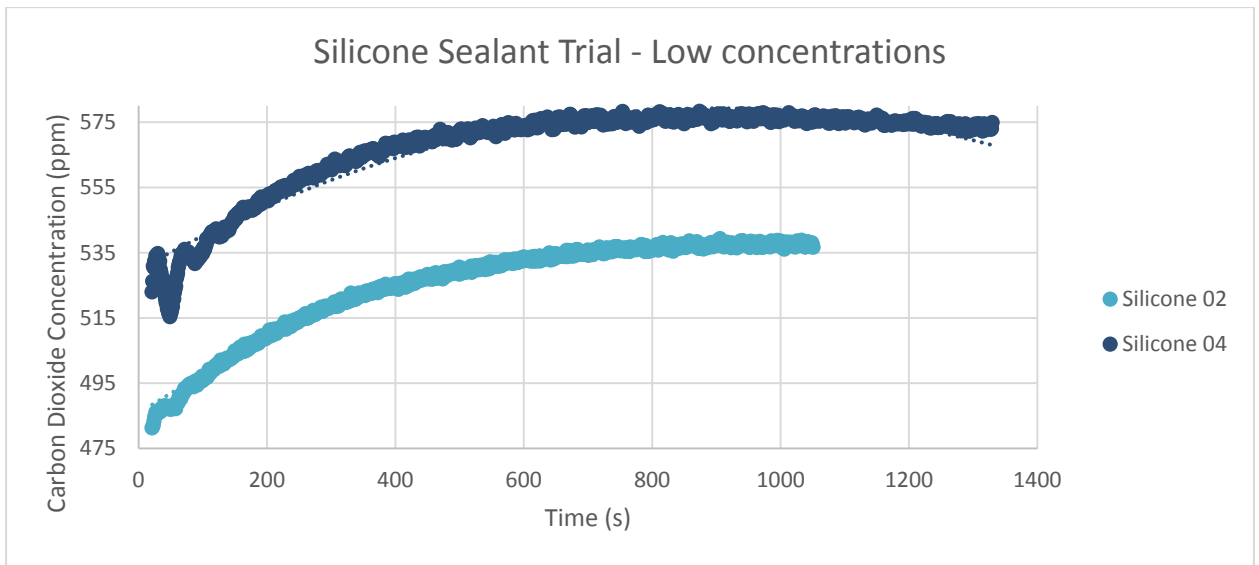


Figure 6. At low concentration trials following the high concentration trials high concentration gas is released back into the tube. This is likely caused by some sort of matrix diffusion of gas into the honeycomb structure of the tube.

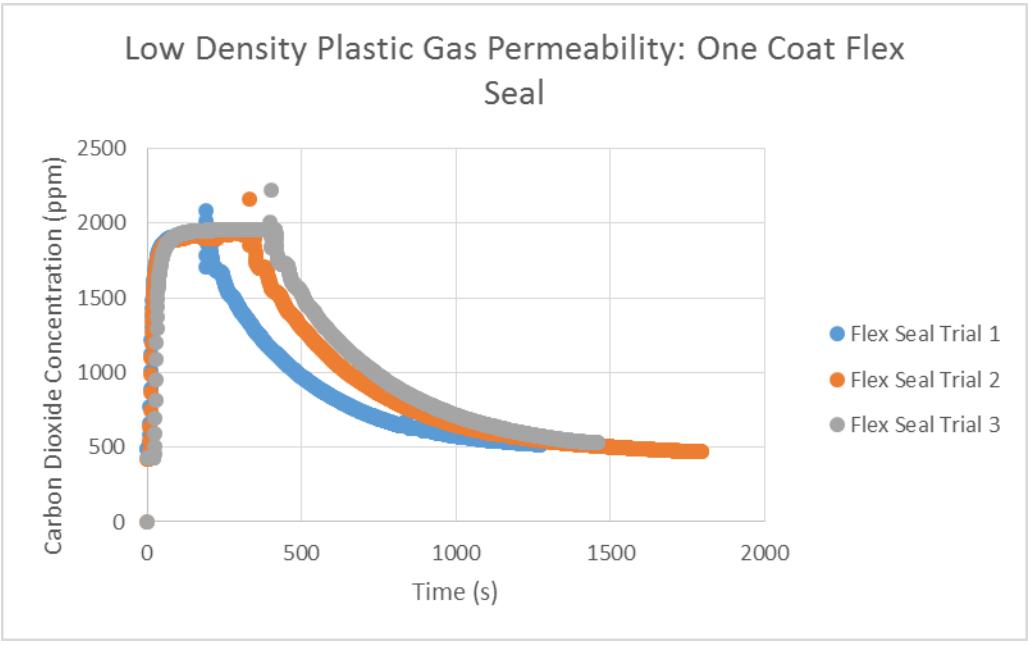


Figure 7. Low density plastic with one coat of flex seal was permeable.

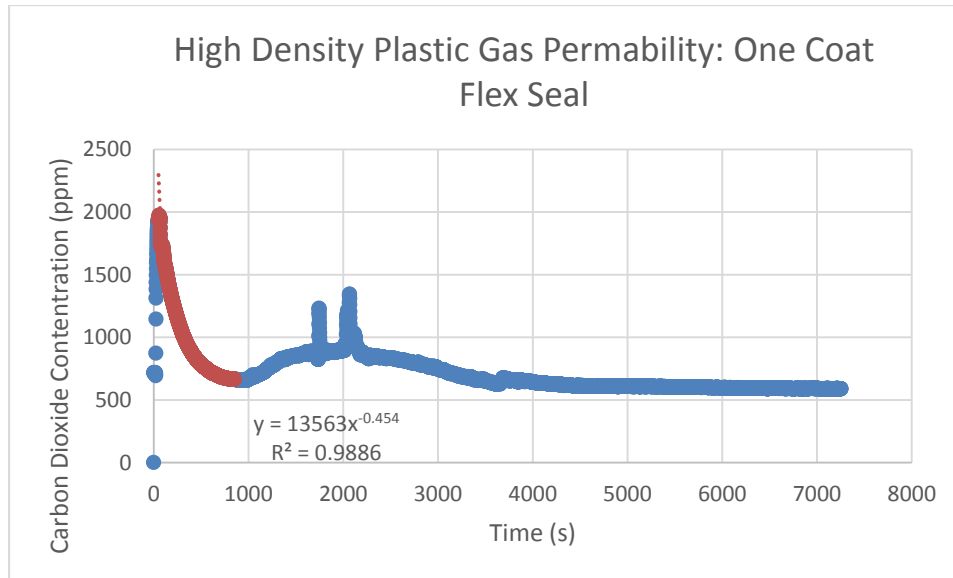


Figure 8. The one coat of flex seal is still highly permeable and is sensitive to outside air movement (ex. someone waving their hand as demonstrated by the bump beginning at time 1000).

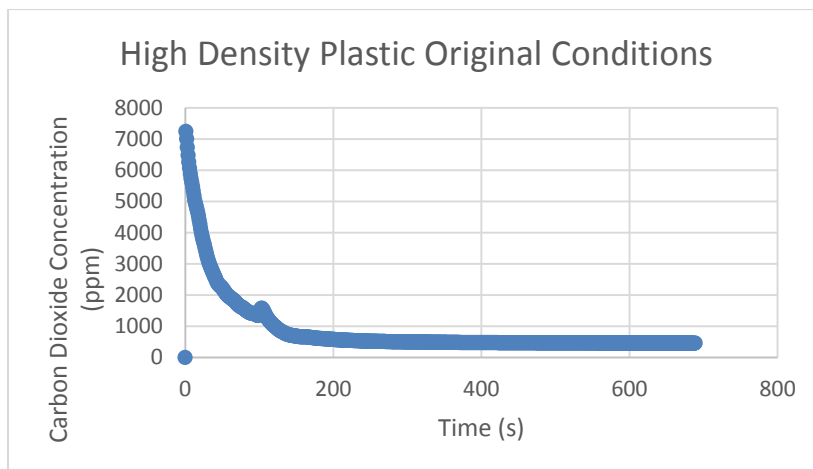


Figure 9. The high density plastic appears to have a very high initial carbon dioxide concentration before it dries out.

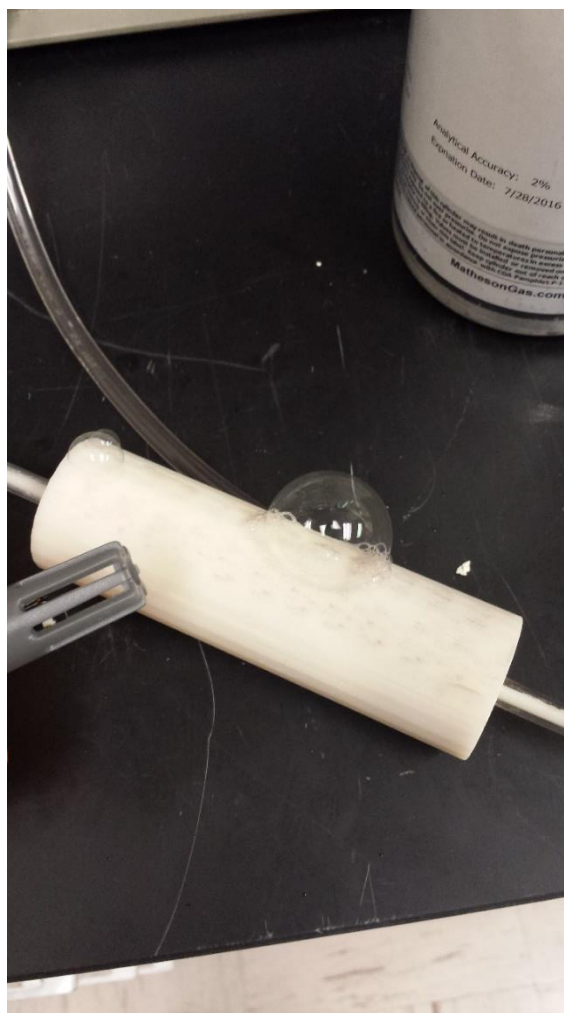


Figure 10. High density plastic not yet dried out.

Appendix B. Water-chemistry Flux

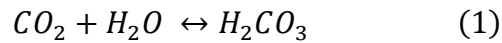
Introduction

The pH levels in the flume experiments were monitored at a point at both the upstream downstream portion of the flume. The change in pH was at or within the uncertainty of the probe used (± 0.01), so it was excluded from the main paper (chapter two). The goal of these measurements was to provide a flux comparable to the floating chamber measurements in the flume experiment.

Methods

Dissolved CO₂ content was calculated using a geochemical speciation model with measured pH and temperature (Orion 8157BNUMD Ross Ultra pH/ATC Triode), alkalinity (titration with 0.017 N HNO₃), and major aqueous cations (ICP-OES) and anions (IC; water chemistry available in Chapter 2: Table 3). Measurements were made and water samples were collected at fixed points near the floating chamber location (Figure 1 of Chapter 2). All water samples were filtered using a 0.45 μm syringe filter within 48 hours of collection. Samples for cation determination were preserved in LPDE containers by acidifying to 2% (v/v) with HNO₃. Cation concentrations were measured using a JY 2000 Inductively Coupled Plasma Optical Emission Spectrometer. Water samples for anions were stored in glass bottles with Teflon-lined lids, refrigerated for preservation, and analyzed using a Dionex 4000i Ion Chromatograph. Samples for alkalinity were stored in glass bottles with Teflon-lined lids, refrigerated for preservation, and titrated using the inflection point method. Results modeled using PHREEQC Interactive 3.1.7-9213 (Parkhurst and Appelo, 1999) indicated that flume water was under-saturated with respect to all minerals (see Appendix E). Assuming precipitation of minerals was negligible, any change in the H⁺ concentration of the water was due to changes in the CO₂ or HCO₃⁻ concentrations (equation (1) and (2), below). HCO₃⁻ concentrations remained consistent throughout the experiment (Figure 2 of Chapter 2), so changes in CO₂ were the primary driver of

changes in pH. Assuming no mineral precipitation (due to under-saturation with respect to all minerals), any changes in CO₂ over the length of the flume were related to gas evasion or gas invasion. The pH was used as a proxy of CO₂ content for the experiments in the flume by the relationship shown in the following equations, and used as a model input to determine CO₂ fluxes (equation (4)).



$$pH = -\log(H^+) \quad (3)$$

$$F_{Flume} = \left(\frac{\Delta CO_2}{A_{Flume}} \right) (t_{Flume})^{-1} \quad (4)$$

$$\Delta CO_2 = precipitation + degassing, precipitation = 0 \quad (5)$$

PHREEQC model outputs (see Appendix E) were combined with physical measurements taken in the flume to produce a value for the flux of CO₂ from the flume (F_{flume}), as follows: The modeled change in CO₂ (ΔCO_2) between the upstream sampling point and the downstream sampling point was divided by the product of the surface area of the flume (A_{flume}) and the approximate residence time of the water in the flume between the upstream and downstream sampling points (t_{flume}). This flux was then compared with the flux measured using the floating chamber.

Verifying water chemistry fluxes rates

Compressed cylinders of CO₂ were used to dissolve CO₂ into the flume water reservoir system through diffusion stones. CO₂ dissolved at a constant rate into the water reservoir of the flume system (Appendix D), and when the gas was turned off, it left the water at a constant rate.

Assuming all of the degassing in Figure 4 occurred in the open water of the flume and not the reservoirs, the flux rate would be approximately $0.3 \mu\text{mol m}^{-2} \text{s}^{-1}$. This is an order of magnitude higher than the average observed flux using the water chemistry method of $0.03 \mu\text{mol m}^{-2} \text{s}^{-1}$. Observing the change in $\log p\text{CO}_2$ with the flume channel closed and gas off (so the water is being recirculated between the head tank and the basement reservoir; Appendix D) shows that the system is degassing at all times. Subtracting the rate of degassing observed within the flume system with the valve closed restricting flow of water through the flume channel from the observed rate with the flume water flowing through the open channel then a flux of approximately $0.01 \mu\text{mol m}^{-2} \text{s}^{-1}$ is observed. This flux matches better with the flux values measured during this experiment, and the differences can be explained by differences in the regulated rate of pumping CO_2 from the compressed gas cylinders into the reservoir system. This rate was not constant throughout all experiments due to the regulator freezing as condensation built up.

Results

Assumptions tested

Geochemical speciation modeling confirmed that the flume water was under-saturated during all trials with respect to all minerals, so mineral precipitation was negligible for these experiments (see Appendix E). The water in the flume was always supersaturated in CO_2 compared to the atmosphere of the lab ($\log p\text{CO}_{2\text{-water}}$ between -1.46 and -2.37). Laboratory atmospheric CO_2 concentrations were maintained with the ventilation system in laboratory (Figure 3, and Appendix J), but fluctuated between trials by between 400 and 5,000 ppmv CO_2 with a mean concentration of 2,000 ppmv CO_2 . Alkalinity remained relatively constant between all trials (mean was 136 mg l^{-1} , one standard deviation was 4 mg mg l^{-1} , and range was 14 mg l^{-1}). Negligible mineral precipitation and change in the alkalinity concentration suggests that the

chemistry over the length of the flume would likely only be influenced by degassing. The constant saturation of CO₂, with respect to the laboratory atmosphere, suggests that the channel was most likely to degas CO₂ rather than absorb CO₂ gas. Thus increases in pH observed over the length of the flume channel were likely caused by degassing of CO₂, and not by precipitation or significant changes in carbonate ions. Measured water velocities in the flume ranged from 0.13 to 0.23 m s⁻¹. Air temperature ranged between 23 °C and 29 °C with a mean of 25 °C, and water temperatures ranged from 20 °C to 29 °C with a mean of 24.5°C.

Corresponding measurements of the water-chemistry method were taken for all 39 accepted chamber measurements. Water-chemistry measurements of gas flux from the water surface were significantly lower than those measured using the floating chamber. To obtain the maximum flux value measured across all trials with the floating chamber (52.6 μmol m⁻² s⁻¹), the pH would still change less than 0.01 (modeled pH change of 0.006), and thus could not be accurately measured with the instrumentation available.

Discussion and conclusions

Comparing the two fluxes revealed that there is a difference of several orders of magnitude between fluxes measured using the chamber and fluxes measured using the water-chemistry method (Figure 1, 2 and 3). In every trial, the chamber measured a flux that was higher than the water-chemistry approach.

A model was created using Comsol Multiphysics to test the physical conditions that may be creating additional turbulence and causing the higher comparative fluxes of the floating chamber (Figures 6, 7, and 8). The model was 2D, and assumed laminar pipe flow, with an inlet velocity of 0.01 m s⁻¹, and an outlet water velocity of 0.01 m s⁻¹. The model was created with the

cross-sectional dimensions of the flume channel, and the dimensions of two floating chamber walls were extended into the water column 2.5 cm. The model results suggested that there was a Venturi effect (Figure 7) underneath of the chamber (likely due to the 2D nature of the model), and that the flow was disrupted under the chamber. The front half of the chamber appeared to have slower velocities and lower Reynold's numbers, but the water moved at much higher velocities and experienced higher turbulence at the back of the chamber. The model results had several assumptions that were necessary for model convergence, and this is only the first step in modeling the flow regime under a chamber. It is likely that the chamber experiences some similar stresses to those observed in the 2D model, but in 3D the model is also likely to change significantly.

Our results generally agree with Lorke et al. (2015), but varying between two chamber designs did not significantly impact the readings obtained. The measurements used to calculate the CO₂ flux using the water chemistry equation were less than or right at the margin of error of the pH probe used (± 0.01) because the water in the flume had a residence time of one to two minutes. The results of the stirring plate simulations (chapter two) revealed that the water chemistry method may provide inaccurate results because of the limitation of minute changes in pH. None the less, equation (1) was derived to correct floating chamber measurements. The equation is velocity (v) dependent, and requires a gas transfer coefficient measured using the floating chamber (k_{FC}) to solve for a water-chemistry gas transfer coefficient (k_{WC}).

$$\frac{k_{FC}}{\frac{4E^{-07}v+5E^{-08}}{6E^{-10}v-8E^{-12}}} = k_{WC} \quad (1)$$

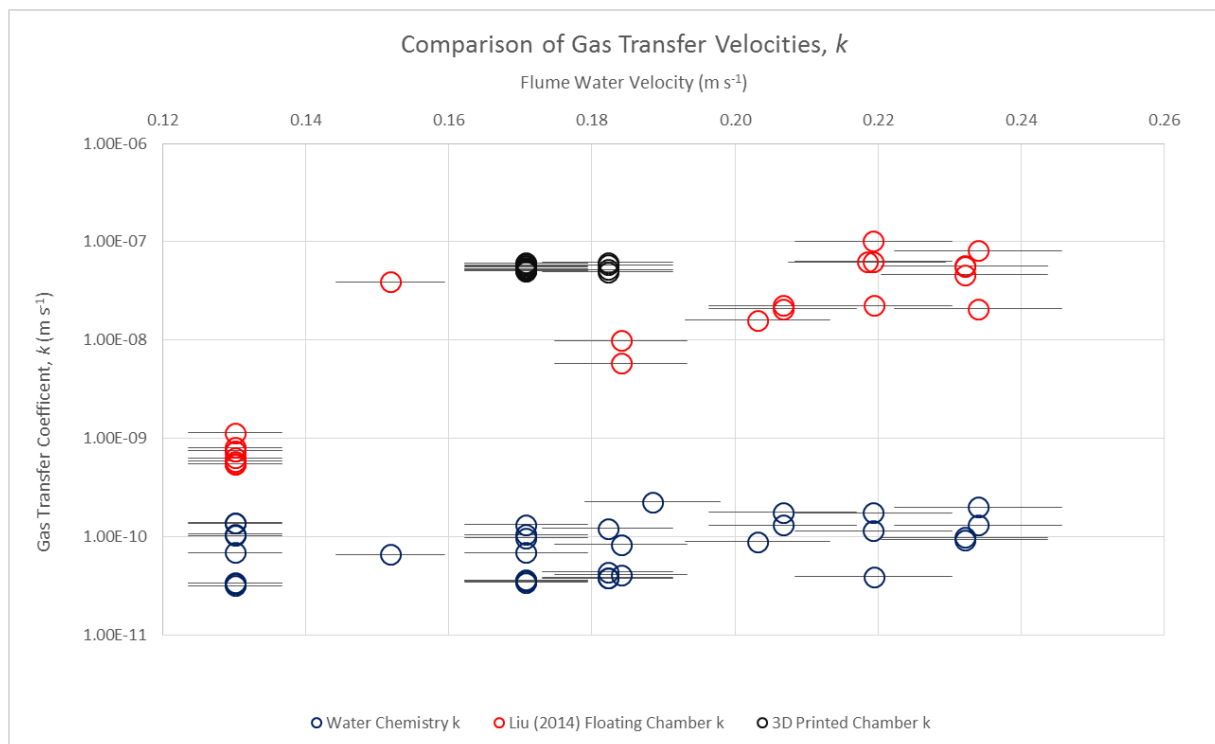


Figure 1. All floating chamber measurements and corresponding water chemistry method measurements of the gas transfer coefficient plotted against water velocity of the flume.

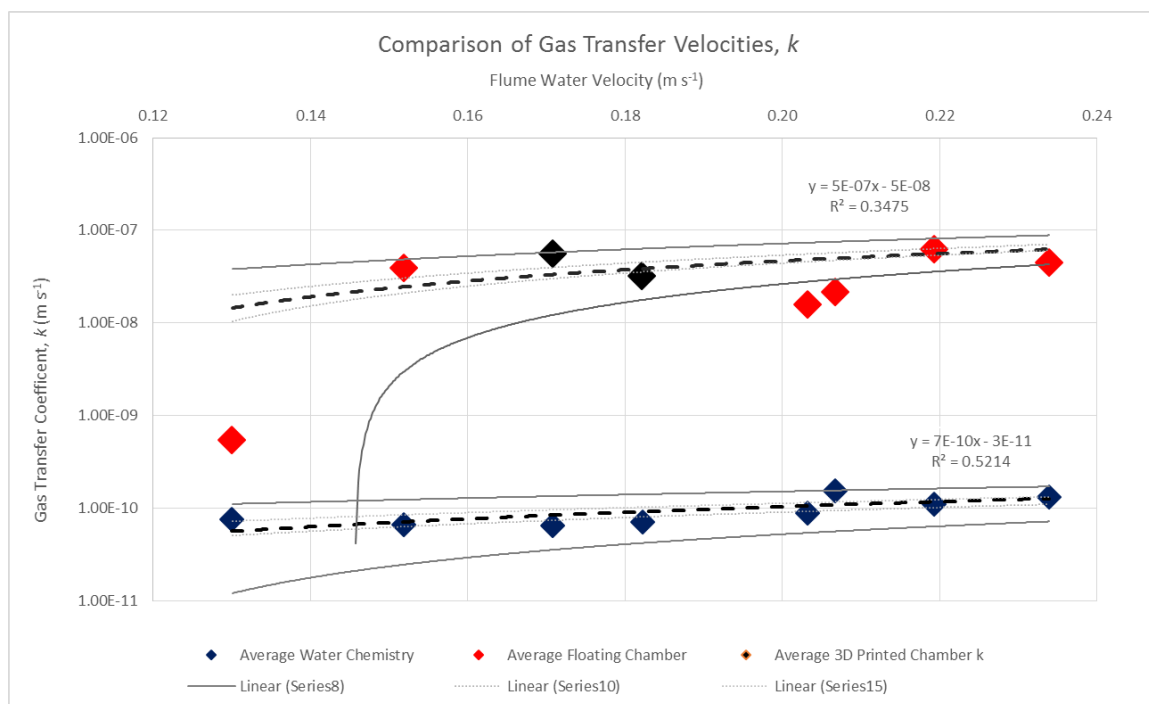


Figure 2. Gas transfer coefficients averaged at individual velocities for the floating chamber method and the water chemistry method.

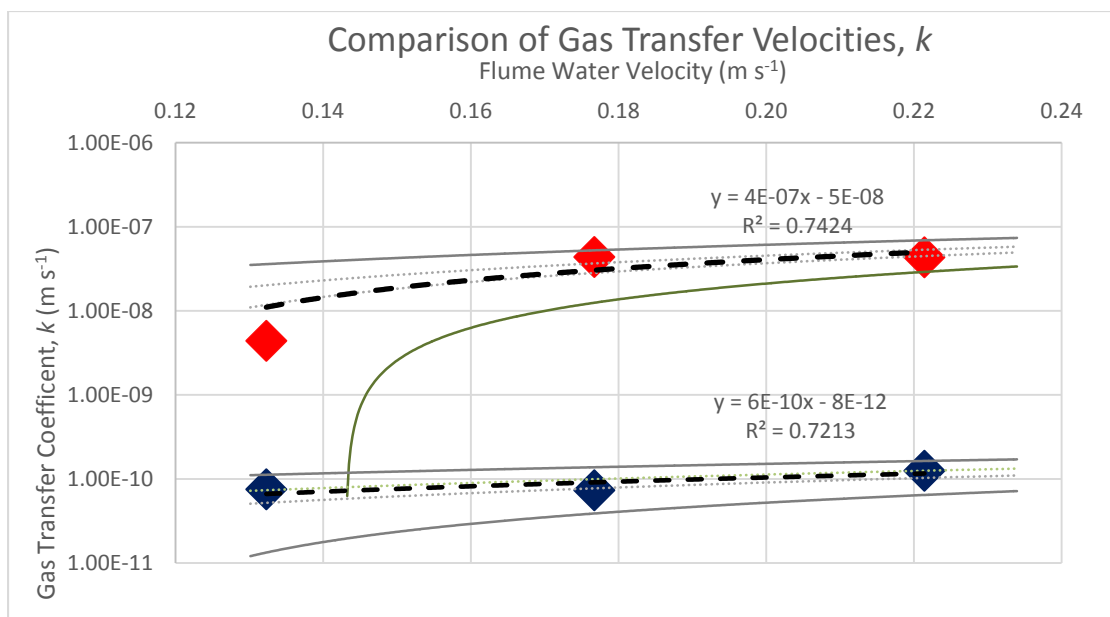


Figure 3. Velocity average values of the gas transfer coefficient for the floating chamber measurements (red) and the water chemistry method measurements (blue).

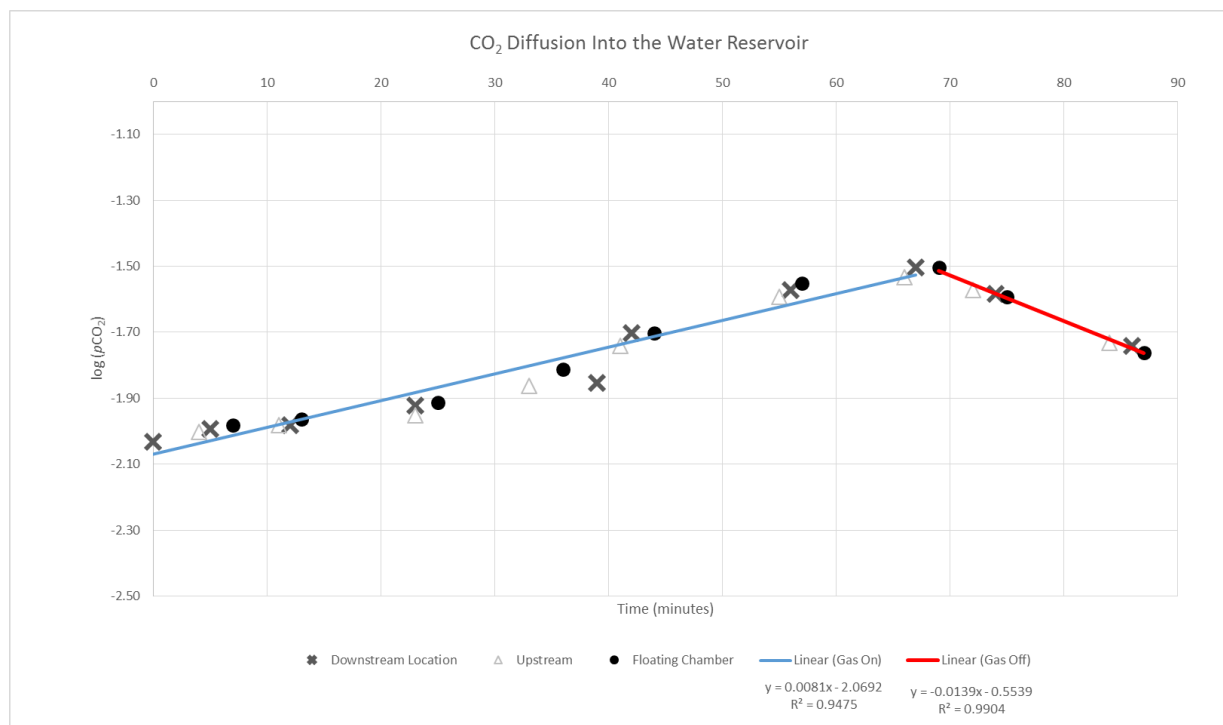


Figure 4. The CO₂ diffuses into the water reservoir system at a constant rate, and also decreases at a steady rate when the gas supply is turned off as shown above. The log (pCO₂) was calculated using the equation from Macpherson (2009).

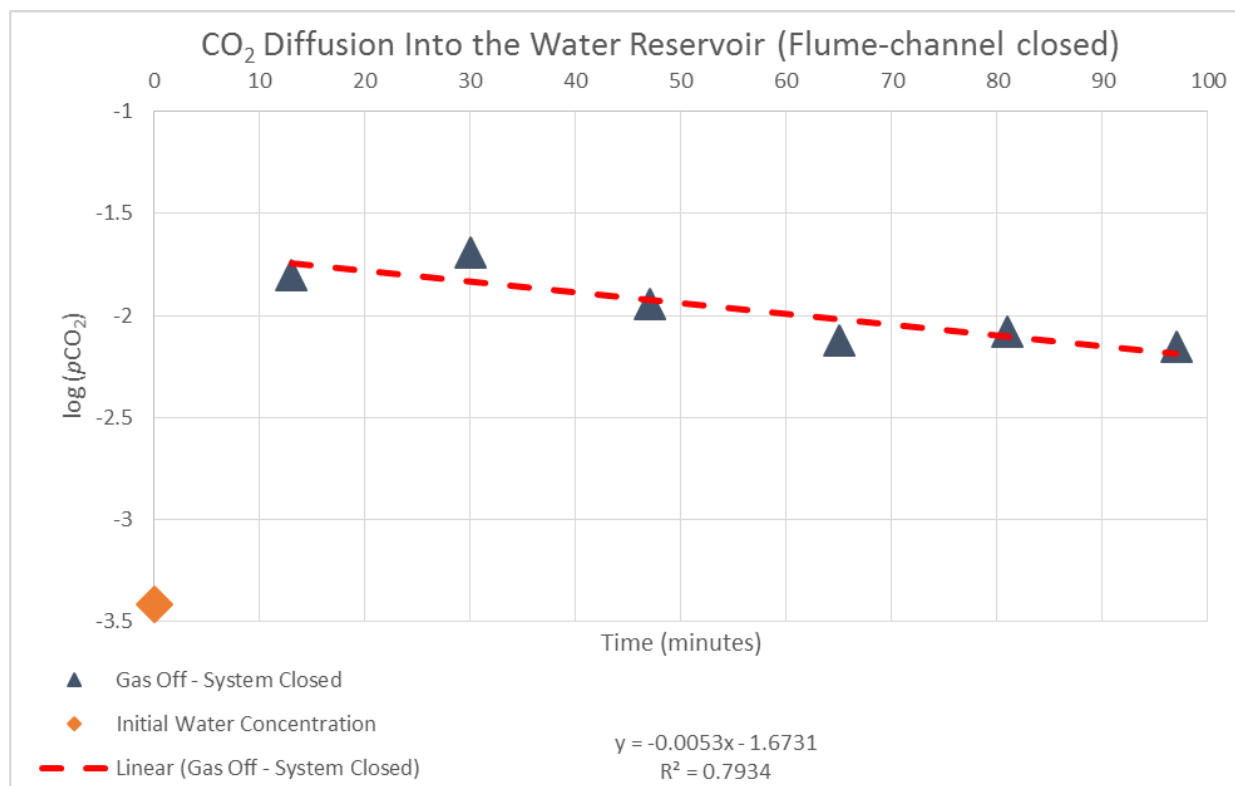


Figure 5. CO₂ partial pressure changes when the flume channel is closed and water is restricted to circulating between the constant head tank and the basement water reservoir.

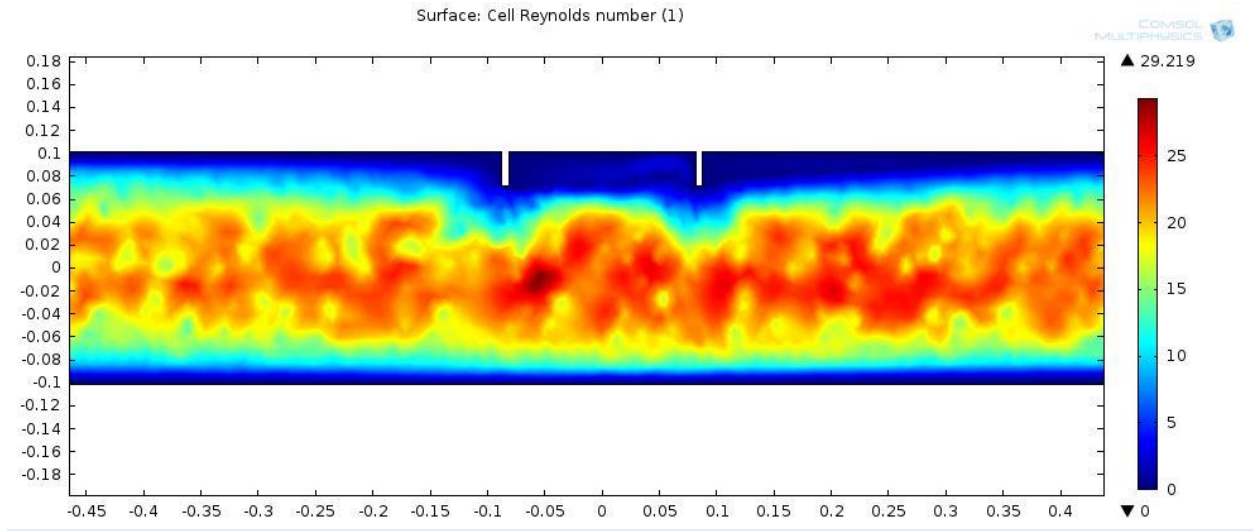


Figure 6. Reynold's number calculations from Comsol Multiphysics model.

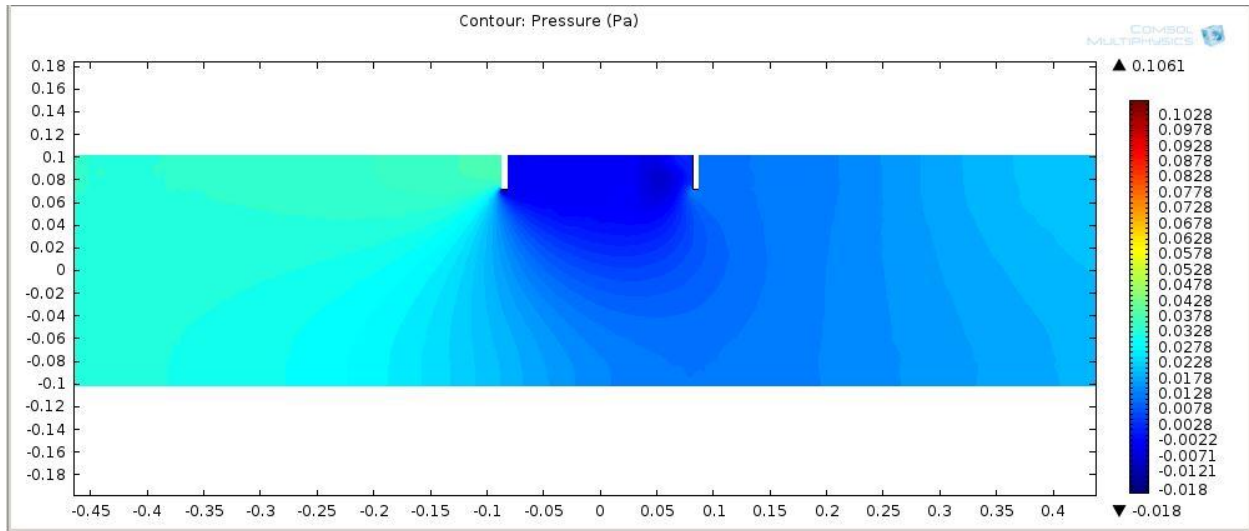


Figure 7. Pressure contour calculations from Comsol Multiphysics model.

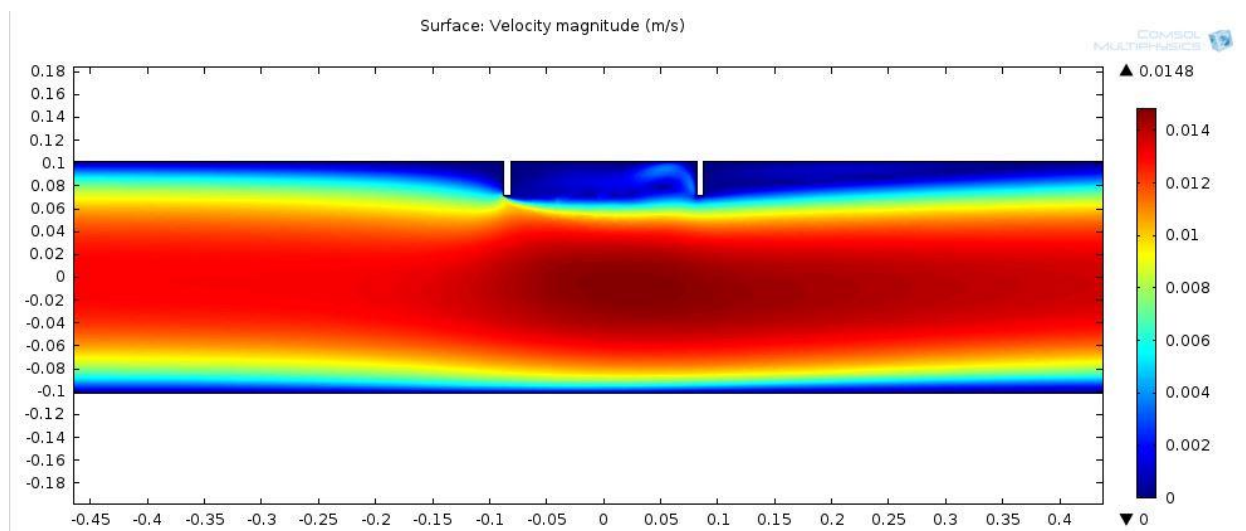


Figure 1 Velocity vector calculations from Comsol Multiphysics model.

Appendix C. Gas analyzer setup and procedure

Field check-list:

- Power strip (4+ outlets)
- Power supply (battery with adapter, generator, or wall outlet)
- Umbrella
- Table
- Chair
- Anemometer
- Hand-held AZ-77535 CO₂ yellow meter
- Backpack carrying case
- Spare tubing (in outer compartment of backpack)
- Knife for cutting tubes
- LI-820 Manual (PDF version on Toughbook desktop)
- CI-301 System
 - Power adapter, tan/black
 - Extra 10 ml Drierite tubes (last approximately 45 minutes each). Drierite tubes are constructed of 10 ml syringes. The plunger of the syringe is removed and replaced with a rubber stopper that has a hole drilled through the stopper. A gas connection glued with an air tight seal into the stopper allows for the sample to be connected to the stopper, then the stopper can be plugged into the top of the 10 ml syringe, and then the syringe can be plugged into the proper inlet to the photosynthesis system. A small tuft of glass wool is also placed on both sides of the Drierite used to fill the 10 ml syringe.
 - Extra Drierite
 - Tubing to connect to LI-820 analyzer
 - Small screwdriver set (to open in case you need to trouble-shoot)
- LI-820
 - Extra parts (bag with fuses, etc.)
 - Calibration Gas, regulator, and flow-meter (all secured in box)
 - Gas impermeable tubing to connect with the chamber
 - Tubing screw-on connections (silver)
 - Green covers for the outlet & inlet
 - Small screwdriver set (just in case power supply comes loose)
- Toughbook
 - RS-232
 - Flash-drive (to back-up data)
 - Power supply chord
- Floating chamber
 - 3D printed chamber
 - Four legs
 - Four floats
 - *All bolts, nuts washers*
 - Crescent wrench (to adjust floats on the chamber)

- Length of string to secure the chamber if necessary

Start-up procedure:

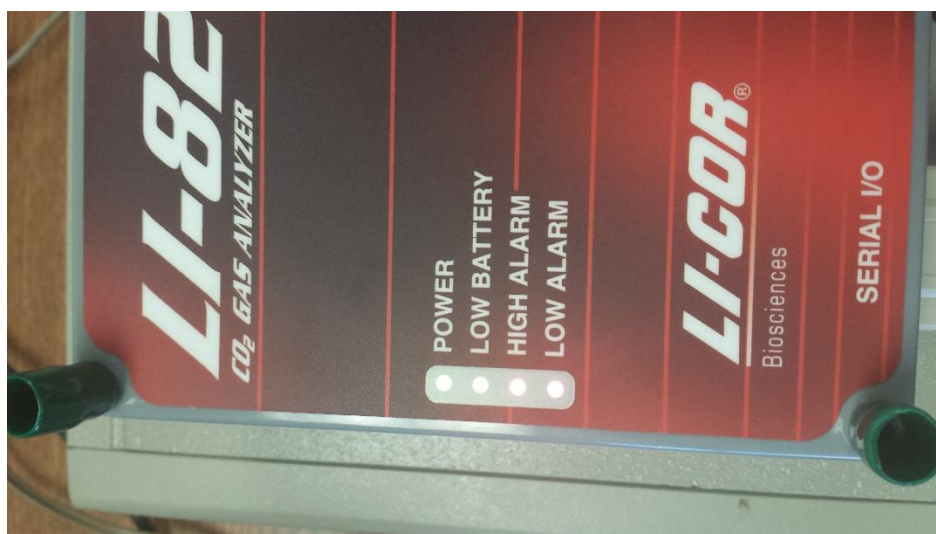
Plug-in the CI-301 Analyzer to the power source. Make sure that the, three way valve is pointed towards the analyzer according to the label on the valve, the inlet tube (labeled to pump) is not blocked, and that the outlet tube from the 3-way valve (labeled to analyzer) is not blocked. This ensures that the pump will not sustain damage. If you hear a whirring from the pump carefully check the entire system to make sure there is no block in the tubing (keep in mind it is an old pump, so sometimes it whirs without any cause to be concerned).

Turn the CI-301 analyzer on by pressing the “On” button on the control panel. The instrument then takes several minutes to warm-up, and then calibrate (the machine thinks it is still an analyzer even though the analyzer portion does not work).

On the CI-301 control panel follow this sequence: Press “Enter”> Press “Enter” > Press “0.2” for sampling rate>Press “Enter” > Press “0.2” LPM for flow rate (note: the LiCOR has a maximum flow rate of 1.0 LPM) > Press “Enter” > Press “Enter”

You should hear the pump turn on (it is quiet). You can then attach the LI-820 to the CI-301.

Plug-in the LI-820. All four lights on the LI-820 should light-up, and then turn off, leaving only the green “Power” light illuminated as shown in the images below. The red electric cable should be plugged into the #1 outlet, and the black cable should be plugged into the #2 outlet on the LI-820.



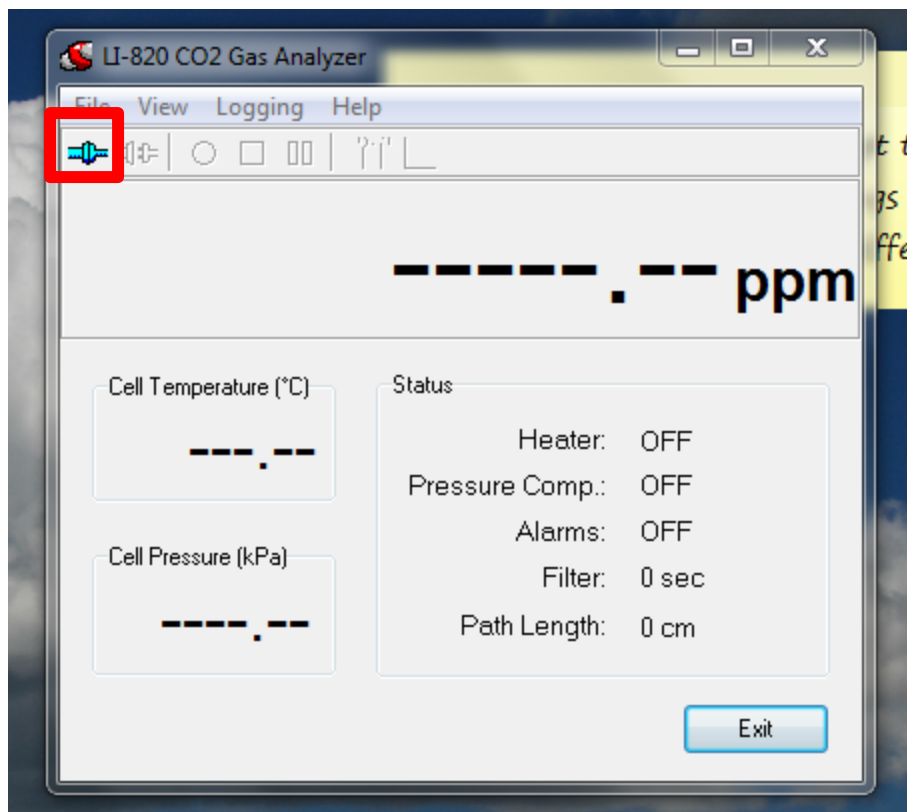


Connect the LI-820 to the Toughbook using the RS-232 cable connection.

Open the LI-820 icon on the desktop. The icon is a CO₂ molecule.



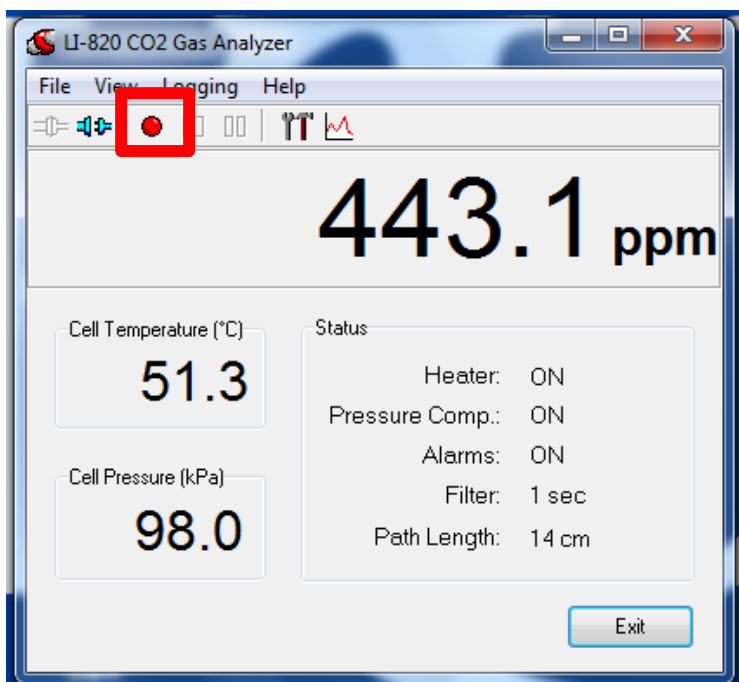
Click the blue connection button to connect with the device.



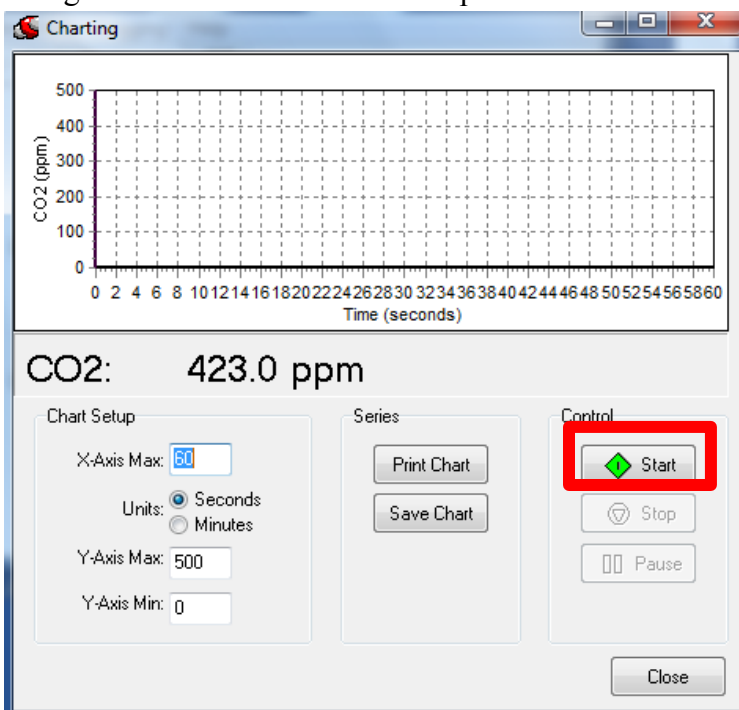
A screen will pop-up. Select an output interval of 1.0 seconds or greater integer, and Com Port one.

An up to the minute reading should appear on the screen showing CO₂ ppm, cell temperature, cell pressure, and instrument status.

Record the warm-up data by pressing the red record button as shown in the image below, and saving the file to the location you desire. The LI-820 recommends a 90-minute warm-up time, but usually reports accurate numbers within 10 minutes of start-up. Make sure that the cell temperature is reading a steady value of about 51° C.



Plot the warm-up data by clicking on the graph icon. Adjust your axis values as necessary, and hit the green “Start” button. This will plot the data in real-time.



While the device is warming up you can connect the floating chamber to the device using gas impermeable tubing, and adjust the flotation devices on the chamber.

After all of your tubing is connected blow for several seconds into the inlet of the chamber, and time how long it takes for the gas from your breath (high concentration CO₂) to reach the analyzer and be read by the computer.

Record this number in your notes, or remember it.

***Span* (monthly):**

On the LI-820 software click “View” > ”Calibration”

Enter the concentration of your calibration gas.

Make sure your calibration gas canister is secured.

Turn the calibration gas on briefly, and ensure that the flow is restricted to less than 1.0 LPM.

Connect the calibration gas to the analyzer using gas impermeable tubing, and turn the gas on.

Click “Span” in the calibration window.

When the span is complete you may close this window, or proceed to Zero the instrument.

***Zero* (monthly):**

On the LI-820 software click “View” > ”Calibration”

Flip the three way valve connected to the CI-301 to inlet labeled “To Na-lime”

Connect the outlet tube labeled “Na-lime to analyzer” to the “In” connection on the LI-820. You should see the concentration on the heads-up display drop to near zero within a few seconds.

Click “Zero” in the LI-820 software calibration window.

When the zero is complete you may close the window and proceed.

Always make sure the 3-way valve is not open to the Na-lime when not in use. This preserves the Na-lime.

Operation:

Hit the record button on the software to name your file, and save it to a specific location (saves as a .txt file) like you did to record the warm-up data.

Quickly, hit save, and then hit the pause button in the software.

Place the chamber onto the surface of the water gently, and simultaneously hit the record button in the software. The lip should be about 2 cm below the surface of the water.

Closely monitor the chamber for “gulping” of air or any bubbles escaping from the chamber.

Record pH, water temperature, and take a water sample for alkalinity titration to determine the theoretical concentration of CO₂ dissolved in the water during the course of chamber measurements.

Take periodic humidity and air temperature measurements using the AZ-77535 hand-held CO₂ analyzer.

Leave the chamber on the surface of the water for at least five minutes, and note any changes to the condition of the chamber. If you are measuring in an area where wind speeds may be greater than 0.5 m/s then you should take periodic wind speed measurements.

Shut-down:

After you are done collecting samples run dry air through the machine for approximately 10 minutes. Then hit “Stop” on the CI-301 system.

Click the disconnect symbol on the LiCOR software.

Unplug the LI-820 from the power source.

Hit the “Off” button on the CI-301 system. The screen should go blank when the instrument turns off. You can then shut-down the computer, and pack up all supplies. The analyzer fits best into the pack as shown below.



Data extraction & interpretation:

Open excel > File > Open > All Files > Navigate to the folder where you saved your data > Click on the file > Open > Select delimited > Select Space > Click Finish

You should have four columns open in excel (time, temperature, pressure, and CO₂). Go to File > Save As > Excel Workbook

Create a new column heading to the right of previous columns titled “Time (s)”. Start a time 0, and assign values for the remaining rows based off of the time interval you selected when you connected the LI-820 to the Toughbook computer.

Plot “CO₂ ppm” on the ordinate, and “Time (s)” on the abscissa.

Add a linear trend line to the data and show the R² value and equation on the chart. R² values should be greater than 0.9. You may have to adjust the section of data that you are using on your curve. Usually there is a lag time when you first place the chamber on the water before the air concentration begins to increase inside of the chamber (due to the uptake time that was recorded after breathing into the chamber). Manipulate the curve to obtain the highest possible R² value while also maintaining a representative sample (usually at least three minutes of good data with a high R² and good linear fit).

After you have a representative amount of data selected with a linear fit curve with a high R² value take the slope of that curve, and input it into the following set of equations or using the provided spreadsheet to calculate flux values.

Floating-chamber calculations:

$$\frac{dc}{dt} = \frac{\Delta ppm}{seconds} = \frac{\Delta \mu mol}{mol second}$$

$\frac{dc}{dt}$ is the slope of the fitted curve in $\mu mol mol^{-1} s^{-1}$, $\frac{\Delta ppm}{s}$ is the slope of the linear fitter curve obtained from plotting the data from the LI-820 analyzer.

$$F_{chamber} = \frac{dc}{dt} \left(\frac{pV}{RT_{KA}A} \right)$$

* $F_{chamber}$ is in $\mu mol m^{-2} s^{-1}$, $\frac{dc}{dt}$ is the slope of the fitted curve in $\mu mol mol^{-1} s^{-1}$ (calculate mols in denominator using ideal gas law $PV=nRT$ as demonstrated below) for the floating chamber measured concentrations over time, p is the pressure in Pa inside the chamber, V is the chamber volume in m^3 , R is the universal gas constant, T_{KA} is the temperature of the air Kelvin, and A is the floating chamber surface area in m^2 (Müeller et al 2015).

K is a piston velocity and can be thought of as the height of water that is equilibrated with the atmosphere per unit of time for a given gas at a given temperature.

$$F_{chamber} = k(C_w - C_a)$$

* C_w is the measured aqueous concentration of CO₂ in $\mu mols m^{-3}$, C_a is the concentration of CO₂ $\mu mols m^{-3}$ if the water were in equilibrium with the overlying atmosphere via Henry’s Law, k is the gas transfer coefficient in $m s^{-1}$, and $F_{Chamber}$ is the chamber flux in $mol m^2 s^{-1}$.

Rearrange, and solve for k (Cole and Caraco, 1998);

$$k = \frac{F_{chamber}}{C_w - C_{fc}}$$

Normalizing the Gas Transfer Coefficient:

K_{600} is calculated for the purposes of comparison with other gas transfer rates at 20 °C. 600 is the Schmidt number of CO₂ at 20 °C in freshwater.

$$\frac{k_{600}}{k} = \left(\frac{600}{Sc_{CO_2}} \right)^{-n}$$

* n is typically between 2/3 to 1 (Cole and Caraco, 1998) with 1/2 being appropriate for rougher surface waters from Jähne et al 1987, 2/3 being appropriate for a smooth surface, and 1.0 would be for a totally nonreactive gas.

$$Sc_{CO_2} = 2073.1 - 125.62(T_c) + 3.6276(T_c)^2 - 0.043219(T_c)^3$$

* T_{cw} , is temperature in degrees Celsius of the water

*Schmidt number calculations from USGS “CO₂calc: A User-Friendly Seawater Carbon Calculator for Windows, Mac OSX, and iOS (iPhone)”

* Sc_{CO_2} (20° C) = 668

The Schmidt number relates diffusivity of gas to viscosity of water as expressed below (ν is the kinematic viscosity of water, and D is the diffusion coefficient for a gas). Kinematic viscosity is the dynamic viscosity divided by the density of the fluid. Dynamic viscosity and density can be found in reference tables like the *CRC Handbook of Chemistry and Physics*. Diffusion coefficients are determined experimentally, or by empirical equations (MacIntyre et al 1995).

$$Sc = \frac{\nu}{D}$$

Modified CI-301 PS & LI-820 Analyzer Setup(7.21.2014)

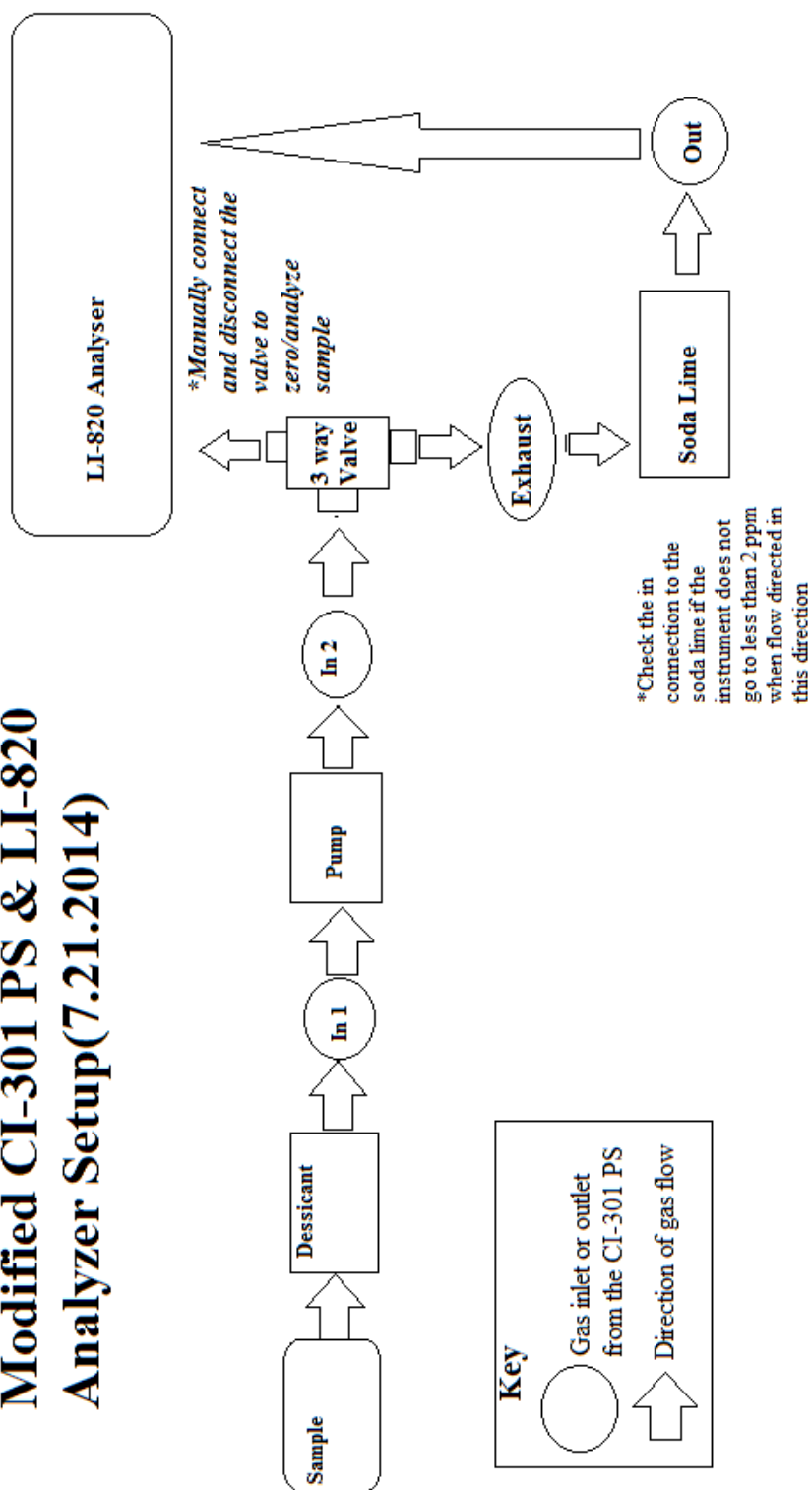


Figure 1. Schematic of gas flow to the IRGA.

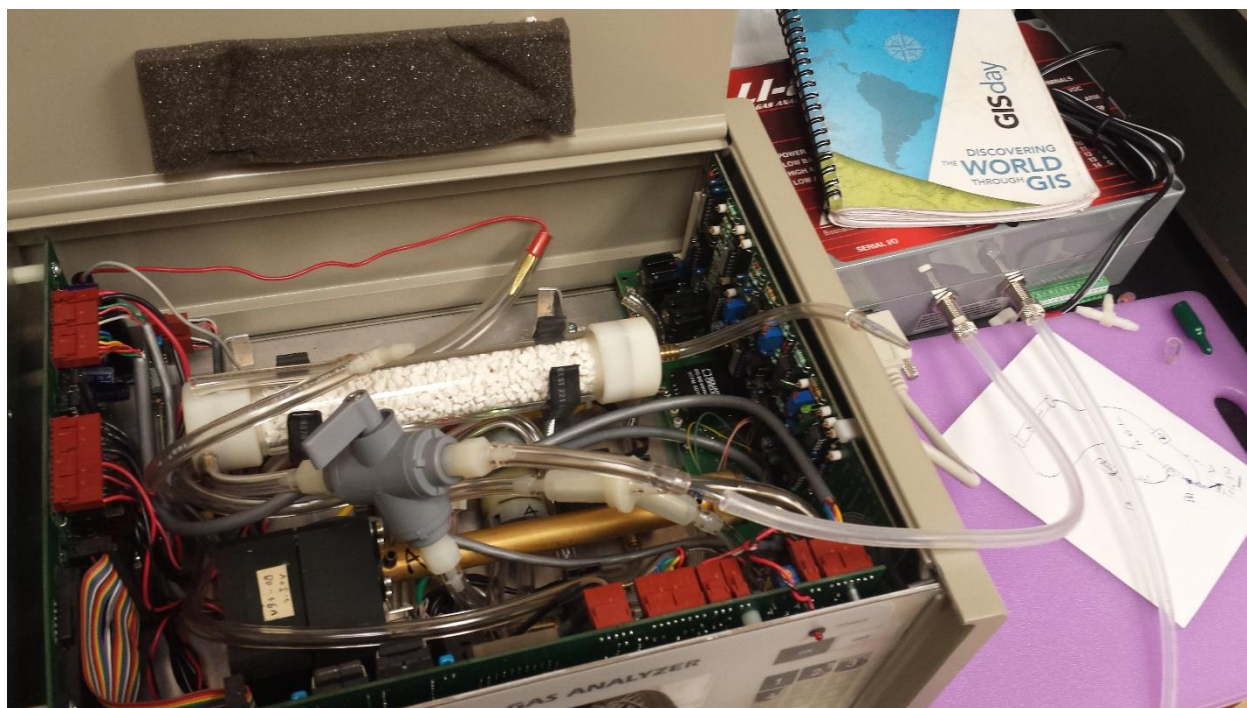


Figure 2. Image of the inside of the converted Gas Analyzer.

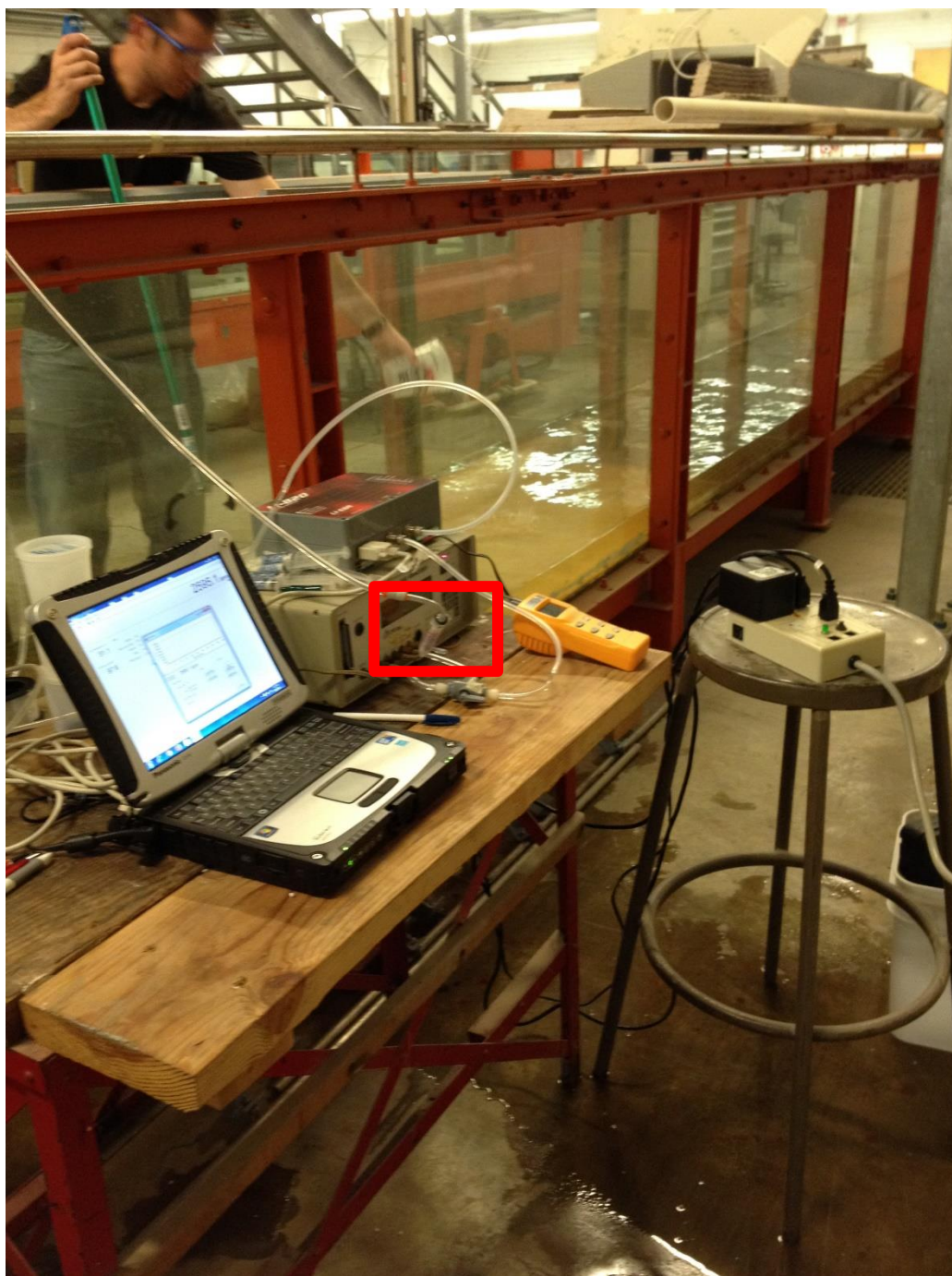


Figure 3. Analyzer setup as used in the flume experiments. Note, the Drierite tube highlighted in the red box.

Appendix D. Flume setup and procedure

Water resources laboratory

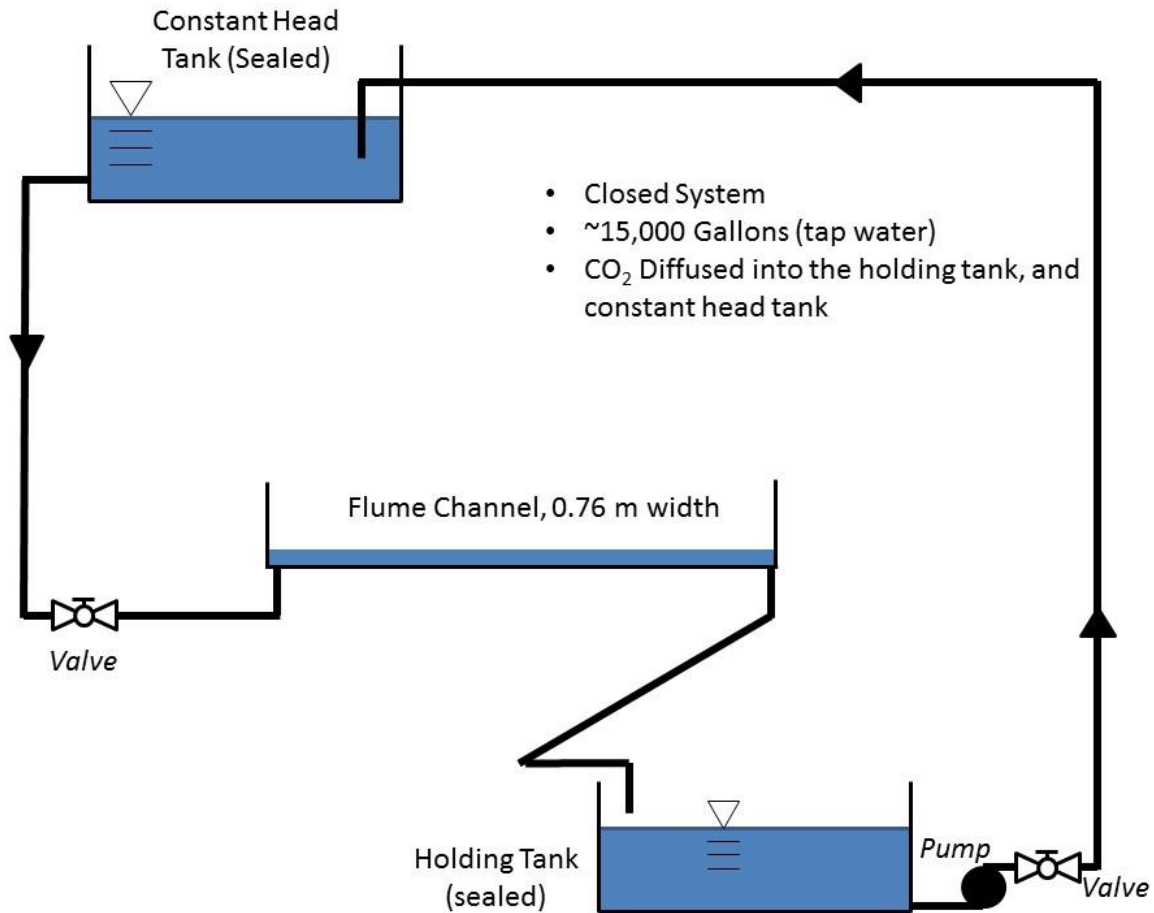


Figure 1. The University of Kansas Water Resources Laboratory contains the flume system described including a re-circulating supply of water. The system was sealed off to the atmosphere except for the flume channel, and CO₂ was dissolved into the holding tank and constant head tank. Water flow through the system is indicated by the arrows in the schematic, and valves were manually opened and closed.

Step by step procedure

- Person 1: Place FC on water, fan out FC in between trials, change computer logging file names
- Person 2: Record height of the backwater, and depth of the water at the upstream and downstream location (0.5, 2, and 4). Control yellow valve.
- Person 2: Record pH, temp., and time
- Person 3: Take water samples, for alkalinity
- Person 5: Pictures

1. Submerge CO₂ diffusing buckets into the basement reservoir
 - a. Make sure all are tied off and rope lengths cannot reach the water intake
2. Seal off the basement reservoir with plastic sheeting and weights
3. Close the trap door to the flume drain
4. Turn on the CO₂ gas tank on the flume level to 15 psi
 - a. Record the initial tank pressure and time
5. Move to the head tank supply and turn on the CO₂ gas tank next to the radio room to below 10 psi
 - a. Record the initial tank pressure and time
 - b. Check the seal on the head tank
 - i. Look for breaks in the seal around the edge
 - ii. Look for tears in the plastic
 - c. Check this pressure periodically
6. Move to the basement and turn the breaker to the on position
 - a. Open the green valve
7. Hit start to turn on the pump
8. Open the blue valve all the way
 - a. Use cheater bar if necessary
9. Record the time
10. Wait 2.5 hours for the CO₂ to dissolve into the water
 - a. Use the CO₂ air monitor to check CO₂ levels at one hour
11. Calibrate the pH meter
- 12. After two hours lift the trap door to the flume drain**
 - a. Secure it to the loop hole on top of the welding machine
13. Move to the upstream portion of the flume and open the yellow valve the appropriate amount
 - a. Read the height of the head over the weir and record it
 - b. Allow the trough to fill up behind the retaining weir and crest over
 - c. Quickly calculate velocity and residence time in the flume
14. Take a pH sample and water at the upstream portion of the reservoir just downstream of the rail that is perpendicular to the surface of the water
 - a. Record with the time
 - b. Precontaminate the sample
 - c. Completely submerge the water sample
 - d. Seal the sample, mark it with the initials MJRS, date, time, location(upstream or downstream), and experiment trial #
 - e. Place in the cooler for preservation
15. Quickly move to the downstream portion(try to match the residence time of the water) of the flume between the rails that are perpendicular to the surface of the water and take a

- pH sample and water at the upstream portion of the reservoir just downstream of the rail that is perpendicular to the surface of the water
- a. Record with the time
 - b. Precontaminate the sample twice
 - c. Completely submerge the water sample
 - d. Seal the sample, mark it with the date, time, location, and experiment trial
 - e. Place in the cooler for preservation
16. Simultaneous to steps 14 and 15 place the floating chamber onto the surface of the water to record the CO₂ flux
- a. Make sure the analyzer has warmed up for 1.5 hours
 - b. Make sure that both the inlet and outlet are connected appropriately to the chamber
 - c. Make sure that the software is logging and you are record the file name for later
 - d. Take a pH sample and water at the upstream portion of the reservoir just downstream of the rail that is perpendicular to the surface of the water
 - i. Record with the time
 - ii. Precontaminate the sample twice
 - iii. Completely submerge the water sample
 - iv. Seal the sample, mark it with the date, time, location, and experiment trial
 - v. Place in the cooler for preservation
17. During the survey continue to record pH, time, and temp. as often as possible.
18. At the conclusion of the survey(10 minutes following start) repeat steps 14 and 15
19. Remove the floating chamber from the surface of the water
- a. Stop the data logging
20. Close the yellow valve
21. Close the trap door after the drain to the flume has completely drained
- a. Secure rope loosely around nearest post
22. Shut-down the flume level CO₂ tank
- a. Close both valves on the regulator
 - b. Record the final tank pressure and time of shut off
23. Move the head tank and shut off that gas tank
- a. Record the final tank pressure and time of shut off
24. Move to the basement
25. Close the blue valve completely
26. Switch the breaker to off
27. Lock the basement door
28. Head upstairs and remove the diffuser buckets from the basement reservoir
- a. Store in a semi-dry or dry place
 - b. Store ropes neatly
29. Record the final time

Appendix E. Geochemical speciation modeling

Modeling completed using PHREEQC Interactive 3.1.1-9213. Alkalinity was derived by titration using the inflection-point method. Anions were determined using the EPA Method 300.0 for determination of inorganic anions by ion chromatography.

Pfaff, J. D., 1993, Method 300.0 Determination of inorganic anions by ion chromatography: USEPA Environ. Monit. Syst. Lab., Cincinnati, OH.

Appendix F. Example calculations

Dissociation reaction constants

$$\log(K_{CO_2}) = 108.39 + 0.019851(T_{KW}) - \frac{6919.5}{T_{KW}} - 40.452 * \text{Log}(T_{KW}) + \frac{669,370}{(T_{KW})^2}$$

$$\log(K_1) = -\left(464.2 + 0.093448(T_{KW}) - \frac{26,986}{T_{KW}} - 165.76 * \text{Log}(T_{KW}) + \frac{2,248,600}{(T_{KW})^2}\right) - K_2$$

$$\log(K_2) = -(107.89 + 0.032528(T_{KW}) - \frac{5151.8}{T_{KW}} - 38.926 * \text{Log}(T_{KW}) + \frac{563,710}{(T_{KW})^2})$$

$$\log(K_W) = -283.971 - 0.05069842(T_{KW}) + \frac{13,323}{T_{KW}} + 102.2447 * \text{Log}(T_{KW}) - \frac{1,119,669}{(T_{KW})^2}$$

* T_{KW} , temperature of the water in Kelvin. Calculations from PHREEQC

Partial pressure of CO₂

pH was measured with a Thermo Scientific Orion, Orion 8157BNUMD Ross Ultra pH/ATC Triode, and alkalinity as bicarbonate was determined using the inflection point method.

$$[H^+] = 10^{-pH}$$

$$\text{Assume, } [H_2CO_3^*] = [CO_2 + H_2CO_3]$$

$$[H_2CO_3^*] \approx [CO_2] \approx \frac{[H^+][HCO_3^-]}{K_1}$$

*Concentrations are in mol/L

* $[HCO_3^-]$ is from titration

Use Henry's Law:

$$[H_2CO_3^*] = K_{CO_2} * pCO_2, \quad K_{CO_2} = 10^{\log(K_{CO_2})}$$

$$\frac{[H_2CO_3^*]}{K_{CO_2}} = pCO_2, \text{ assume activity of } H_2O \text{ is } 1$$

Water-chemistry flux

$$Q = 1.84(b - 0.2)J^{\frac{2}{3}}$$

* Q is discharge in $m^3 s^{-1}$, b is the length of the rectangular weir notch in meters, and J is the height of head over the weir crest in m. From "Fluid Dynamics" by Finnemore et al 2002.

$$V = \frac{Q}{x_c}$$

* V is velocity in meters per second, X_c is the channel cross-sectional area in m^2 .

$$t_{\text{residence time}} = \frac{L}{V}$$

Residence time in seconds can be determined with the length of the flume (L) divided by the velocity. Development of eddies and friction that slowed down flow of flume sides resulted in a much slower residence time than the calculated residence time average residence time, so a dye tracer was used to establish residence time. This was found to be error prone so residence time was later approximated using a dye release and tracking flow of the dye visually.

$$A_{\text{Flume}} = L_{\text{flume}} * W_{\text{flume}}$$

*The flume surface area (A_{Flume}) is equal to the length of the flume (L_{Flume}) multiplied by the flume width (W_{Flume}). All units were in meters for this calculation.

Calculate $\log p\text{CO}_2$ at the upstream and downstream area as discussed in the previous $\log p\text{CO}_2$ section. A theoretical gas transfer velocity can be derived from this flux, but is early trials due to fluxuating atmospheric CO_2 concentration variations during the course of the trial in the flume laboratory.

$$p\text{CO}_{2\text{upstream}} - p\text{CO}_{2\text{downstream}} = \Delta p\text{CO}_2$$

$$\Delta p\text{CO}_2 * K_{\text{CO}_2} = \Delta[\text{H}_2\text{CO}_3^*]$$

$$\frac{\Delta[\text{H}_2\text{CO}_3^*] * 10^6}{t_{\text{residence time}} * A_{\text{flume}}} = F_{\text{flume}}$$

* $\Delta[\text{H}_2\text{CO}_3^*]$ is in mol/L and represents the approximate change in CO_2 over the length of the flume, $t_{\text{residence}}$ is residence time is in seconds, A_{flume} is flume surface area in meters squared, and F_{Flume} is the flume flux in $\mu\text{mol s}^{-1} \text{m}^{-2}$.

Floating-chamber calculations:

$$\frac{dc}{dt} = \frac{\Delta \text{ppm}}{\text{seconds}} = \frac{\Delta \mu\text{mol}}{\text{mol second}}$$

$\frac{dc}{dt}$ is the slope of the fitted curve in $\mu\text{mol mol}^{-1} \text{s}^{-1}$, $\frac{\Delta \text{ppm}}{s}$ is the slope of the linear fitter curve obtained from plotting the data from the LI-820 analyzer.

$$F_{\text{chamber}} = \frac{dc}{dt} \left(\frac{pV}{RT_K A} \right)$$

* F_{chamber} is in $\mu\text{mol m}^{-2} \text{s}^{-1}$, $\frac{dc}{dt}$ is the slope of the fitted curve in $\mu\text{mol mol}^{-1} \text{s}^{-1}$ (calculate mols in denominator using ideal gas law $PV=nRT$ as demonstrated below) for the floating chamber measured concentrations over time, p is the pressure in Pa inside the chamber, V is the chamber

volume in m^3 , R is the universal gas constant, T_{KA} is the temperature of the air Kelvin, and A is the floating chamber surface area in m^2 Müeller et al 2015.

K is a piston velocity and can be thought of as the height of water that is equilibrated with the atmosphere per unit of time for a given gas at a given temperature.

$$F_{chamber} = k(C_w - C_{fc})$$

* C_w is the measured aqueous concentration of CO_2 in $mols\ m^{-3}$, C_a is the concentration of CO_2 $mols\ m^{-3}$ if the water were in equilibrium with the overlying atmosphere via Henry's Law, k is the gas transfer coefficient in $m\ s^{-1}$, and $F_{chamber}$ is the chamber flux in $mol\ m^2\ s^{-1}$.

Rearrange, and solve for k (Cole and Caraco, 1998);

$$k = \frac{F_{chamber}}{C_w - C_{fc}}$$

Appendix G. Flushing the chamber between trials

To verify the results of Liu (2014) an experiment was completed in January of 2014 to compare flushing the floating chamber (FC) with room air versus letting the chamber sit on the ground for fifty minutes. This was done to replicate a field trial where the chamber was not flushed out in between uses, and the CO₂ content appeared to accumulate rather than dissipate to atmospheric concentrations in-between trials. It is common with the FC method to flush the chamber out in between measurements although not all published FC methods explicitly incorporate this technique.

Three trials were performed as part of this experiment:

- **Trial one:** The chamber was sealed with an aqueous reservoir of CO₂ that was super-charged with CO₂ with respect the atmosphere, and CO₂ concentration changes inside of the chamber were measured over a period of five minutes. This was the control trial (see Figure 1, and Table 1).
- **Trial two:** At the end of trial one the chamber was placed onto the floor for fifty minutes and considered “non-flushed”. The same steps described for trial one are repeated (see Figure 2, and Table 2).
- **Trial three:** Between the second and third trial the chamber was flushed with room air for longer than twenty seconds by waving the chamber, and then reapplied to the water. The same steps described for trial one were repeated (see Figure 3, and Table 3).

For each trial, gas samples were taken from the floating chamber per the methods described in Liu (2014). The gas samples were then analyzed within a week using the ThermoFinnigan GASBENCH II in the University of Kansas Keck-NSF Paleoenvironmental and Environmental Laboratory. Water super-saturated with CO₂ with respect to the atmosphere was

created by bubbling compressed CO₂ gas into a large sink (located in the University of Kansas Hydrogeology Lab) through a diffusion stone until the water reached an equilibrium pH (where it appeared to no longer decrease). pH was measured using a Thermo Scientific Orion, Orion 8157BNUMD Ross Ultra pH/ATC Triode, and was considered a proxy for aqueous CO₂ content. The FC was sealed against the water in the sink, and gas samples were taken approximately every minute for five minutes beginning at time zero.

The chamber appeared to equilibrate with the atmosphere within 50 minutes without flushing (Figures 2 and 3, Tables 1-3) as demonstrated by the miniscule differences in the y-intercepts of the fitted slopes. This result provides positive support for the results demonstrated in Liu (2014), and suggests that this is an acceptable method for using the floating chamber. Although this method may be acceptable in this instance, it is not recommended, and chamber flushing helps to eliminate any accumulation of CO₂ during the course of multiple consecutive floating chamber trials.

Table 1. Trial One	
Time (sec)	CO₂ (ppm)
0	740
60	580
120	784
180	836
240	939

*Sat chamber on floor for 50 minutes

Table 2. Trial Two	
Time (sec)	CO₂ (ppm)
0	505
90	410
120	848
180	975
240	950

*Flushed chamber with room air in between trials

Table 3. Trial Three	
Time (sec)	CO₂ (ppm)
0	471
60	583
120	838
180	733
240	931

Table 4. pH Measured As a Proxy For Aqueous CO₂	
Relative Timing of Measurement	pH
Before trial one	5.48
End of trial one	5.48
Before trial two	5.48
End of trial two/start of trial three	5.45

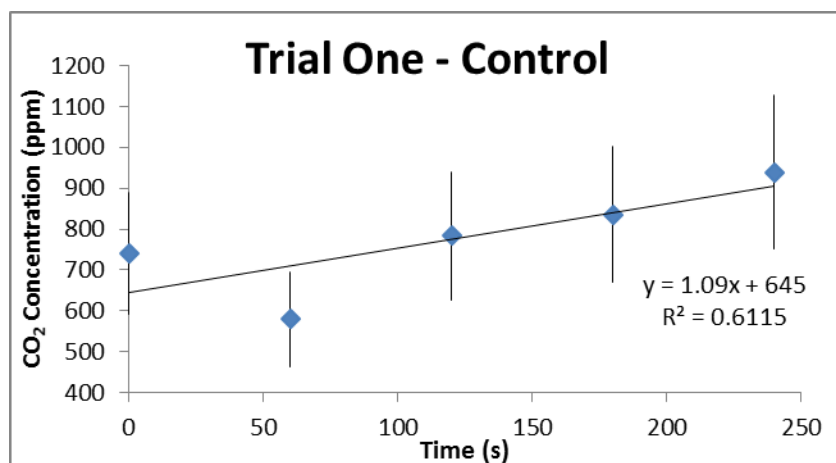


Figure 1. After trial one the chamber was placed onto the floor for fifty minutes.

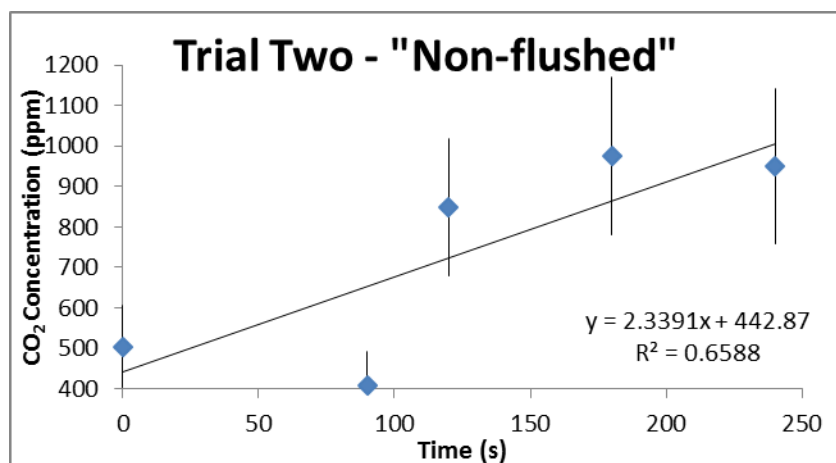


Figure 2. After trial two the chamber was flushed with room air for longer than twenty seconds, and then reapplied to the surface of the water.

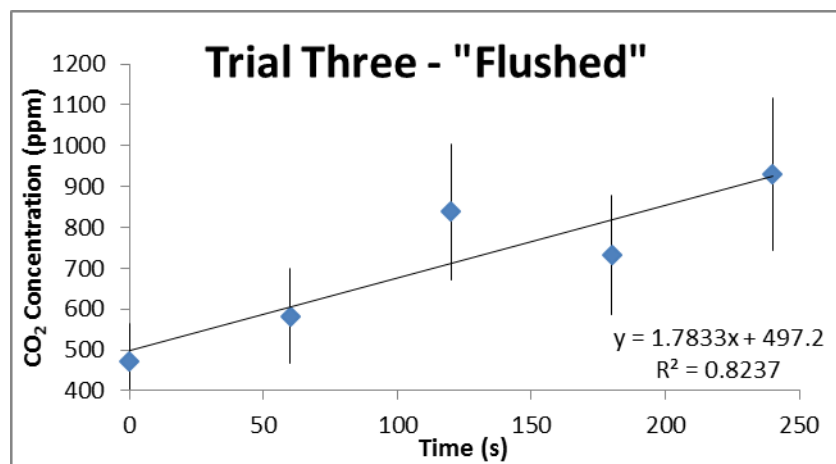


Figure 3. This final FC measurements in trial three showed that the chamber had equilibrated with atmospheric conditions, and did not appear to accumulate CO₂ concentrations from the previous trial.

Appendix H. Supply numbers and orders

Part #	Description	Image URL	Provider	List Price (\$)	Price Paid (\$)
SXGMT100266R	2000 PPM CO ₂ in air 103 liters 180 calibration gas	N/A	Mattheson	156	118.41
SEQRFM0029XX	Regulator/flowmeter 1.5 liters per minute CGA 180 PELGAS for calibration gas	N/A	Mattheson	446.25	310.97
N/A	Model 18 series single-stage general purpose brass regulator for use in regulating CO ₂ diffusion rate	N/A	Mattheson	N/A	121.46
N/A	CO ₂ 50 lb cylinder for flume gas supply	N/A	Mattheson	N/A	7.00
N/A	Gas diffusion stones for diffusing into flume water reservoir	URL	Great Fermentations	N/A	41.97
N/A	¼ inch I.D. tubing to carry gas from the compressed gas cylinders to the flume water reservoir	URL	FreshWaterSys ems.com	N/A	10.00
N/A	10 pack 1/8 inch I.D. Y barb connectors for the flume diffusion system	URL	Fisher Scientific	N/A	36.48
N/A	Tygon tubing 1/8 inch I.D. ¼ Inch OD, 1/16 Inch wall for carrying gas through the IRGA system, and recirculating to the chamber	N/A	Fisher Scientific	N/A	12.45

Appendix I. Results of CO₂ concentration titration

The CO₂ content of the high CO₂ concentration stirring plate experiment was also verified using a colorimetric titration (Method 8205) Model AL-DT Hach Test Kit. Titrating the sample with NaOH suggested that the water held approximately 440 ppmw of CO₂ while PHREEQC calculations suggested a concentration of approximately 800 ppmw CO₂. The end-point titration was above 9, and was greater than the theoretical end-point of 8.33. It was later found that the NaOH container had expired, and was not longer the original titrant strength needed for proper calculations. It would be possible to determine the CO₂ concentration if the NaOH titrant strength was known, but this would require another titration to verify the NaOH titrant strength. Determining the NaOH titrant strength by titration was deemed unnecessary, and outside the scope of this research project.

Appendix J. Stirring plate experiment with tap water

An experimental trial of the stirring plate simulations (Chapter 2, Section 3) was run using tap water from the water supply in the University of Kansas Water Resources Laboratory. This tap water was obtained from the same source that is used to provide the 35,000 liter water supply for the flume system. The experiment had a duration of 45 minutes, and had two simulations as shown in Figure 1 below. Two water samples were tested. Both water samples consisted of tap water charged with a high amount of CO₂ (pH ≈5.20). One of the water samples was allowed to sit non-stirred, and the other water sample was stirred at rate of 90 rpm to simulate the water velocity in the flume experiments. The experiment was designed to test if the particulate matter in the flume water was making it more difficult for CO₂ to exsolve from the water and move to the atmosphere. The results of the experiment showed that the gas transfer coefficient was similar to the flume water. The conclusion of the experiment was that the particulate matter did not affect the CO₂ gas efflux rate in any significant matter.

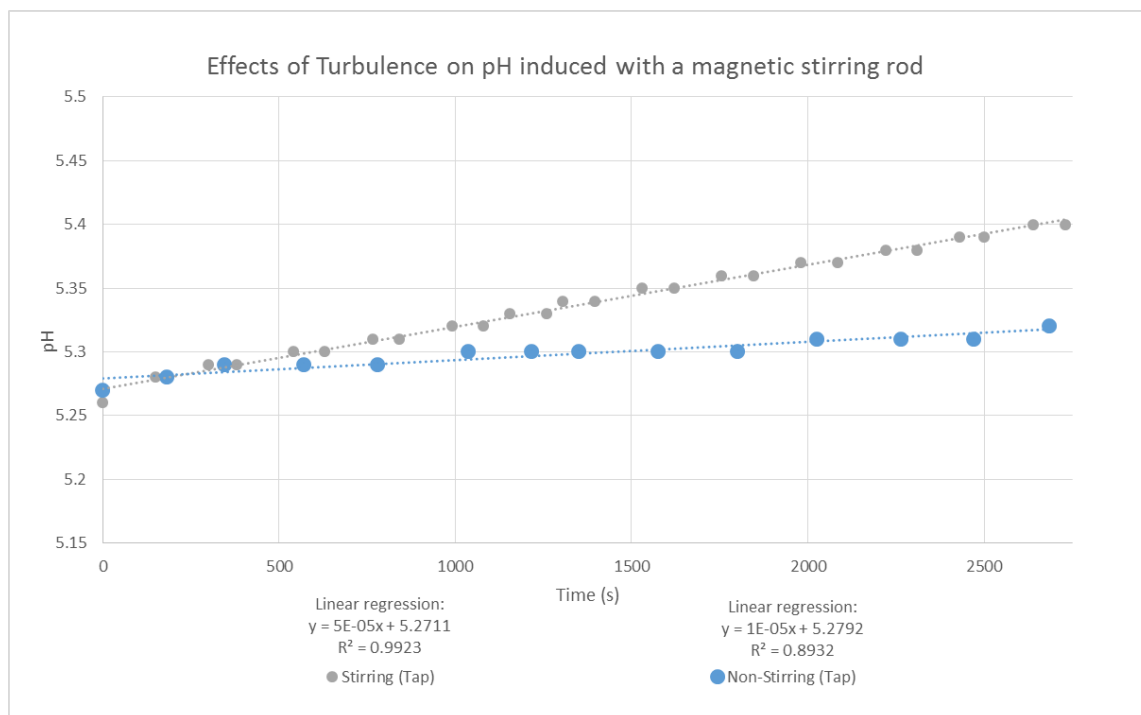


Figure 1. Change in pH over time of the two water samples.

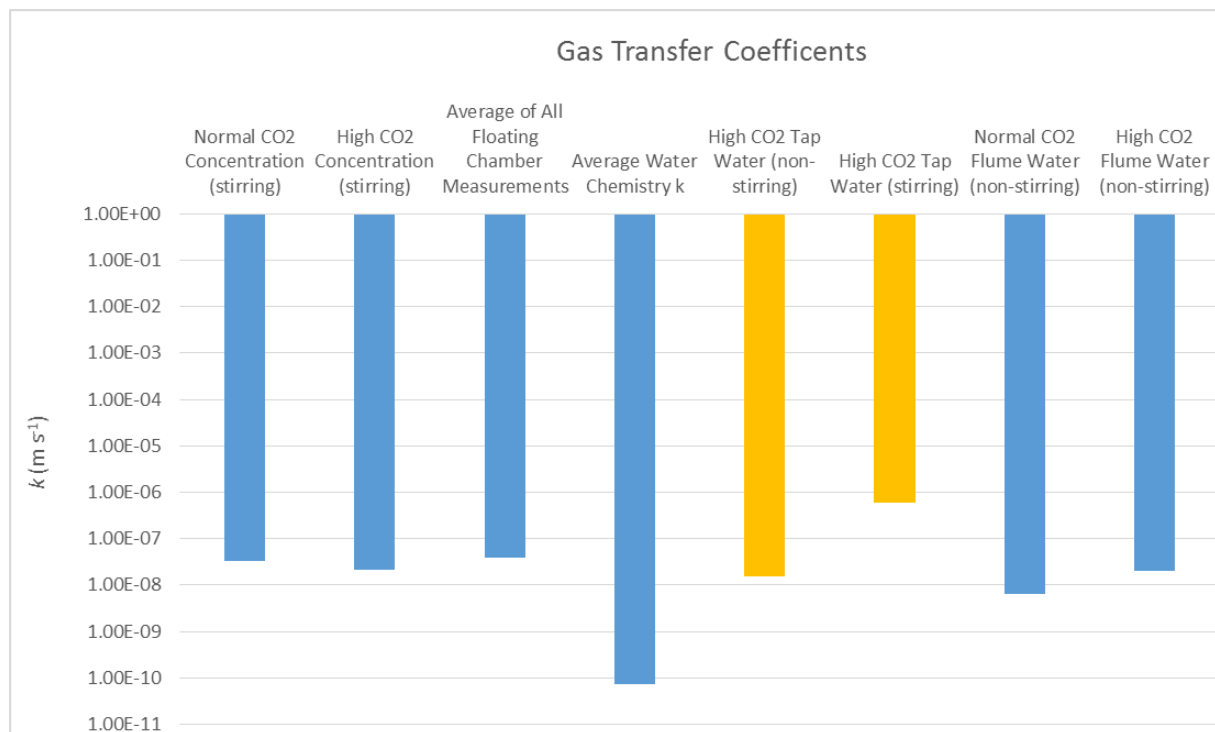


Figure 2. Comparing the gas transfer coefficient of the tap water stirring plate simulation to other known gas transfer coefficients obtained during experiments.

Appendix J. Controlling room atmospheric CO₂

Laboratory concentrations of atmospheric CO₂ were regulated using the ventilation system in the lab. Gas escaping from a leaky seal between the basement water reservoir of the flume system and the flume channel (Appendix D) was responsible for the dramatic increase in laboratory atmospheric CO₂ beginning at time 6,000 seconds. The ventilation system was turned on at approximately 6,500 seconds in Figure 1. As demonstrated turning on the ventilation system decreases the atmospheric CO₂ and holds it relatively constant below about 1,000 ppmv following ventilation system being turned on.

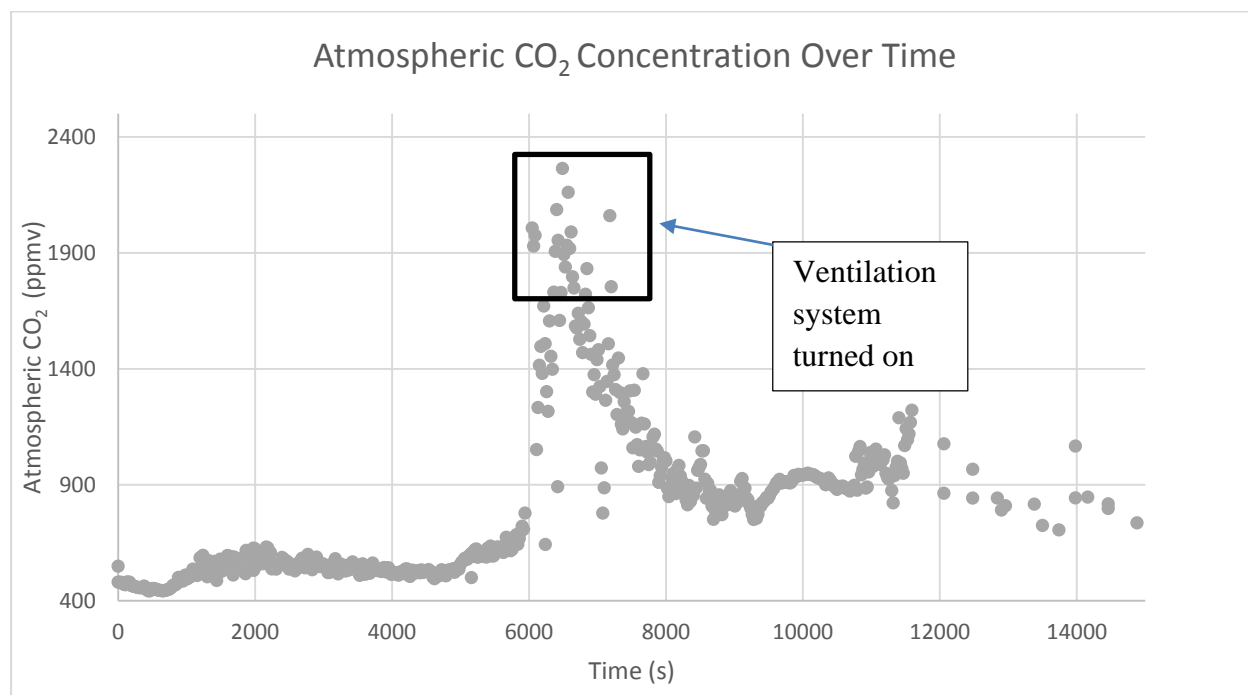


Figure 1. Atmospheric concentrations were monitored over time using three monitoring techniques.

References cited in all appendices

- Cole, J. J., and Caraco, N. F., 1998, Atmospheric exchange of carbon dioxide in a low-wind oligotrophic lake measured by the addition of SF₆: *Limnology and Oceanography*, v. 43, no. 4, p. 647-656.
- Haynes, W. M., 2014, *CRC handbook of chemistry and physics*, CRC press.
- Liu, H., 2014, *Inorganic and Organic Carbon Variations in Surface Water, Konza Prairie LTER Site, USA and Maolan Karst Experimental Site, China* [M.S. thesis]: University of Kansas Geology.
- Lorke, A., Bodmer, P., Noss, C., Alshboul, Z., Koschorreck, M., Somlai, C., Bastviken, D., Flury, S., McGinnis, D., and Maeck, A., 2015, Technical Note: Drifting vs. anchored flux chambers for measuring greenhouse gas emissions from running waters, vol. 12, no. 17.
- MacIntyre, S., Wanninkhof, R., and Chanton, J., 1995, Trace gas exchange across the air-water interface in freshwater and coastal marine environments, *Biogenic trace gases: Measuring emissions from soil and water*, p. 52-97
- Macpherson, G., 2009, CO₂ distribution in groundwater and the impact of groundwater extraction on the global C cycle: *Chemical Geology*, v. 264, no. 1, p. 328-336.
- Müller, D., Warneke, T., Rixen, T., Müller, M., Jamahari, S., Denis, N., Mujahid, A., and Notholt, J., 2015, Lateral carbon fluxes and CO₂ outgassing from a tropical peat-draining river: *Lateral*, v. 12, p. 10389-10424.
- Parkhurst, D. L., and Appelo, C., 1999, *User's guide to PHREEQC (Version 2): A computer program for speciation, batch-reaction, one-dimensional transport, and inverse geochemical calculations*.

Robbins, L. L., Hansen, M. E., Kleypas, J. A., & Meylan, S. C., 2010, CO2calc: A user-friendly seawater carbon calculator for Windows, Mac OS X, and iOS (iPhone), US Geological Survey: No. 2010-1280.